ABSTRACT

WANG, CHENG. Soil Suction Characterization and New Model for Predicting Suction in Residual Soils. (Under the direction of Dr. Roy H. Borden and Dr. Mohammed Gabr).

Soils encountered in construction are often unsaturated. If the magnitude of matric suction is quantified, it can be incorporated as a stress variable of the shear strength in the unsaturated state, which will influence the calculated safety of geo-structures. The objective of this study is to provide a detailed characterization of the suction profile in a North Carolina residual soil and propose an empirical model to predict soil suction based on basic soil indices. A field test site was chosen in Greensboro, North Carolina. In addition, three slopes of varying steepness were cut (0.25:1, 0.5:1, and 1:1) and one cantilever sheet pile wall was installed. The soil between the intended slopes and the sheet pile wall was excavated via stage excavation to a depth of 22 feet. Two major residual soil groups, a high plasticity silt (MH) and a low plasticity silt (ML), were encountered at the site. The suction of these soils, retrieved using thin-walled sampling tubes, was tested using tensiometers, the filter paper method, and pressure plate tests. Sixteen Fredlund Thermal Conductivity *(*FTC) suction sensors and sixteen moisture sensors were installed in the field for measurements over time. The monitoring process was from June 27, 2013 to March 10, 2014. Man-made infiltration (ponding of water) on the horizontal ground surface at the top of the slopes was maintained from February 6, 2014 to March 10th, 2014.

A comprehensive suction-related soil property database was established by testing soil from 64 Shelby tube samples obtained from soil borings. Twelve SWCCs were obtained using pressure plate tests. A field curve concept is demonstrated that considers the actual

suction conditions of the soil, as measured from a tensiometer inserted into the Shelby tube, and the hysteresis of soil water characteristic curves (SWCCs). By using the actual one-point reading as a reflection point, the drying curve of SWCC can be adjusted to account for the actual field condition of the soil. The reliability of the paired T5 and T5x tensiometers used in this study was validated by testing uniformly laboratory-compacted soil samples.

An empirical suction prediction model was developed using multivariate analysis. The proposed statistical model for predicting the suction of the test-site residual soils better represents measured soil suction than models found in the literature. The proposed model was verified using limited data from Rahardjo (2012) who also studied soil water characteristic curves of residual soils.

For the field instrumentation, the field sensors were able to predict the changes in suction and water content quantitatively. FTC suction sensors captured the changes in suction, but the absolute values at the initial and final stages did not reflect the actual suction conditions measured on retrieved samples, at the beginning and end of the monitoring period. The water content sensor measurements are shown to be more reasonable.

Soil Suction Characterization and New Model for Predicting Suction in Residual Soils

by
Cheng Wang

A dissertation submitted to the Graduate Faculty of
North Carolina State University
in partial fulfillment of the
requirements for the degree of
Doctor of Philosophy

Civil Engineering

Raleigh, North Carolina

2014

APPROVED BY:

_____	_____
Dr. Brina M. Montoya	Dr. Shamimur M. Rahman
_____	_____
Dr. Mohammed Gabr Co-Chair of Advisory Committee	Dr. Roy H. Borden Co-Chair of Advisory Committee

BIOGRAPHY

Cheng Wang was born on January 1, 1985 in Dalian, China. In the fall of 2003, he enrolled.in Civil Engineering at Northeastern University in Shenyang, China, for a B.S. degree.

After graduating in June, 2007, he continued his study for a M.S. degree at Northeastern University. During this time, he was involved in the monitoring of metro infrastructure during shield tunneling construction.

In August, 2010, he started his pursuit of Ph.D. degree at North Carolina State University in Civil Engineering with a specialization in Geotechnical Engineering.

ACKNOWLEDGMENTS

The author would like to express sincere appreciation and gratitude to the following people:

Dr. Mohammed Gabr and Dr. Roy Borden, my advisors, for the opportunities given to me for getting involved in the unsaturated soil behavior research project and also their consistent guidance, encouragement and mentorship. It would have been impossible to complete this dissertation without their help and support.

Dr. Shamimur Rahman and Dr. Brina Montoya for reviewing the dissertation and providing important advices for the research.

Dr. K J Kim and Mr. Michael Valiquette from North Carolina Department of Transportation Geotechnical Engineering Unit for supporting this research project and for their generous help with the field work.

The graduate students, Chien-ting Tang, Jungmok Lee and Justin Pescosolido, for the effort they made for the soil properties characterization and the installation of field monitoring sensors. With all of their help, the laboratory testing and field monitoring work could be completed in time. It is a very cooperative group and it is a great honor to have had the opportunity to work with these hard-working graduate students.

Lab managers, Jake Rhoads and Jerry Atkinson, for their suggestions and assistance in the laboratory testing set-up. Whenever there were some problems with the laboratory equipment, it was their insights and suggestions that often enabled the testing to continue without extensive delay.

Dr. Alyson Wilson, Associate Professor in the Statistics Department of North Carolina State University, for her generous help and suggestion for the statistical multivariate analysis used in my research.

T J Ju, Geotechnical Engineer at Subsurface Construction, former graduate student of North Carolina State University, for his generous help with the use of the SoilVision software.

My parents, for all the years of their support and encouragement. It is their love and support that has given me the courage and persistence to move forward until the completion of my studies.

TABLE OF CONTENTS

LIST OF TABLES

LIST OF FIGURES

1. INTRODUCTION

1.1. Background: Unsaturated Soil Properties in Practice

Unsaturated soil properties are well recognized and used in many engineering practices, such as earth-fill dams, highways, and airport runways, which all use compacted soils in unsaturated conditions (Fredlund and Morgenstern 1977). The shear strength of unsaturated soil can be expressed in terms of two independent stress state variables: net normal stress (σ-u_a) and matric suction (u_a-u_w) (Fredlund et al. 1978), where σ, u_a, and u_w refer to total normal stress, air pressure, and water pressure, respectively.

Matric suction has been shown to contribute significantly to the shear strength of unsaturated soil. One example is seen in rainfall-induced slope failure. Especially in slopes composed of residual soils, the groundwater table is deep, and the unsaturated soil profile has a significant thickness (Rahardjo et al. 2011). When water infiltrates the soil, the pore water pressure near the surface of the slope starts to build and the matric suction decreases. Thus, the shear strength of the soil decreases, and the factor of safety also decreases. Rainfall-induced slope failure due to the loss of soil matric suction and shear strength is widely recognized and has been studied extensively (Rahardjo et al. 2011, Anderson and Richards 1987, Sweeney 1982, Au 1998)

Many relatively steep natural slopes are found to be stable, even without any reinforcement, because the soil exists in an unsaturated condition and the matric suction increases the shear strength of the unsaturated soil. However, attempts to analyze these natural slopes based on the strength of laboratory-saturated samples collected from the field

and using conventional effective stress analysis without accounting for existing suction lead to the assumption that the natural slopes would, theoretically, often fail. These contradictory observations suggest that matric suction, which is often excluded from current engineering design, can in fact be an important factor in evaluating the stability of geotechnical structures.

So, from a design point of view, if temporary slopes and retaining walls are designed based on effective stress analysis, which considers the *in situ* soil without suction, the design will be overly conservative. However, if soil suction is included in the design, the resulting design will be more economical, effective, and sustainable. Therefore, in order to consider soil suction for effective engineering design in North Carolina Piedmont residual soil areas, an extensive research program related to soil suction properties is needed.

1.2. Problem Statement

The current design procedures that are based on effective stress theory for temporary slopes and shoring walls typically do not consider soil suction in residual soils. Therefore, they may result in overly conservative designs and excessive costs. Even when engineers are aware of this over-conservatism of the current design, no rational means or procedures are in place to include soil suction in designs that have been validated.

A test site in Greensboro, North Carolina was chosen to study the potential effects of soil suction on the performance of geotechnical structures. Three slopes with different degrees of steepness, 0.5:1, 0.25:1, and 1:1, and a sheet pile wall were constructed. An experimental program involving primarily the characterization of suction-related soil properties was carried out. Field instruments (suction and water content sensors) were

installed and monitored to investigate the changes in the suction and moisture profiles under the influence of surface water infiltration.

1.3. Objectives

The objectives of this study are to:

1. Characterize soil suction and set up an extensive database for Piedmont residual soils.
2. Take suction measurements using tensiometer, filter paper and pressure plate tests and propose reliable suction measurement techniques.
3. Propose an empirical model to predict soil suction based on basic soil properties that can easily be incorporated into current design.
4. Monitor the change of suction and moisture profiles by field installed sensors and suggest future uses of the field installed sensors.

1.4. Scope

Chapter 1 provides background information regarding unsaturated soil properties in practice as well as the problem statement, objectives, and scope of this study. Chapter 2 describes the database and characterization of the unsaturated properties of North Carolina residual soils. Chapter 3 investigates the reliability of the T5 tensiometer and offers a proposed suction correction factor for adjusting the actual measurements for design purposes. Chapter 4 sets forth a proposed empirical model to predict residual soil suction based on basic soil properties. Chapter 5 looks at the changes in soil suction and moisture profiles by analyzing the data obtained from the field instruments and laboratory tests. Chapter 6 provides a summary and the conclusions drawn from the study.

2. CHARACTERIZATION OF SUCTION-RELATED SOIL PROPERTIES OF RESIDUAL SOILS

2.1. Introduction

Residual soil is formed by in-place decomposition or the chemical weathering of parent rocks. The engineering properties of residual soil are dependent on the parent material, climate, topography and drainage, vegetation, and age (Townsend 1985). Its heterogeneity, which has led to wide variations in engineering properties and testing difficulties, has been documented by Townsend (1985); Sowers and Richardson (1983); Wang and Borden (1996) among others. Due to the difficulties associated with the laboratory testing of residual soil, databases of residual soil properties are very limited, especially for North Carolina, which is one of the Piedmont residual soil regions. A database of suction-related residual soil properties for Piedmont residual soils is even harder to find, with the exception of some published data (William 1986).

An experimental program was set up to study the unsaturated soil properties of North Carolina residual soils for this research. Undisturbed Shelby tube samples were obtained from the field, and the soil samples' matric suction values were measured using different approaches, the pressure plate test, tensiometers, and the filter paper method. Basic soil properties, such as grain size distribution, Atterberg limits, specific gravity, and natural water content, also were measured following ASTM standards.

The objectives of this study are to: 1) generate data regarding suction values and other basic soil properties of Residual soils, 2) investigate the corresponding measurement techniques and compare different suction measurement approaches and propose a reliable suction measurement technique, and 3) obtain soil water characteristic curves by pressure plate test and provide a reliable and comprehensive database that can be considered for design purposes.

2.2. Background

The suction of soil generally refers to total suction, which includes matric suction and osmotic suction. Osmotic suction is the result of dissolved solutes in the water. In general applications of geotechnical engineering, osmotic suction is not considered to be a significant influencing factor for soil suction. So, the type of suction studied here is matric suction. The suction of soil can be characterized using different measurement techniques, as shown in Table 2.1. The different suction measurement techniques presented in Table 2.1 have been widely used. The advantage and limitation of each approach is discussed in the following sections.

Table 2.1 Different Suction Measurement Techniques after Fredlund et al. (2012) and Lu and Likos (2004)

Name of Test	Suction Component Measured	Range, kPa	Type	Comments
Psychrometer	Total	100 to~8000	Lab and field	Constant temperature
Noncontact filter paper	Total	1,000-500,000	Lab	
Chilled mirror hygrometer	Total	1,000-450,000	Lab	
Tensiometer	Pore-water pressure or matric suction	0-90(high capacity tensiometer can attain 1000 kPa)	Lab and field	Difficulties with cavitation and air diffusion through ceramic cup
Contact filter paper	Matric		Lab	
Pressure plate	Matric	0-1,500	Lab	
Thermal conductivity sensors	Matric	10 to ~1,500	Field	Indirect measurement

Pressure plate method

The pressure plate method is the most common way to determine soil water characteristic curves (SWCCs). However, research studies have been undertaken to investigate the potential inaccuracies of this method by Bittelli and Flury (2009). Such research notes that low plate and soil conductance, lack of plate-soil contact, and soil

dispersion make this method often unreliable at 'low water potentials', which means within a high-suction range. Bittelli and Flury (2009) performed pressure plate tests on silty loam soil and compared the results to those obtained using a dewpoint meter. Their study derived different results between the pressure plate and dewpoint meter measurements at potentials less than -10 m H_2O (higher than 100 kPa), with the pressure plate apparatus providing higher water contents than the dewpoint meter at the same water potential.

Many factors affect the SWCCs of soil, such as soil type, stress history, hysteresis, and the natural condition (e.g., dry density and overburden pressure) which were studied by Vanapalli et al. (1999), Iyer et al. (2012), Yang et al. (2004), and Tarantino and De Col (2008).

Vanapalli et al. (1999) conducted pressure plate tests on compacted soil and found that:

> …. the stress history and initial molding water content seemingly have the most influence on the soil structure (and aggregation), which in turn dominates the nature of the soil-water characteristic for fine-grained soils. Specimens of a particular soil, in spite of having the same texture and mineralogy, can exhibit different soil-water characteristics if they are prepared at different initial molding water contents and possess different stress histories (Vanapalli et al. 1999).

The findings of Vanapalli et al. (1999) are similar to the observations of Iyer et al. (2012) and Yang et al. (2004). Iyer et al. (2012) stated that the initial water content can affect the initial portion of the SWCC at less than 500 kPa and that the specimen thickness does not

significantly affect the shape of the SWCC. Yang et al. (2004) found that the dry density can affect the shape of the SWCC. Soils with lower densities have lower air-entry values and less residual matric suction than soils with high dry density values.

Tarantino and De Col (2008) observed that for the same void ratio and degree of saturation, the matric suction will change after unloading and reloading because of "the redistribution of water between micro- and macro-pores." Also, the matric suction will increase when the soil is compressed at the post-compaction stage compared to the non-compaction state.

The Fredlund and Xing (1994) model is used widely as a SWCC fitting equation, as expressed in Equation (2.1).

$$\theta = \left[1 - \frac{\ln(1 + \frac{\psi}{\psi_r})}{\ln(1 + \frac{10^6}{\psi_r})}\right] \times \frac{\theta_s}{\left[ln\left[\exp(1) + \left(\frac{\psi}{a}\right)^n\right]\right]^m} \tag{2.1}$$

where ψ_r is the residual matric suction (kPa), ψ is the matric suction of the soil (kPa), θ_s is the saturated volumetric water content, θ is the volumetric water content of the soil, and a, n, and m are the curve-fitting parameters.

As aforementioned, the pressure plate method is the most common way to obtain SWCCs. However, because this method can be used only in the lab and is time-consuming, other tools have been developed for taking field suction measurements more quickly and effectively.

SWCC and hysteresis

The SWCC determined by the pressure plate method generally provides the drying curve which is the boundary of the suction at a given volumetric water content. If soil suction is predicted based on the drying curve, the suction inevitably will be over-predicted due to the hysteresis of the SWCC. At a given volumetric water content, the matric suction of soil is not unique, which is known as the hysteresis effect of the SWCC. The actual suction in the soil might be located on the scanning curves that lie between the drying and wetting curves, as shown in Fig. 2.1. The hysteresis history of the *in situ* soil is difficult to know. So, in order to improve the ability to predict suction, the suction measured from the drying curve must be corrected by considering the hysteresis effect.

Numerous research studies have been conducted to consider the hysteresis effect on the suction of soil. Instead of relying merely on the drying curve to predict soil suction, an actual one-point measurement on the SWCC, and modification approach was proposed by Houston et al. (2006). By using the Zapata and Houston (2008) suction prediction model, a group of predicted SWCCs can be obtained as a function of *w*PI which is the product of the percent passing the No. 200 sieve (*w*) and the plasticity index of soil (PI). By measuring one actual point of suction and degree of saturation for a sample, an optimized *w*PI can be determined that considers the actual density and hysteresis condition of the soil. By inputting the optimized *w*PI into the prediction model, a more precise predicted SWCC can be obtained.

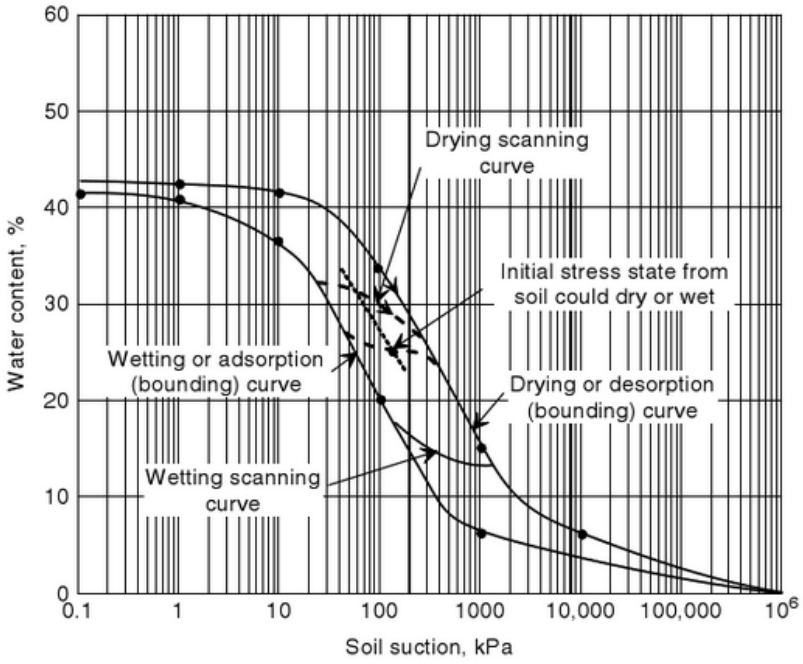

Fig. 2.1 Hysteresis of SWCCs (Fredlund et al. 2012)

Chin et al. (2010) proposed another one-point measurement method by using the database in the SoilVision program. For fine-grained soils (P200 ≥ 30%), the Fredlund-Xing SWCC parameters, i.e., *a*, *n*, and *m*, were found to be a function of eP200, which is the product of the void ratio and the percentage passing the #200 sieve. For coarse-grained soils (P200 < 30%), the *a* value correlated with D50, and the *n* and *m* values correlated with D60. By measuring one point on the SWCC, the predicted SWCC could be shifted to the point being measured. These one-point methods take into consideration the uncertainty associated with the estimation and thus provide an improved correction for the model.

Yang et al. (2004) studied the hysteresis effect on sandy soils and found that D10 has a strong correlation with the air-entry value, residual matric suction, and total hysteresis, and

that all of these parameters tend to decrease with an increase in D10 for sandy materials. Also, Yang et al. found that taking measurements for the wetting curve can be inaccurate and time-consuming due to the low permeability of the ceramic stone embedded in the pressure plate device.

Pham et al. (2003) proposed a simplified method to estimate the wetting curve by determining the drying curve and measuring two points on the wetting curve. They found the estimated wetting curve to be close to the measurements.

Fredlund et al. (2011) found that the log cycles of the shift of the *a* value differ according to soil type. For the same material, the estimated SWCC determined from the grain size distribution using the Fredlund et al. (1997) curve-fitting equation is close to the measured SWCC. The magnitude of the hysteresis was found to be 0.2 log cycle for fine sands and 1.1 log cycle for clayey sand.

So, instead of using the dry curves obtained from the measured or predictive method, the actual one-point measurement is suggested here for considering the actual suction conditions of the soil. By shifting the drying curve to the actual measured point, a SWCC that takes into account the actual condition of the soil can be obtained.

Tensiometer method

The tensiometer is the most common and convenient tool that is used to measure matric suction. The tensiometer studied here is a portable device that can be used for measuring pore water pressure and matric suction directly. Simply by inserting the tensiometer into the soil, the matric suction value can be obtained after the ceramic tip (a

high-air-entry ceramic cup) of the sensor reaches equilibrium with the surrounding soil. However, disadvantages of the tensiometer include its low-suction measurement range and the fact that it requires refilling de-aired water due to the cavitation phenomenon.

Take and Bolton (2003) found that the initial saturation of the tensiometer is crucial in taking suction measurements. They found that "the stepwise pressurization process shows that poor saturation of tensiometer will limit the measurable suction and cause pressure hysteresis." A high degree of saturation is required to obtain a reliable suction measurement.

Mahler and Mendes (2005) used a high-suction range tensiometer (EQ2, Delta-T Devices, Cambridge, UK) to measure soil suction in conjunction with the filter paper method. This tensiometer uses electronic humidity sensors to obtain high-suction ranges. A good correlation between the results from the filter paper method and the tensiometer was observed, as shown in Figure 2.2.

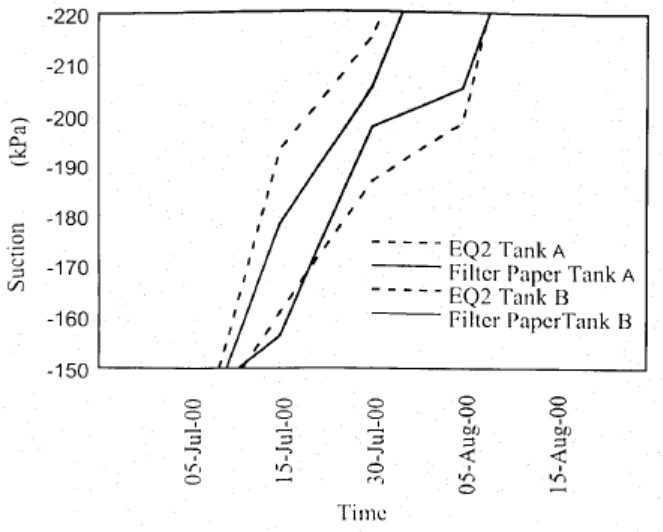

Fig. 2.2 Suction values obtained using filter paper method and tensiometer at 200 kPa (after Mahler and Mendes 2005)

Cui et al. (2008) found that field monitoring using the tensiometer produces variations in suction values with changes in air temperature and soil water content. They applied a tensiometer within a low-suction range (20 kPa -160 kPa) and observed no cavitation during the two or three weeks before the tensiometer was resaturated. In the high-suction range, however, the duration was shorter, probably due to significant air diffusion.

In short, a tensiometer can be used for taking low-suction measurements and is easy to use. It can be employed in the laboratory and in the field to obtain suction values within a relatively short time. However, one of its limitations is that it requires refilling with de-aired water.

Filter paper method

The filter paper method (ASTM D5298) is an indirect method that is used to measure soil matric suction. After placing the filter paper between two soil samples in a desiccated glass jar, the water content of the filter paper can be measured after seven days of equilibrium. The matric suction can be determined using a calibration equation. The contact filter paper method is for measuring the matric suction of soil. And if the filter paper is placed on top of sample without contact, this non-contact filter paper method is for measuring the total suction of soil. Advantages of the filter paper method include its simplicity and cost-effectiveness. However, its results are very sensitive to the mass of the filter paper, so a high precision balance (0.0001 g) must be used to ensure accuracy of the results. Whatman #42 filter paper is used following the recommendations found in ASTM D5298. The test results also are highly dependent on the operators.

The results of filter paper method has been investigated by several researchers. Chandler and Gutierrez (1986) observed that the filter paper technique leads to better results when applied using clayey soils. Houston et al. (1994) found that filter paper measurements are fairly reliable and provide confidence in a given measurement of suction. They also found that the filter paper method can be "enhanced by obtaining replicate measurements due to the simplicity and low cost of the method." Also, different batches of filter papers can lead to different calibration curves. So, individual calibration for each batch of filter paper is recommended (Likos and Lu 2002).

Randy Rainwater et al. (2001) found that one primary limitation of the filter paper test method is the difficulty in measuring very small changes in the filter paper mass as water is absorbed; these small changes correlate with large changes in soil suction.

Leong et al. (2002) investigated various factors that affect measurements obtained using the filter paper method. These factors include different calibration curves, the quality of the filter paper, the suction source used in the calibration, hysteresis, and equilibration time. The soil suction measurements indicate that Whatman #42 filter paper can be used reliably with the ASTM D5298 equation to obtain the matric suction of the soil via the contact method.

Power et al. (2008) found that applied pressure on the filter paper can alter the measured suction value and that 1 kPa is appropriate to ensure good contact without altering the measured suction value.

Marinho and da Silva Gomes, J. E. (2012) studied the effects of contact on the filter paper method. They found that lack of contact that exceeds 20% leads to an inadequate

matric suction measurement. They compared the matric suction values obtained using the filter paper method to those obtained using the traditional pressure plate test and found that the filter paper values were higher. This finding suggests that the measured suction values obtained using the filter paper method reflect a combination of the total and matric suction values and do not represent the actual pressure plate test values.

In short, the filter paper method is easy to perform, but it is highly operator dependent. Lack of contact area, not enough equilibrium time, and differences in calibration curves are all factors that affect the accuracy of the results. In this research, the filter paper method is used in conjunction with the tensiometer to obtain suction values for the natural state of the soil.

Comparison of pressure plate, tensiometer and filter paper methods

Because all three of these approaches are commonly used to measure suction within a reasonable range, deciding which method can provide results that are closest to the actual suction of the soil becomes a significant question. The discrepancy between pressure plate test results and tensiometer readings was noted by Tarantino et al. (2011), who observed that the suction values obtained using the pressure plate method are higher than those of the tensiometer in the medium range of suction values from 150 kPa to 400 kPa (as shown in Figure 2.3).

Similar results also were obtained by Noguchi et al. (2011), who pointed out that the measured suction values obtained from the pressure plate method were higher than those derived from both the filter paper method and tensiometer. The reason for this discrepancy

was the occluded water that was present in the samples. When the pressure plate test was initiated, the initial water content in the sample was high enough that the water could exit the sample. During the test, especially high pressure was applied, 100 kPa or higher, and the boundary of the sample became drier, but some water bubbles were still entrapped in the sample. The permeability of the boundaries was so low that the water bubbles could not exit the sample freely.

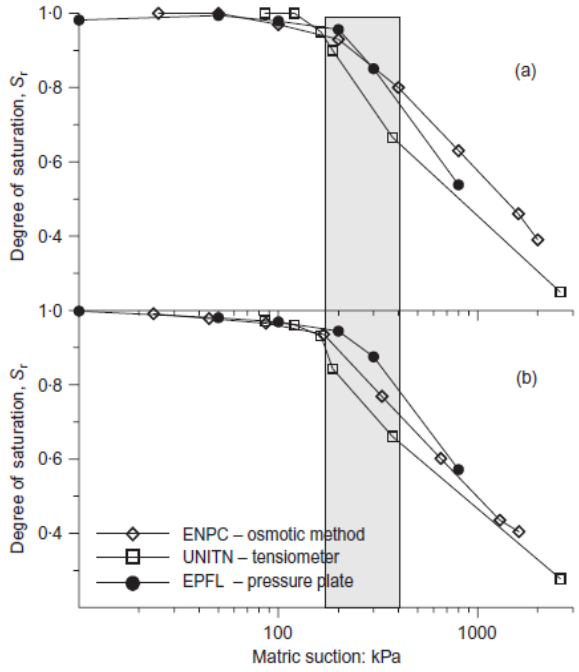

Fig. 2.3 Comparison of pressure plate method, osmotic method, and tensiometer readings in terms of saturation (Tarantino et al. 2011)

Summary of different suction measurement technique

The pressure plate method is a common approach used to obtain SWCCs under laboratory conditions. In order to determine the matric suction of a natural soil sample, both filter paper method and tensiometer can be used. The tensiometer allows for quick measurement of soil suction and can be used in the field as well as in the laboratory. The filter paper method requires at least one week equilibrium and, because it is an indirect method, some factors might affect the results, such as the contact area between the soil and the filter paper, the calibration equation being used, and the operation of the test. Taking into account these different factors, all three of these approaches are adopted in this study, and the results are discussed later in this paper.

2.3. Experimental Program

2.3.1. Site and Test Description

In order to accomplish the stated objectives of developing a residual soil database of suction parameters, an experimental program was undertaken using a North Carolina Department of Transportation (NCDOT) construction site in Greensboro, North Carolina as shown in Fig.2.4. The Project No. 39406.1.1 highway construction site is located at Alamance Road, Greensboro, Guilford County, North Carolina. Three slopes and one sheet pile wall were constructed in the field.

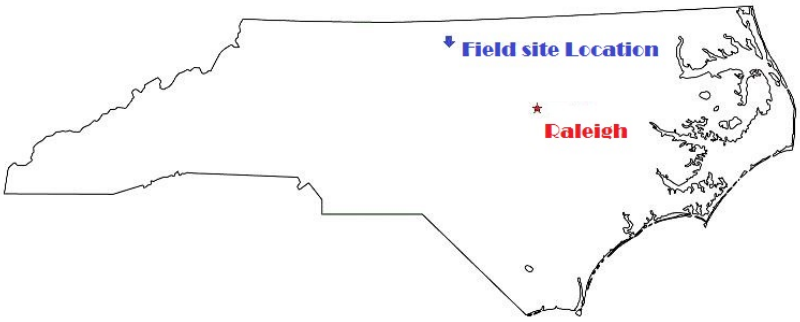

Fig. 2.4 Location of test site

The site s located in the south of Guilford County which is in the Piedmont physiographic province. The main rock type at the site is sheared granite reported by Mundorff (1948). The features of this sheared granite has also been explicitly described by Mundorff (1948):

"The granite is generally a moderately coarse pink schistose and gneissic rock consisting chiefly of quartz, biotite, and feldspar. The granite has been considerably

metamorphosed and intensely sheared. The outstanding feature of the granite is the schistose and slaty dikes, which are green in color and greatly resemble the greenstone schists."

The soils comprising the site are mainly red, yellow clay and sandy silt. Sixty-four Shelby tube samples were obtained from the field and the location of each boring was marked as a station number, as shown in Table 2.2. The samples were obtained from 2 to 52 ft depth, and the relative locations of the auger borings are shown in Fig. 2.5.

Table 2.2 Sample Information

Station		Soil Description (AASHTO and USCS)	Shelby Tube	Quantity
403+45	1:1 slope	Upper 7 ft: A-4 sandy silt Below 10 ft: A-7-5 silty clay	3 ft LT: ST59-ST69	10
404+50	0.25:1 slope	Upper 20 ft: A-7-5 silty clay Below 20 ft: A-4 sandy silt	3 ft LT: ST47-ST58	11
405+70	0.5:1 slope	Upper 30 ft: A-7-5 silty clay Below 30 ft: A-4 sandy silt	3 ft LT: ST36-ST46 9 ft RT: ST88-ST94	10 6
404+50 94'RT	Sheet pile wall	Upper 10 ft: A-7-5 silty clay Below 10 ft: A-4sandy silt	86 ft RT: ST81 ST87 94 ft RT: ST26-ST35 102ft RT: ST70-ST80	6 11 10

Note: LT is left of the center line, and RT is right of the center line.

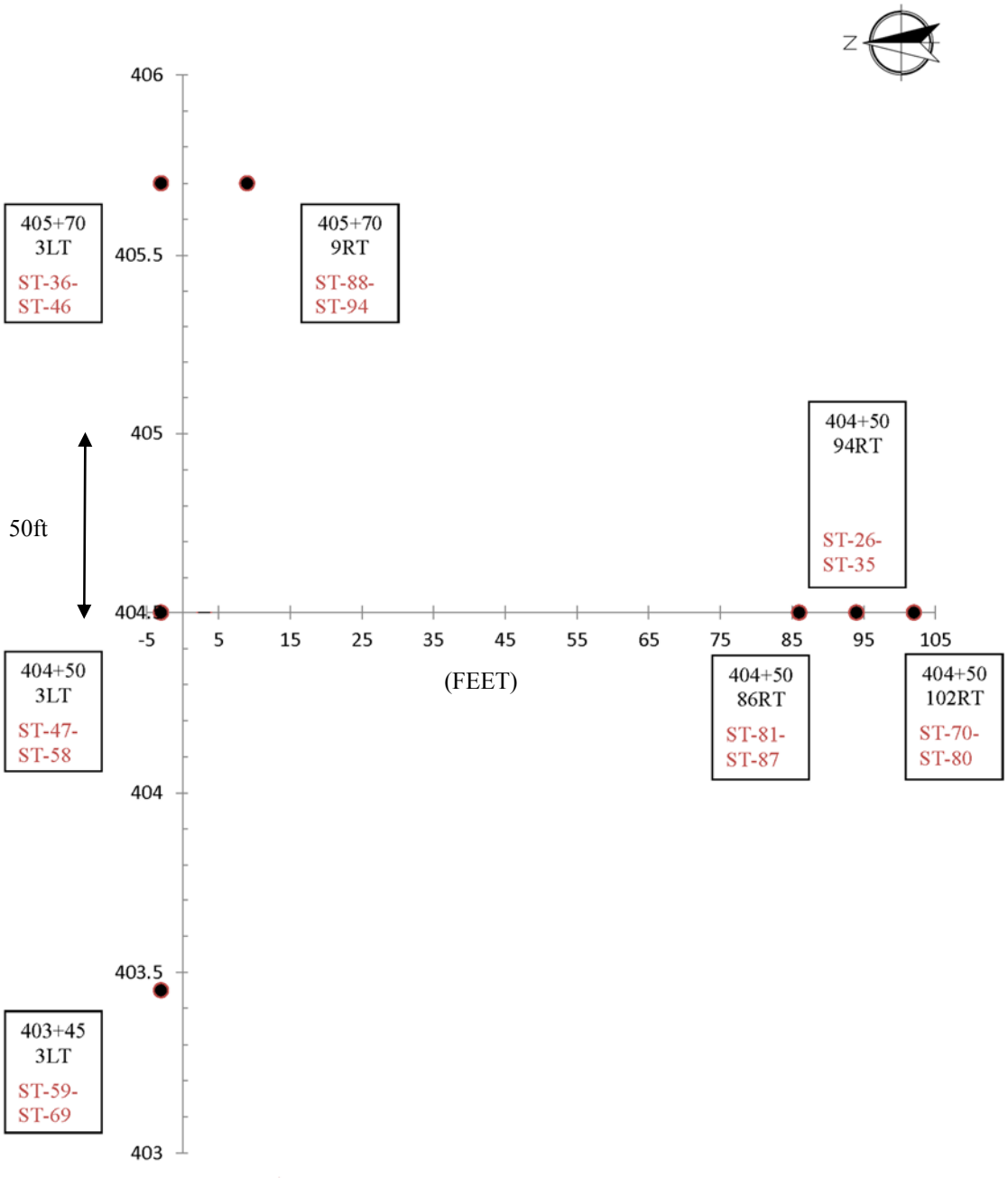

Fig. 2.5 Plan view of the samples' location

2.3.2. Laboratory test procedure and set-up

Standard penetration tests (SPT in figures) were performed for the site investigation and Shelby tube samples were collected for laboratory testing. In the lab, once the Shelby tube was opened, matric suction values were directly determined using paired T5 and T5x tensiometers (described in detail in Chapter 3). In order to study the matric suction comprehensively, pressure plate tests (ASTM 6836) were performed to generate SWCCs, and filter paper tests (ASTM 5298) also were used for comparison. Subsequent soil characterization tests, which included natural water content (ASTM D4959), grain size distribution (ASTM D422), specific gravity (ASTM D854) and Atterberg limits (ASTM D4318), also were conducted by following ASTM standards.

The experimental test set-up, lab testing procedure, and theory behind each matric suction measurement method are presented in the following sections.

Pressure plate extractor

The pressure plate cell design developed by Wang and Benson (2004) was used in this study for obtaining the SWCCs. Fifteen-bar ceramic stone normally is used to determine the SWCCs in a full suction range from 0 kPa to 1500 kPa. However, 5-bar ceramic stone was used in this study because it allows for a less time-consuming process due to the fact that the hydraulic conductivity of 5-bar stone is two orders of magnitude higher than that of 15-bar stone. This set-up also allows for less suction ($\leq$ 500 kPa), which is the research concern of this study.

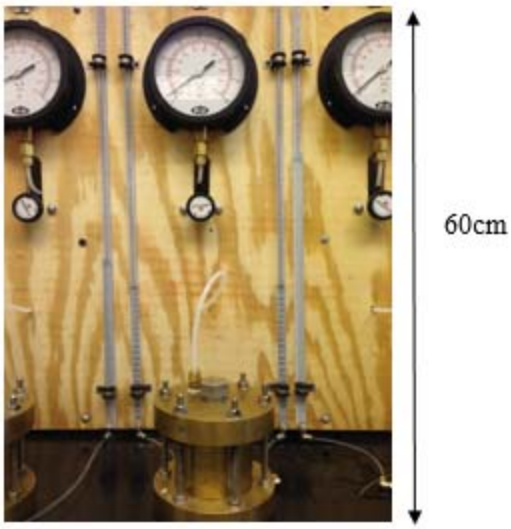

Fig. 2.6 Pressure plate test set-up

First, ensuring that the porous stone is fully saturated is crucial to the test. If the stone is not fully saturated, air will escape through the stone. For air pressure less than 500 kPa and the case of saturated stone, the surface tension is enough to sustain the air pressure. A tank of pressurized air was used as the source of the pressure supply in this study. Air could not escape from the stone, but water could slowly drain out due to the low hydraulic conductivity of the porous stone. An O-ring was used to ensure a good seal. The chamber and the base were tightened together by six bolts. The same amount of torque was applied to each bolt; the necessary amount of torque is 5 kN·m.

Second, constant air flushing is important when measurements are taken. Air bubbles can easily form at the base of the porous stone and in the tubes, so a small manual air pump was used in this study to push water from one tube to the other as an effective way to remove the air bubbles.

After flushing, a small cap was put on the tubes to avoid water evaporation. This air flushing process was conducted every seven to eight hours. During the tests, the air entry value is an important point to be determined because it marks when the soil begins to desaturate.

Tensiometer

Tensiometers allow the direct and precise measurement of small amounts of tension in the soil. In this study, T5 and T5x laboratory tensiometers were used for measuring the matric suction. The tensiometer was inserted into the soil, and the output was recorded as voltage. The voltage corresponds directly to the matric suction.

Fig. 2.7 T5 tensiometer

Fig. 2.8 Tensiometer test set-up

The working range of T5 tensiometers is from +100 kPa (as positive pore water pressure) to -85 kPa (as matric suction). The T5x, a special version of the T5 tensiometer, can measure matric suction up to -160 kPa. The advantage of the T5x is its fast response and easy operation. Before each measurement was taken in this study, the saturation of the sensor had to be checked to ensure the accuracy of the readings.

Filter paper method

Filter paper also can be used for testing the matric suction of Shelby tube samples. For this study, two 1-inch thick soil biscuits were cut, and Whatman #42 (42 mm diameter) filter paper was placed between the two soil biscuits. To prevent contamination, the Whatman #42 filter paper was placed between two Fisherband P8 (5.5 cm diameter) filter papers.

Fig. 2.9 Filter paper specimen

Fig. 2.10 Filter paper sample in equilibrium

The moistened filter paper was weighed using an analytical balance with a four-decimal precision 0.0001 g balance. Then, the filter paper was placed in an oven at 105 Celsius degrees for 24 hours. After the drying process was completed, the filter paper was weighed again, and the matric suction was calculated based on the calibration found in ASTM 5298.

2.4. Residual Soil Characterization Profiles

A comprehensive database was constructed from the data gathered for each of the three slopes and behind the sheet pile wall, as described in Appendix A. The major soil types in this study are A-7-5, MH (red color silty material) and A-4, ML (tan color silty material) based on AASHTO and USCS soil classification.

The database includes: the soil sample number and location, depth, soil type (AASHTO and USCS), natural gravimetric water content (w, %), dry density (γ_d, pcf), total density (γ_t, pcf), specific gravity (G_s), degree of saturation (S, %), void ratio (e), volumetric water content (θ_w), saturate volumetric water content (θ_s), percentage passing the #No. 200 sieve (< = 0.075 mm, %), percentage passing 5 μm (%), percentage passing 2 μm (%), liquid limit (LL), plastic limit (PL), plasticity index (PI), date of suction testing by tensiometer, suction readings by tensiometer (ψ_t, kPa), date of finishing filter paper testing, suction measured by filter paper method (ψ_f, kPa), and gravimetric water content of the filter paper test samples (w_f, %).

Representative suction-related soil profiles at 0.5:1 slope 405+70 3'LT are shown in Figure 2.11 and Table 2.3; the rest of the soil profiles and the corresponding database are presented in Appendices A and B. In general, the matric suction values decreased from the top to the bottom of the profiles at all four locations (i.e., the three slopes and sheet pile wall). Within the top ten feet, the tensiometer readings are around 100 kPa. The suction range is from 60 kPa to 100 kPa for the upper 30 feet of the clayey silty zone. Once the material transitions to the sandy silty zone, the suction drops to below 50 kPa.

This observation shows that suction is strongly related to soil type. This finding is consistent with the water contents and degree of saturation profiles because below 30 feet the soil is close to a fully saturated condition. However, the filter paper method yielded higher results than the tensiometer readings for the upper 20 feet. Therefore, a comparison of the results from these two methods is discussed in the following section.

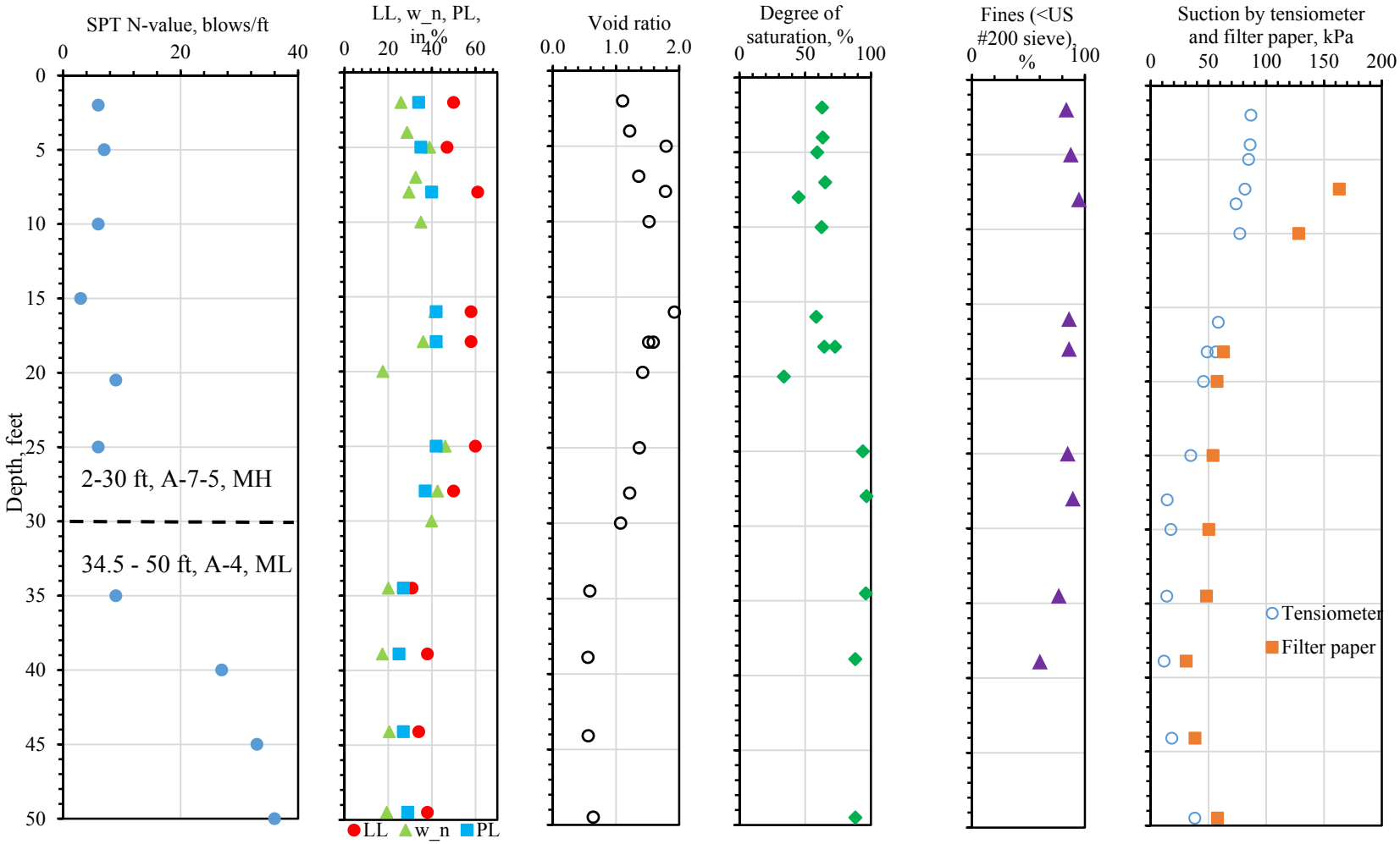

Fig. 2.11 Profiles of SPT N-value, moisture content, void ratio, degree of saturation, fines, and suction for 405+70 3'LT

Table 2.3 Database at 0.5:1 slope 405+70 3'LT

0.5:1 slope 405+70 3'LT																					
#	Depth	Soil Type		w	γ_d	γ_t	G_s	S	e	θ_w	θ_s	#200	5μm	2μm	LL	PL	PI	Tensiometer	ψ_t	Filter paper	ψ_f	w_f
	(ft)	(AASHTO)	(USCS)	(%)	(pcf)	(pcf)		(%)				(%)	(%)	(%)				time	(kPa)	time	(kPa)	(%)
ST36	2.0	A-7-5	MH	25.8	80	100	2.69	63	1.11	0.33	0.53	83.5	32.5	22.3	50	34	16	7/12/13	86.7			
	4.0			28.6	76	97		63	1.22	0.35	0.55							7/12/13	86.1	7/19/13	268.6	27.6
																		9/18/13	86.0	9/30/13	179.3	
ST37	5.0	A-7-5	MH	38.9	61	84	2.72	59	1.79	0.38	0.64	87.4	22.8	14.0	47	35	12	7/17/13	84.8			
	7.0			32.6	72	95		65	1.36	0.38	0.58							7/17/13	81.6	7/24/13	163.2	29.8
ST38	8.0	A-7-5	MH	29.5	61	79	2.72	45	1.79	0.29	0.64	94.6	31.7	21.5	61	40	21	7/17/13	73.9			
																		10/18/13	79.6	10/30/13	441.2	29.1
	10.0			35.0	67	91		62	1.52	0.38	0.60							7/17/13	77.1	7/24/13	128.1	33.0
ST39	16.0	A-7-5	MH	41.3	58	82	2.72	58	1.93	0.38	0.66	85.8	17.2	8.8	58	42	16	7/18/13	58.5			
																		10/16/13	58.7	10/30/13	53.9	40.9
	18.0			36.0	67	92		64	1.52	0.39	0.60							7/18/13	56.4	7/26/13	62.9	37.9
ST40	18.0	A-7-5	MH	42.2	66	94	2.74	73	1.59	0.45	0.61	85.8	17.2	8.8	58	42	16	7/18/13	48.8			
																		10/17/13	49.2	10/30/13	47.0	39.4
	20.0			17.5	71	83		34	1.42	0.20	0.59							7/18/13	45.7	7/26/13	57.4	20.3
ST41	25.0	A-7-5	MH	46.1	73	107	2.79	94	1.37	0.54	0.58	84.7	5.7	2.2	60	42	18	7/19/13	34.7	7/27/13	53.9	45.1
ST42	28.0	A-7-5	MH	42.6	78	111	2.76	97	1.22	0.53	0.55	89.2	10.9	5.0	50	37	13	7/26/13	14.2			
																		10/28/13	28.6	11/6/2013	45.3	40.6
	30.0			39.9	83	116		102	1.07	0.53	0.52							7/26/13	17.5	8/2/13	50.3	37.0
ST43	34.5	A-4	ML	20.1	110	133	2.81	96	0.59	0.36	0.37	76.7	8.0	2.0	31	27	4	7/30/13	13.9	8/6/13	48.3	20.4
ST44	38.9	A-6	ML	17.3	114	133	2.84	88	0.56	0.32	0.36	60.1	4.0	1.0	38	25	13	7/30/13	11.5	8/6/13	30.7	18.5
ST45	44.1	A-4	ML	20.5	115	139	2.88	105	0.56	0.38	0.36	68.2	14.7	10.4	34	27	7	8/6/13	18.3	8/14/13	38.3	19.6
ST46	49.5	A-4	ML	19.3	111	133	2.92	88	0.64	0.34	0.39	48.5	10.0	5.0	38	29	9	8/7/13	38.2	8/15/13	57.8	25.1

Note: ψ_t is suction tested by tensiometer

ψ_f is suction tested by filter paper method and w_f is the water content of samples tested by filter paper method

2.5. Tensiometer Method versus Filter Paper Method

The suction readings obtained from the tensiometer are compared with those obtained using the filter paper method in Figure 2.12. Instead of the 1:1 ratio line, which would indicate that the suction values obtained by the filter paper method are the same as those obtained using the tensiometer, the suction by filter paper is higher than the one by tensiometer.

As Figure 2.12 shows, most of the data fall above the 1:1 ratio line. At a certain level of suction, for example at 40 kPa, the filter paper method measured the suction to be 50% higher than the tensiometer reading. At 20 kPa, the measurements reached 75% or even 150% higher than by the tensiometer.

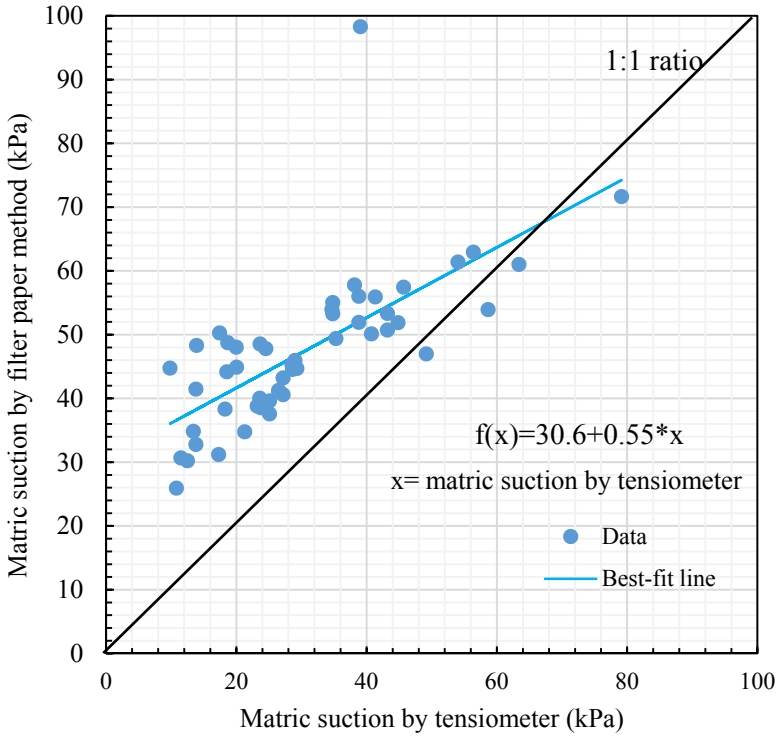

Fig. 2.12 Suction comparison between tensiometer and filter paper method

Reasons that may explain these differences include:

The material tested here is silty soil, and the water content of the filter paper may not be 100% representative of the water content of the soil. Close contact between the filter paper and the soil sample was not ensured. The contact and non-contact filter paper method respectively measure the matric suction and total suction. So, instead of the matric suction measurements being from the contact filter paper method, it is actually a combination of the contact and noncontact methods that caused the high measured suction values (Marinho and da Silva Gomes, J. E. 2012).

The heterogeneity of the Shelby tube samples also can affect the measurements. In general, the sample properties throughout one Shelby tube can be assumed to be consistent. However, for residual soil, the heterogeneity is obvious, as shown in Figure 2.13. This heterogeneity may affect the results because the tensiometer test uses only a relatively small area of soil (diameter of tensiometer tip is 5 mm), and the filter paper method requires samples that are 70 mm in diameter and 50 mm thick which may contain more soil variabilities.

The calibration equation that is applied might also cause significant suction measurement variation. The filter paper method is an indirect suction measurement method that employs the calibration curves found in ASTM 5298. The calibration equation can be different for different types of filter papers, which is a phenomenon that has been studied by Leong et al. (2002), and even for different batches of the same type of filter papers (Likos and Lu 2002). Likos and Lu (2002) investigated the calibration curves for filter papers from different batches for the noncontact filter paper method. The calibration curves for the different filter papers varied significantly from batch to batch, which could cause a potential suction measurement as high as 92% compared with the suction values obtained using ASTM D5298. This variation seems to increase with a decrease in suction. So, without a tailored calibration, a different calibration equation for the filter paper being used would be expected.

Fig. 2.13 Heterogeneity of residual soil sample

The difficulties associated with the filter paper test protocol also must be acknowledged. The filter paper method is very operator-dependent. The measuring precision of the filter paper during the measuring process must be 0.001 g. Also, the transportation of the filter paper must take place quickly to prevent evaporation. This process requires practice on the part of the operator to produce consistent and reliable results.

2.6. Soil Water Characteristic Curves of Residual Soils

The soil water characteristic curve (SWCC) describes the unique relationship between volumetric water content and the soil suction. The volumetric water content of soil can be measured directly. So, knowing the SWCC of soil, the suction can be certainly quantified. The pressure plate test was performed here to obtain the SWCCs of soil.

Twelve SWCCs were obtained from pressure plate tests and the experimental data was curve-fitted by Fredlund-Xing (1994) equation. The dry curves were plotted in conjunction with their respective field curves as shown in Fig. 2.14 - 2.25.The field curve is the shifted drying curve considering the suction value tested by tensiometer (discussed in section 2.7). The summary of the soil properties and Fredlund-Xing parameters (a, n, and m) are shown in Table. 2.4

The air entry value (AEV), also called bubbling pressure is the first inflection point on the SWCC that the decreasing volumetric water content has a strong influence on the increasing matric suction. The air entry can be obtained by construction method on the SWCC. Here, for better accuracy, the AEV values were calculated based on the equation proposed by (Zhai and Rahardjo 2012)

$$AEV = a * 0.1^{\frac{3.72*1.31^{n+1}(1-e^{-\frac{m}{3.67}})}{n*m*\ln(10)}} \quad (2.2)$$

From Table 2.4, the range of AEV values are from 2.1 to 19.2 kPa. This is consistent with the reported AEV: 10kPa for silt soil tested by (Pham 2002) and 2 to 7kPa for Singapore residual soil tested by Rahardjo et al. (2012).

Table 2.4 Summary of soil properties for testing SWCCs

#	Depth	Type		P200	P2 μm	Cu	Cc	LL	PI	θ_s	Gs	ρ_d	a	n	m	AEV[1]
	(ft)	(USCS)	(AASHTO)	(%)	(%)							(g/cm^3)				(kPa)
ST36	2.2	MH	A-7-5	83.5	22.3	30	2.8	50	16	0.541	2.69	1.235	14.9	0.78	0.60	2.1
ST47	2.2	MH	A-7-5	87.4	25.0	13	1.1	61	22	0.615	2.75	1.058	38.5	2.04	0.30	13.0
ST70	5.2	CL	A-7-5	72.1	17.1	32	0.8	45	19	0.533	2.70	1.262	30.9	0.85	0.64	5.1
ST38	8.2	MH	A-7-5	94.6	21.5	14	1.5	61	21	0.611	2.72	1.060	36.3	1.64	0.61	11.4
ST50	10.2	MH	A-7-5	88.5	14.9	12	2.4	59	23	0.594	2.79	1.133	72.4	1.14	0.97	18.0
ST40	18.0	MH	A-7-5	85.8	8.8	8	1.1	58	16	0.580	2.74	1.150	49.8	0.76	1.63	8.8
ST61	10.0	ML	A-4	81.3	16.1	12	0.8	34	8	0.422	2.78	1.608	44.6	1.65	0.33	13.4
ST28	15.2	ML	A-4	66.3	8.8	9	0.9	36	7	0.435	2.69	1.521	49.9	1.66	1.03	16.7
ST64	27.0	ML	A-7-5	84.7	2.2	4	1.1	45	12	0.442	2.81	1.569	69.2	1.03	1.73	17.8
ST32	34.2	ML	A-4	53.1	4.7	32	0.3	38	8	0.509	2.77	1.360	73.6	1.1	1.45	19.2
ST79	44.2	ML	A-4	60.5	3.8	14	0.6	28	3	0.456	2.83	1.540	33	1.42	1.12	10.1
ST34	44.3	ML	A-4	61.5	7.3	14	0.8	38	10	0.490	2.79	1.425	36.3	1.01	1.32	8.5

Note: 1. AEV (air entry value) is calculated based on Zhai and Rahardjo (2012) equation.

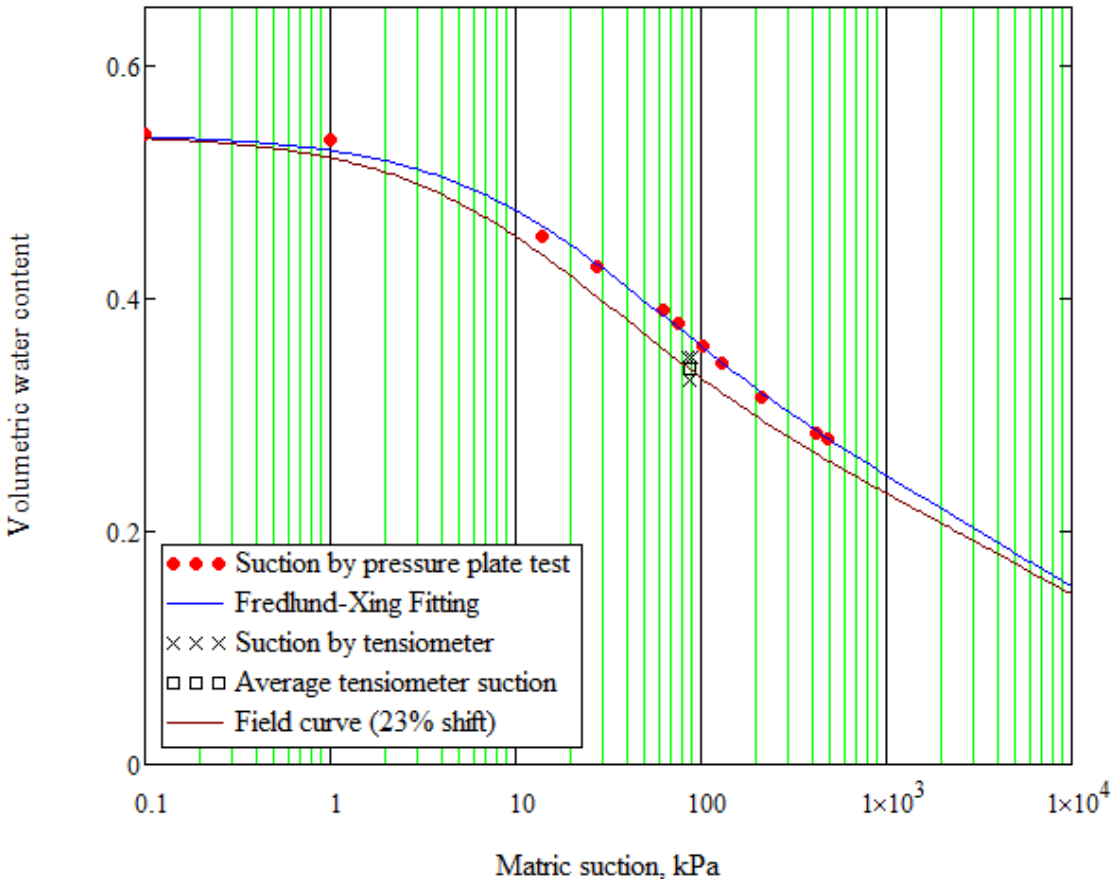

Fig. 2.14 SWCC of A-7-5 (MH) soil at 2.2 ft, ST36

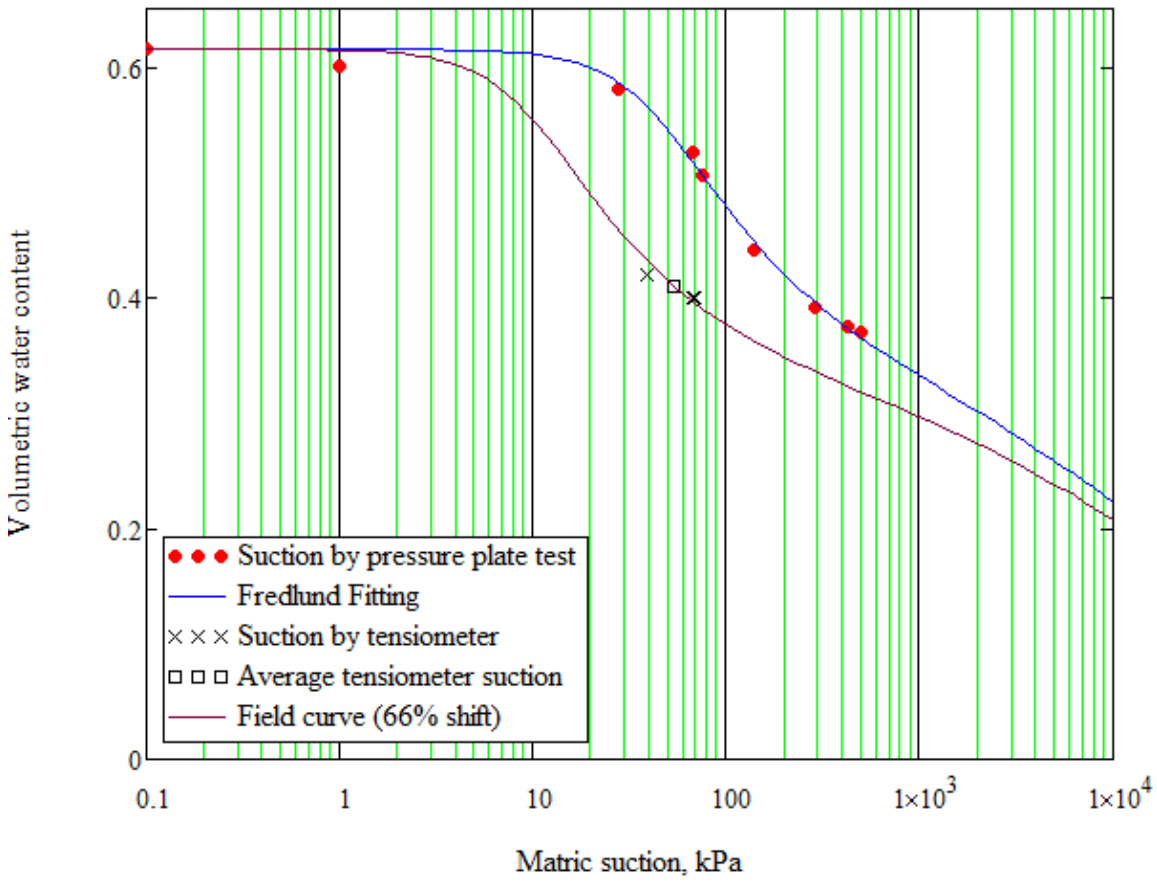

Fig. 2.15 SWCC of A-7-5 (MH) soil at 2.2 ft, ST47

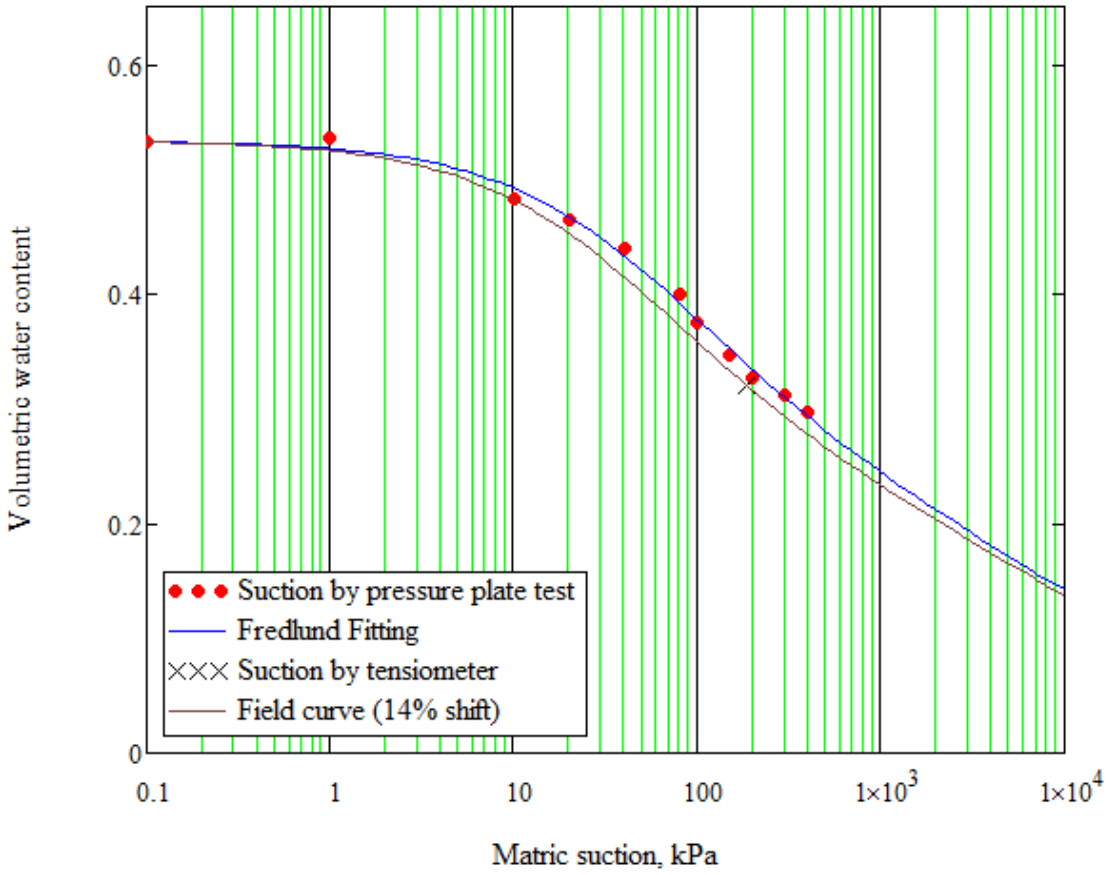

Fig. 2.16 SWCC of A-7-5 (CL) soil at 5.2 ft, ST70

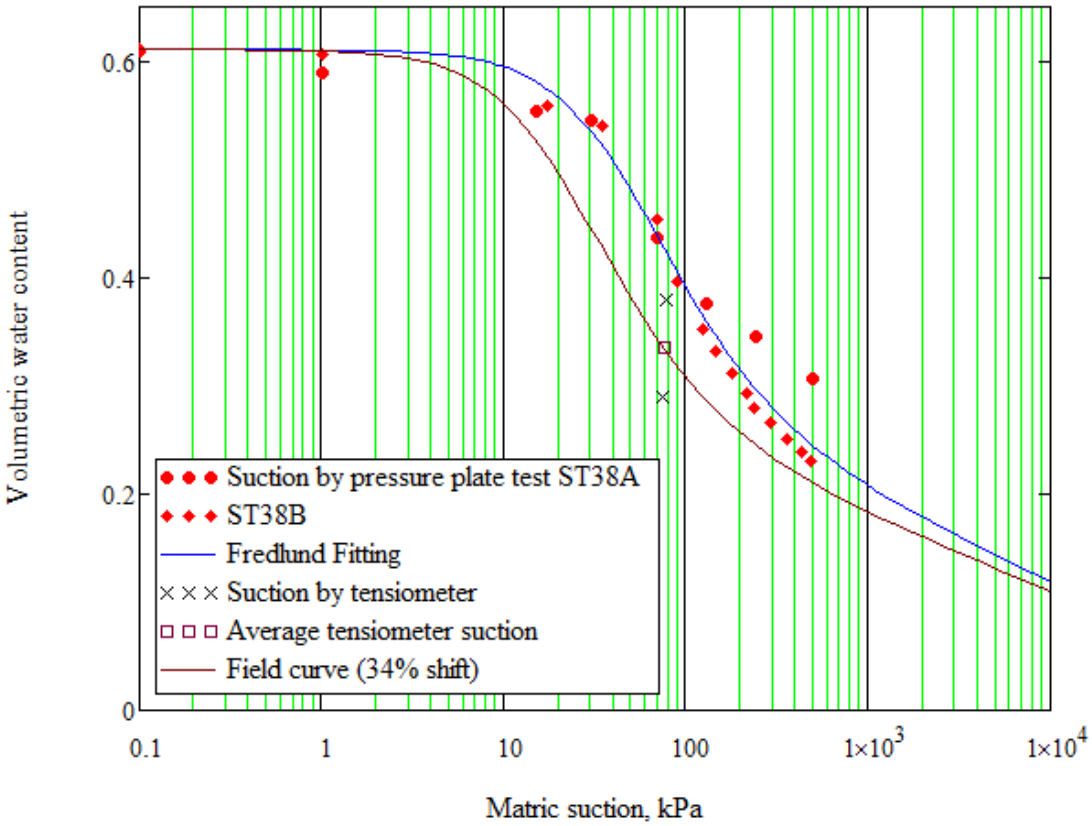

Fig. 2.17 SWCC of A-7-5 (MH) soil at 8.2 ft, ST38

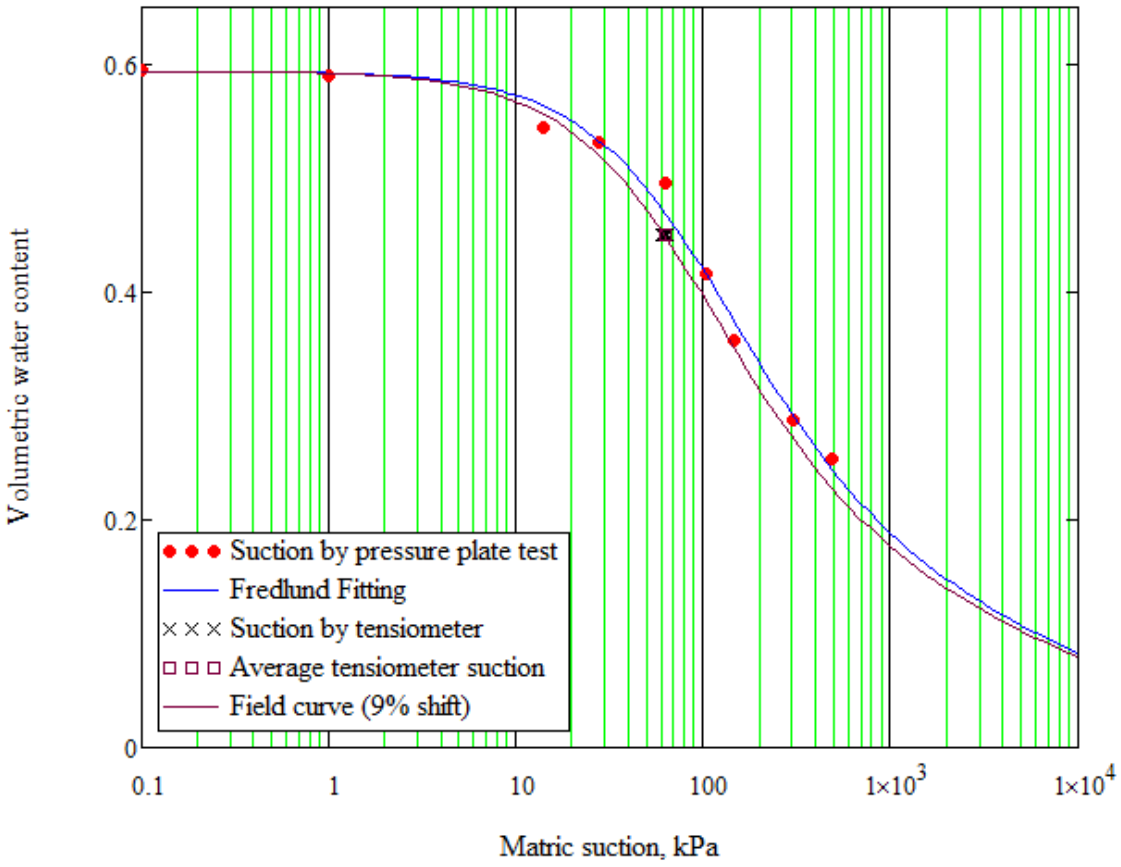

Fig. 2.18 SWCC of A-7-5 (MH) soil at 10.2 ft, ST50

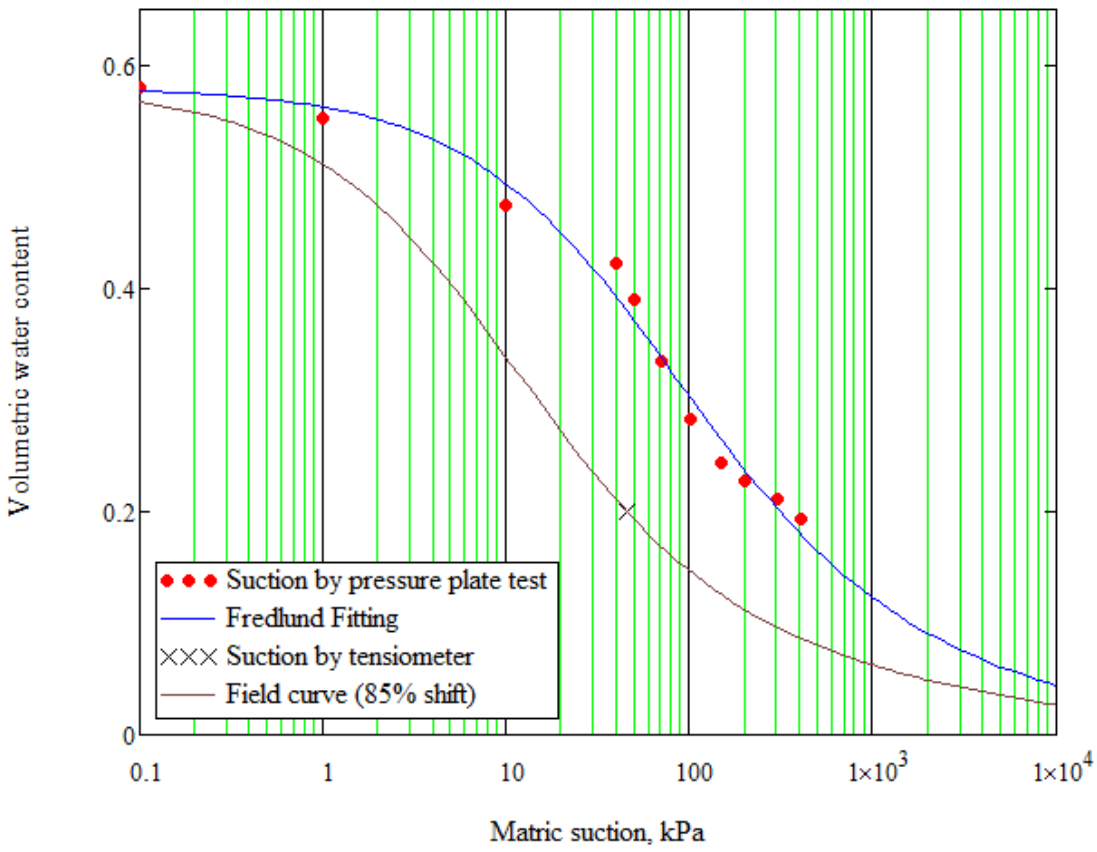

Fig. 2.19 SWCC of A-7-5 (MH) soil at 10.2 ft, ST40

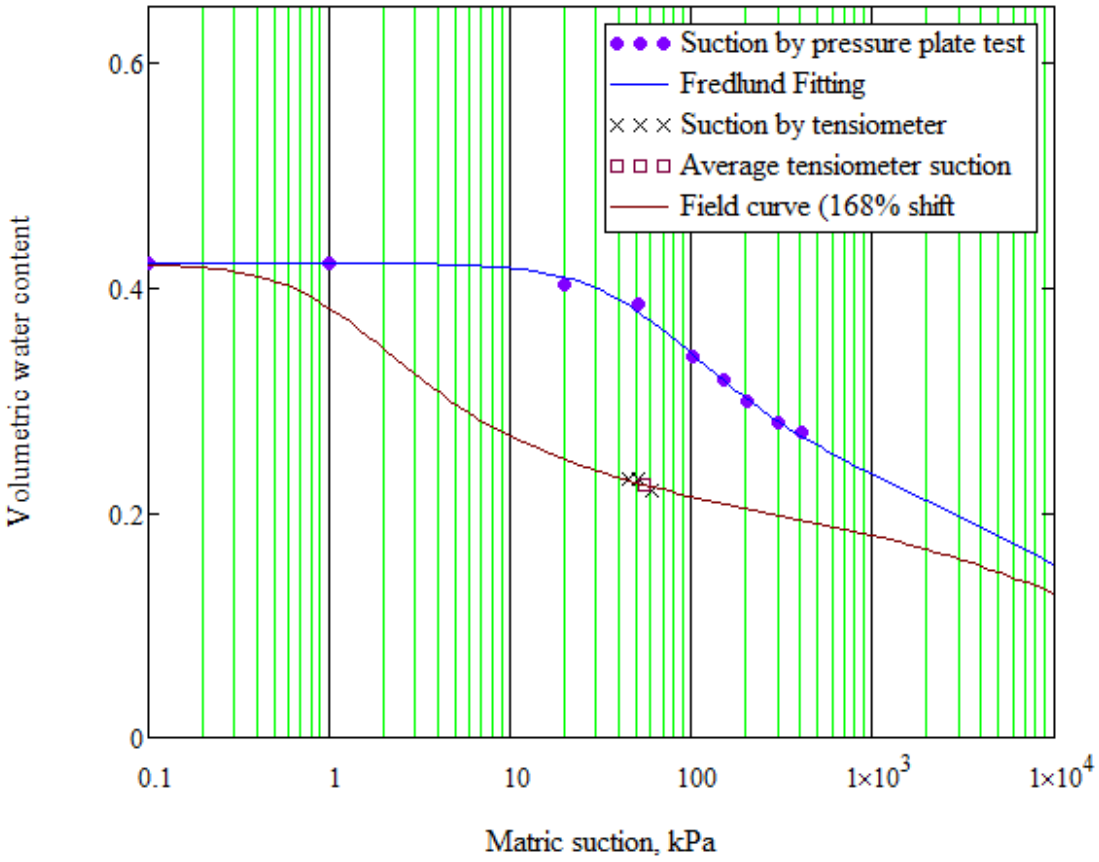

Fig. 2.20 SWCC of A-4 (ML) soil at 10 ft, ST61

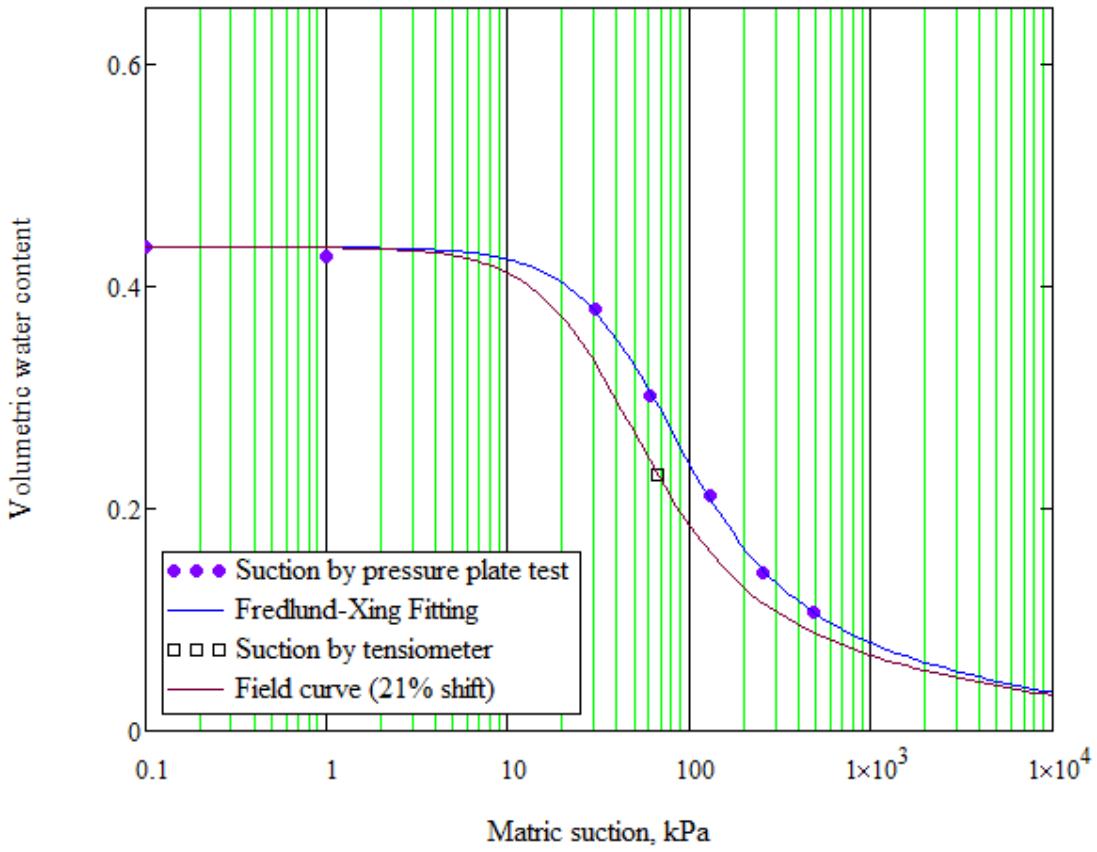

Fig. 2.21 SWCC of A-4 (ML) soil at 15 ft, ST28

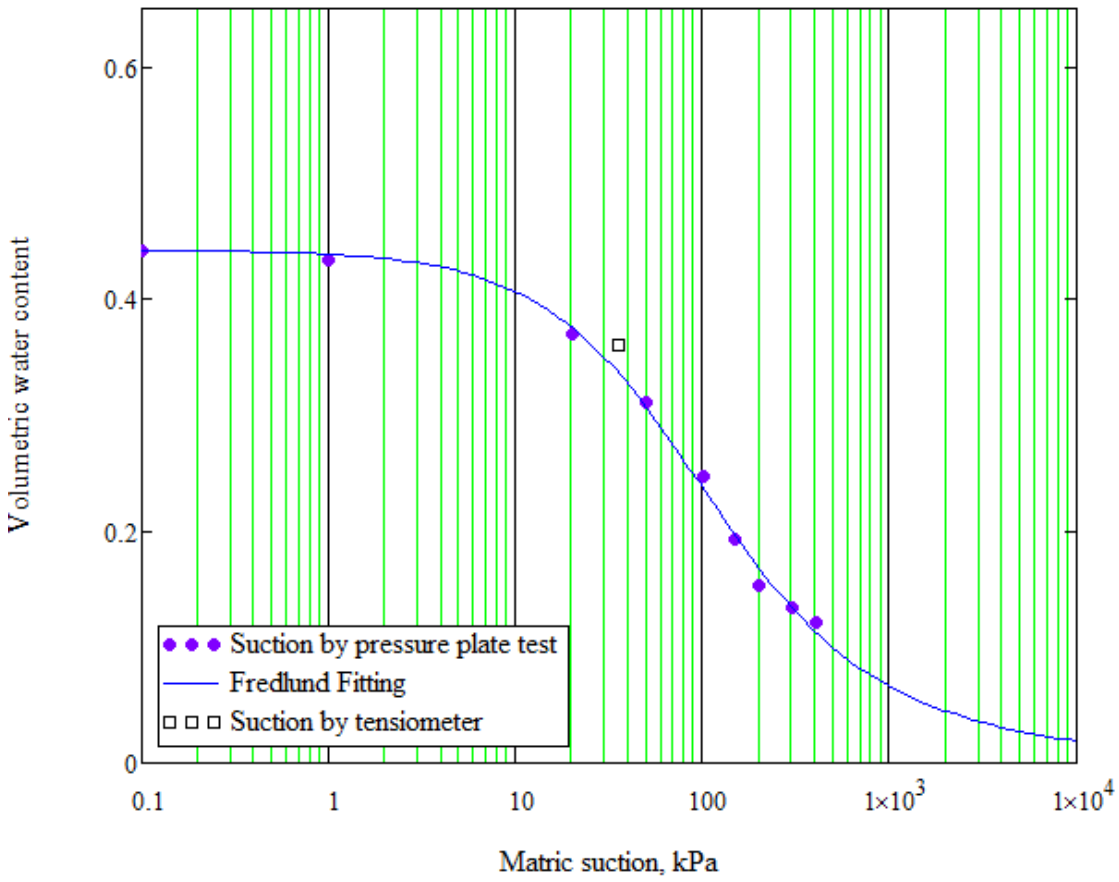

Fig. 2.22 SWCC of A-7-5 (ML) soil at 27.1 ft, ST64

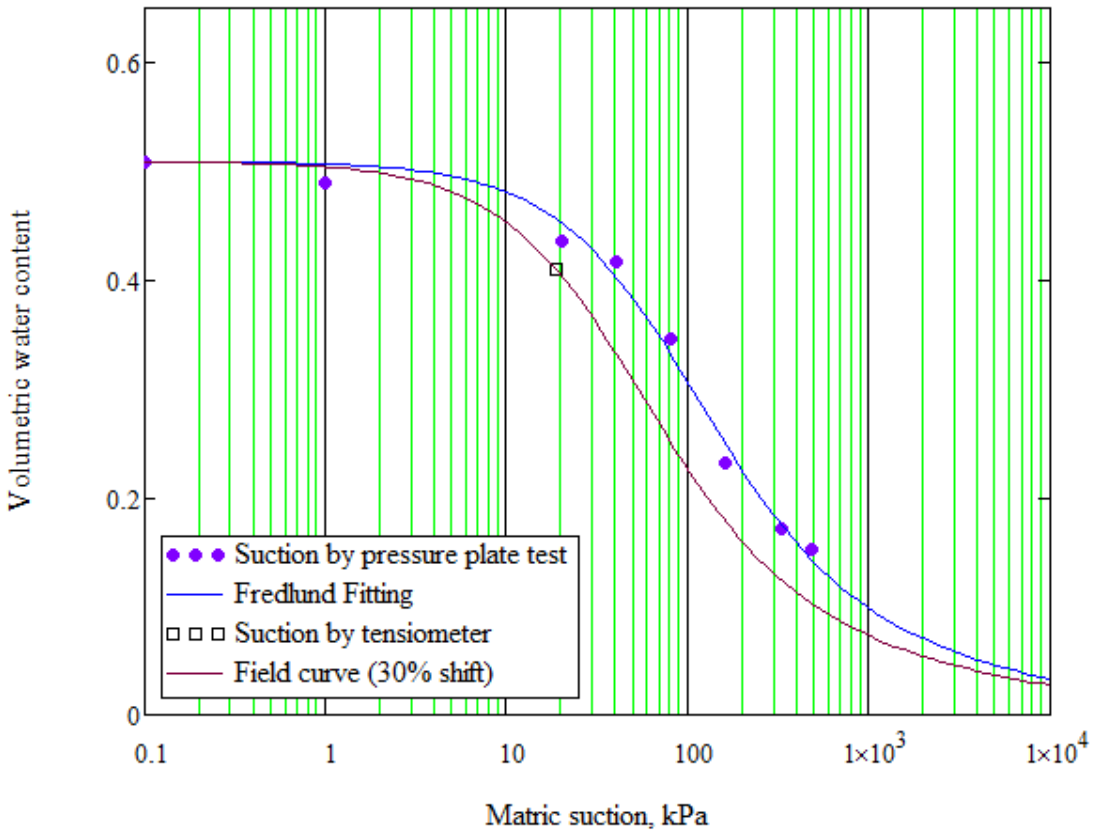

Fig. 2.23 SWCC of A-4 (ML) soil at 34.2 ft, ST32

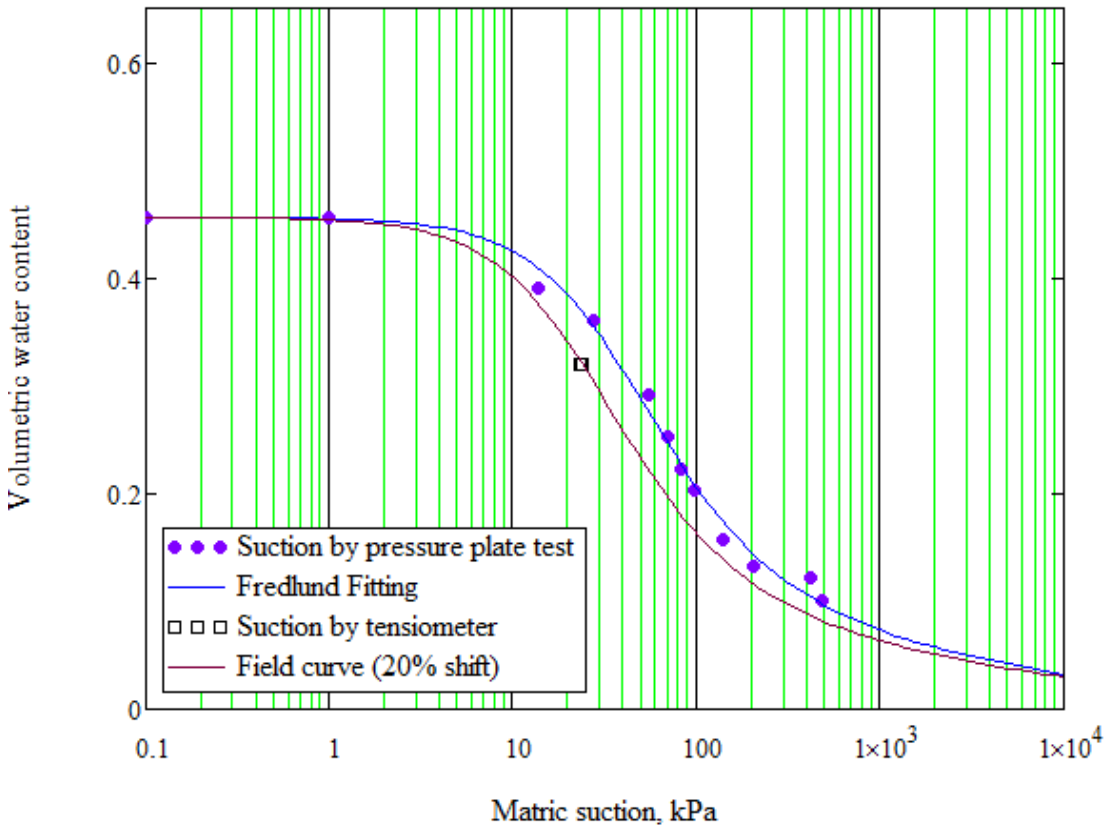

Fig. 2.24 SWCC of A-4 (ML) soil at 44.2 ft, ST79

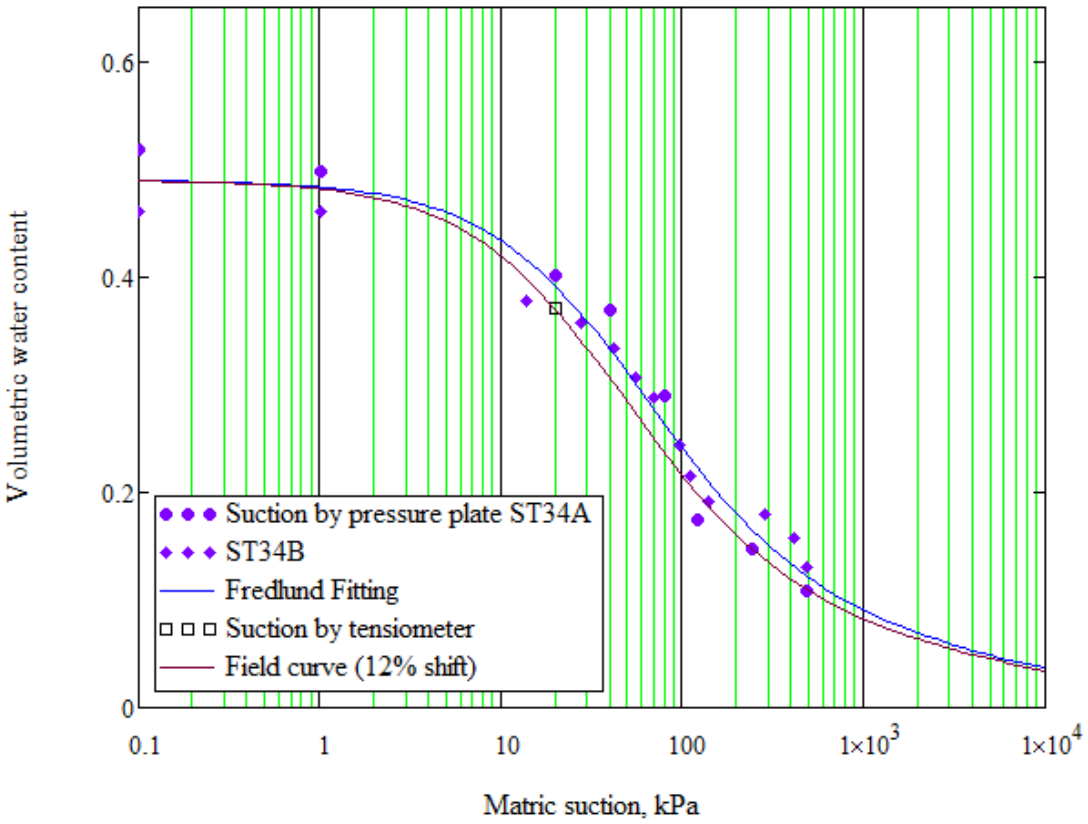

Fig. 2.25 SWCC of A-4 (ML) soil at 44.2 ft, ST34

Discussion on the SWCCs

The three Fredlund-Xing parameters, *a*, *n*, and *m* define the shape of SWCCS. If *n* and *m* remain the same, *a* parameter is related to the air-entry value and *a* value is generally higher than the air-entry value. The parameter n controls the slope of the SWCCs and m value controls the tail of the SWCCs which is the slope in the high suction range (Fredlund et al. 2012). The influence of a, n, and m parameter to the shape of the SWCCs are shown in Fig.2.26 – 2.28 after Fredlund and Xing (1994)

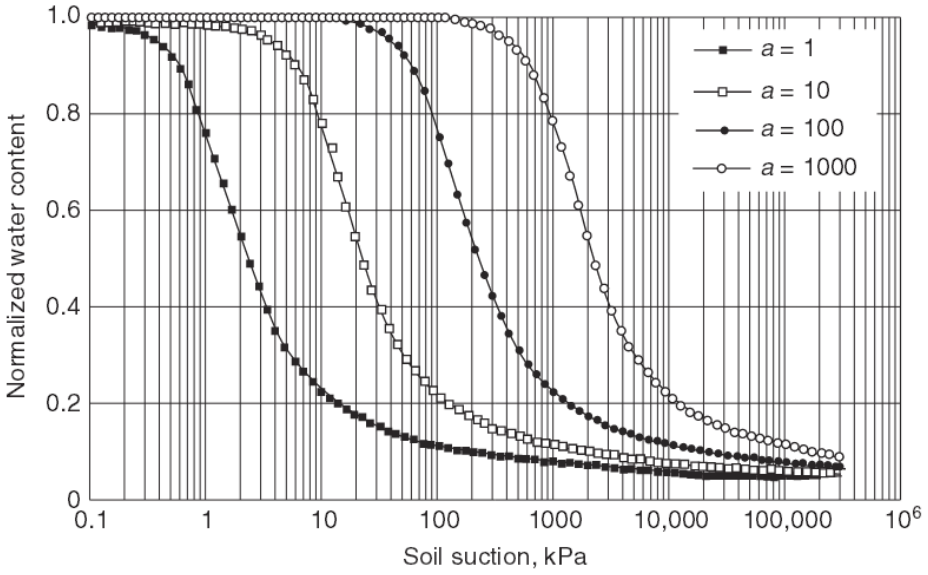

Fig. 2.26 Effect of *a* parameter on SWCC when *n*=2 and *m*=1 (after Fredlund and Xing, 1994)

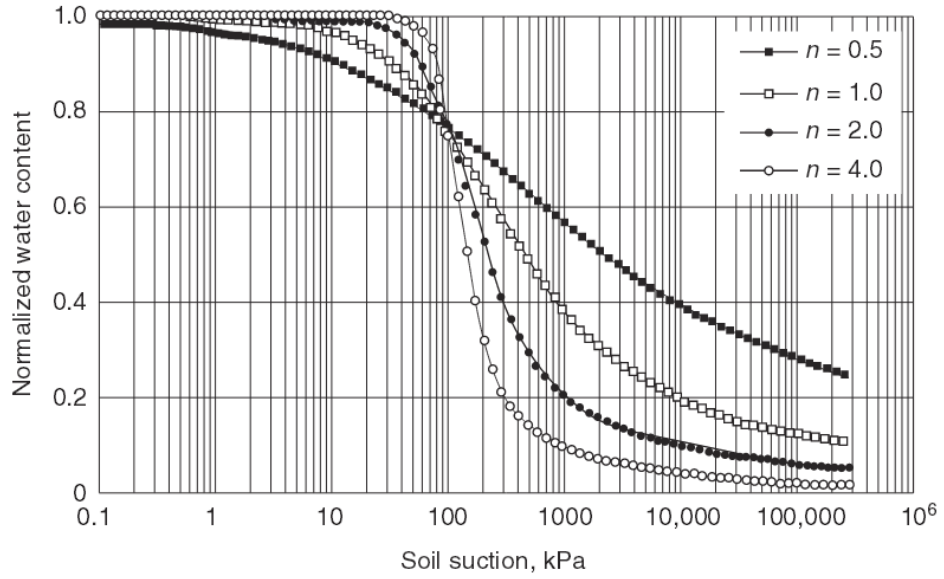

Fig. 2.27 Effect of *n* parameter on SWCC when *a*=100 and *m*=1 (after Fredlund and Xing, 1994)

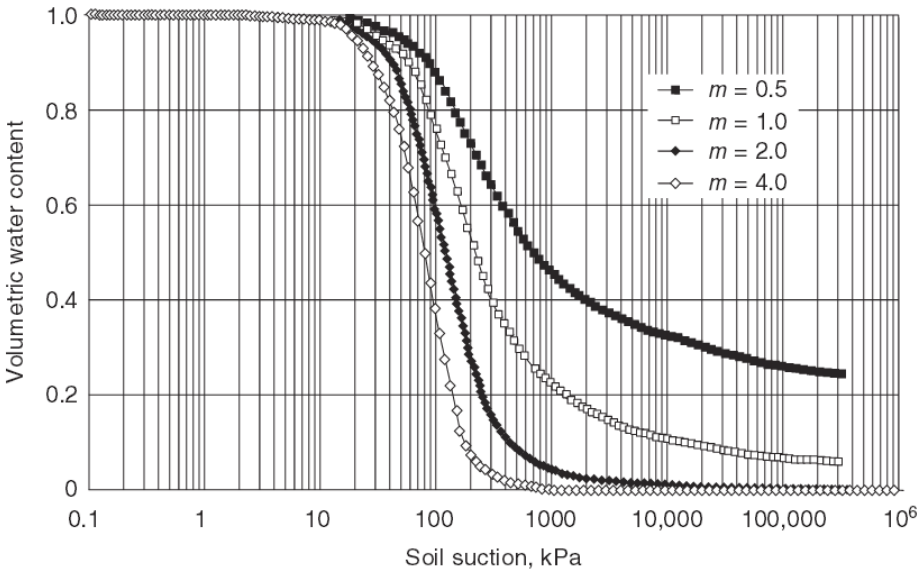

Fig. 2.28 Effect of *m* parameter on SWCC when *a*=100 and *n*=2 (after Fredlund and Xing, 1994)

The air entry values were plotted against *a* value as shown in Fig. 2.29. It is obvious that the air entry value increased with the increasing of *a* value and a value is generally larger than air entry value. This is exactly consistent with the statement from Fredlund (2012).

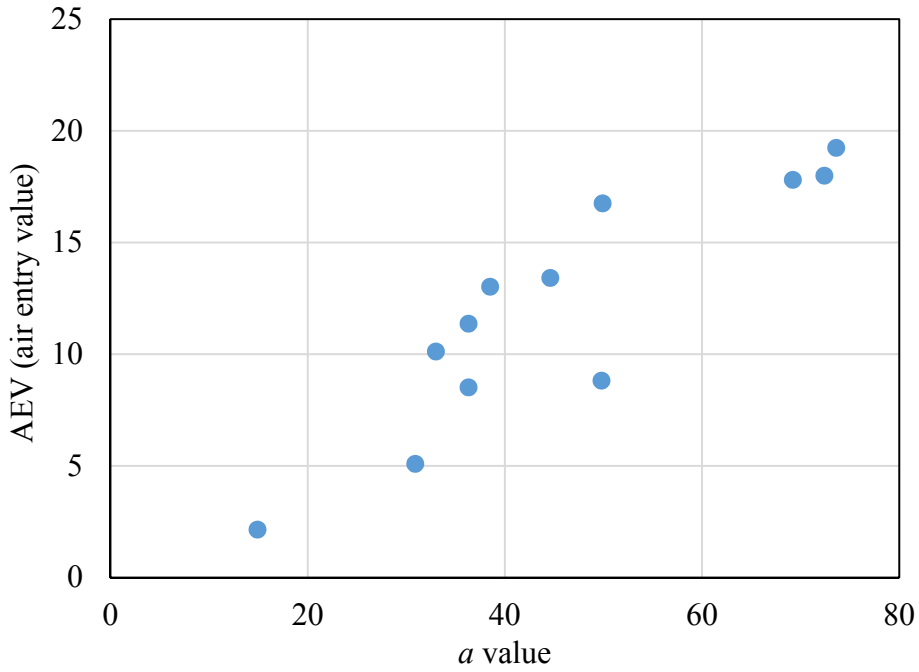

Fig. 2.29 *a* value versus air entry value

Also, m value is plotted against the clay percentage as shown in Fig. 2.30. From the figure, it was observed that *m* value decreased with the increasing clay percentage. So, if the soil is more clayey, m value will be smaller and the tail of the SWCC will get closer to the low suction range as shown in Fig. 2.29. This is also consistent with the observation from Fredlund (2012) as shown in Fig. 2.31. At the same volumetric water content, clay has higher suction than silt and sand. At the same *a* and *n* value, *m* will be smaller for clayey soil compared with sand and silty soil.

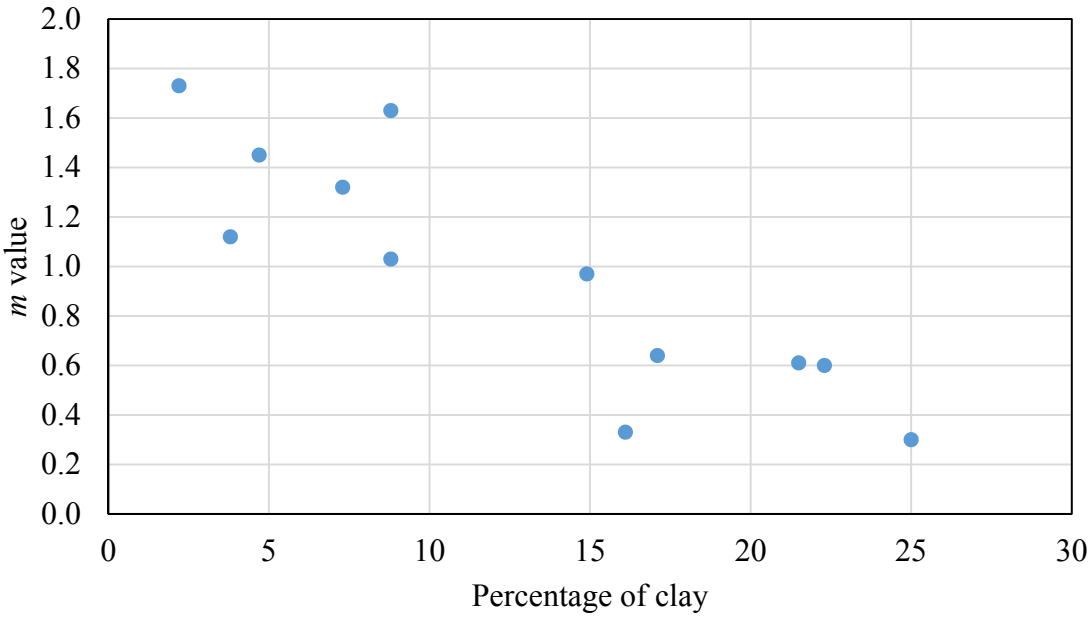

Fig. 2.30 Percentage of clay versus *m* value

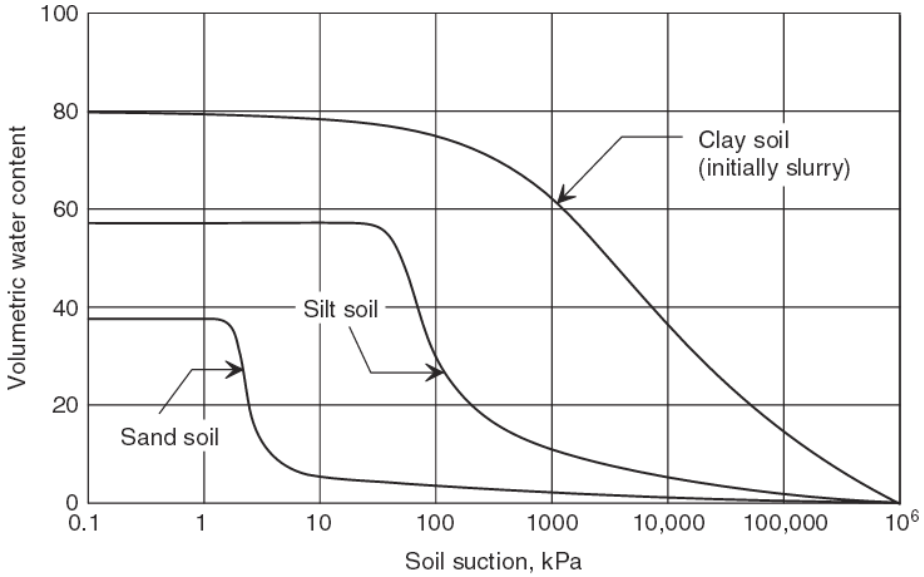

Fig. 2.31 Comparative desorption SWCCs for sand, silt, and clay soils

2.7. Field curve

A field curve concept based on the actual tensiometer suction measurements is proposed for this study. The basis for the field curve concept is the fact that the actual suction conditions in the soil are different from the suction on the drying curve due to the existing hysteresis history in the soil. Fredlund et al. (2011) recommended shifting the wetting curves, as shown in Table 2.5.

Table 2.5 Suggested Shifts of Inflection Point between Drying and Wetting Curves for Various Soils (Fredlund et al. 2011)

Soil Type	Range of Typical Shifts (% of a log cycle)	Average Shift (% of a log cycle)
Sand	15-35	25
Silt and loam	35-60	50
Clay	-	Up to 100

Based on the concept of shifting the drying curve to a certain inflection point (Fredlund et al. 2011), the wet curve can be obtained. The same concept is used here; that is, the drying curve developed from the pressure plate test is shifted to the point where the tensiometer suction measurement is taken. The shifted curve is called the 'field curve' because it actually corresponds to the natural soil suction, which is the field condition.

In order to consider the actual suction conditions in the soil, one set of optimal procedures to determine the field curve of the soil is proposed. First, the drying curve of the sample must be determined using the pressure plate test or another prediction model.

The Fredlund-Xing curve-fitting parameters then are determined. Second, the suction and water content of the natural soil are determined using the tensiometer. Then, the one-point data from the tensiometer measurements are plotted against the drying curve. Third, in order to shift the drying curve to the point where the tensiometer suction measurement was taken, a series of drying curves must be generated by reducing the *a* value in the Fredlund-Xing equation. The reduction of the *a* value can be stepwise at a rate of 5 percent. After the third step, two shifted curves that are closest to the point of the tensiometer reading can be determined. Then, in between the two chosen curves, a set of ten decomposed curves is generated. The best fit to the one-point tensiometer measurement is quantified using the least-square method. And then the field curve will be determined as shown in Fig. 2.32.

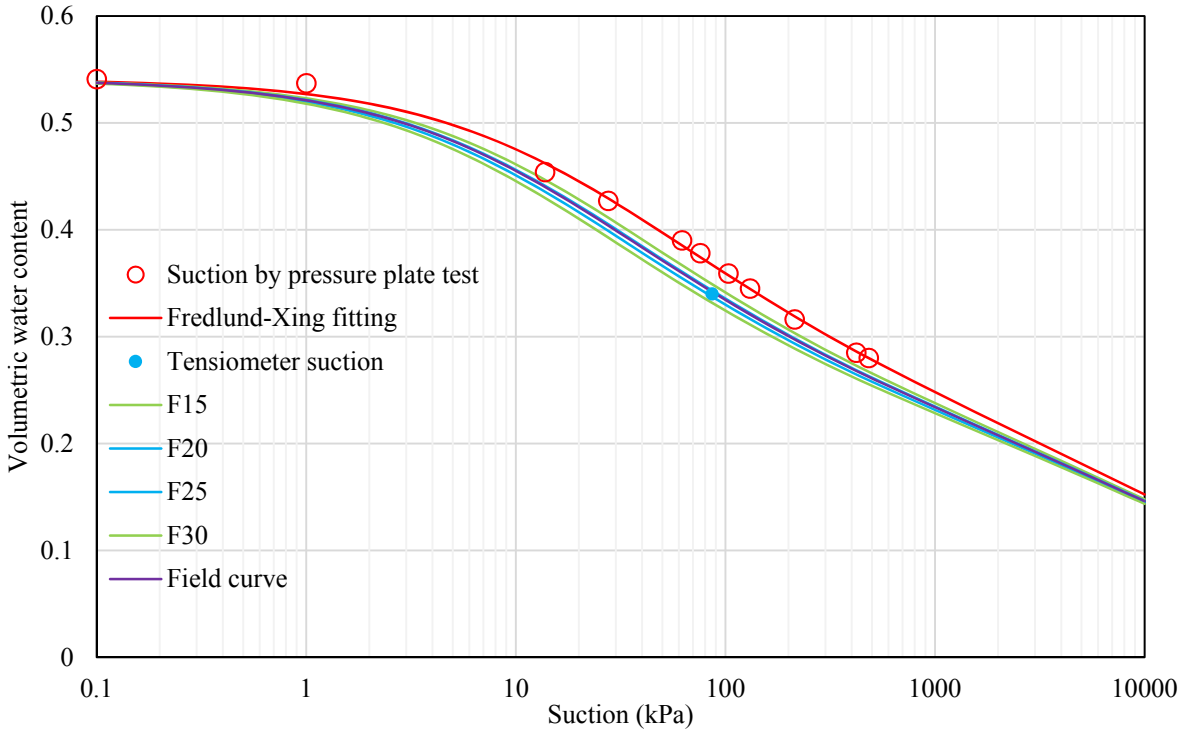

Fig. 2.32 Field curve determination

2.8. Summary and Conclusions

A comprehensive experimental program was undertaken to characterize the suction-related properties of residual soils. The matric suction of the soil was measured using different techniques: tensiometers, pressure plate method, and filter paper method. The corresponding basic soil properties, which included grain size distribution, Atterberg limits, specific gravity, natural water content, and dry density, also were investigated. The profiles of the soil properties showed reasonable results, as expected. The suction range of the soil profile was from 60 kPa to 100 kPa for the upper 30 feet of the clayey silty zone. Once the material transitioned to the sandy silty zone, the suction dropped to below 50 kPa. Based on the suction-related soil properties profiles, it can be concluded that soil type, water content, and the volume-mass relationship all affect changes in the suction profile.

The matric suction measured by the filter paper method tended to be 50% to 150% higher than that measured by the tensiometers. This discrepancy could be due to the fact that the tested material was silty soil and the contact area between the filter paper and the soil sample was not 100% ensured, which may have caused the actual measured matric suction to be a combination of both matric suction and total suction. Other reasons, such as the heterogeneity of the soil, the calibration used for the filter paper method, and the operation of the filter paper test, also could affect the results.

Compared to the filter paper method, the tensiometer is recommended as a direct suction measurement tool for future use because of its advantages of a quick response and ease of operation.

A field curve concept is implemented to adjust for the suction obtained from the drying curve. This concept is based on work by Fredlund et al. (2011) and Houston et al. (2006) who determined that the wetting curve, or the actual SWCC can be obtained by shifting the drying curve, and that the magnitude of the shift is related to the soil type. By measuring the suction of the Shelby tube samples using tensiometers, which represents the field condition of the soil, a field curve can be used to correct for the suction obtained from the drying curve.

Twelve SWCCs were obtained by pressure plate tests and the corresponding field curves were also determined by the tensiometer-measured suction. The accuracy of the measured SWCCs are supported by the observations from the published literature. The air entry values of each tested SWCC are consistent with the data of published residual soil from Rahardjo et al. (2012). For the modeling of SWCC curves, the air entry value is shown to increase with increasing *a* value and the air entry value is consistently smaller than the *a* value. For *m* value, it is shown to decrease with the increasing clay percentage (Fredlund, 2012).

3. RELIABILITY AND VARIABILITY ANALYSIS OF SUCTION MEASUREMENTS BY TENSIOMETER

3.1. Introduction

If unsaturated soil properties are to be considered in engineering design, it is very important to quantify the matric suction accurately. A tensiometer is a portable tool that can be used to measure matric suction directly. It uses a high-air-entry ceramic cup as the interface between the measuring system and the negative pore-water pressure in the soil (Fredlund et al. 2012). Also, the tensiometer is convenient to use because it can simply be inserted into the soil and is compatible with current geotechnical lab set-ups. The tensiometer suction test is a simple protocol that can be combined easily with basic soil parameter testing. For example, after the tensiometer suction reading is taken, the same piece of soil sample can be used again to determine water content.

A commercially available set of T5/T5x tensiometers was used in this study for taking the matric suction measurements. The difference between these two sensors is the measurable matric suction range. T5 is similar to other traditional tensiometers that can measure matric suction up to 100 kPa. The special version, T5x, can measure matric suction up to 160 kPa. The advantage of T5/T5x tensiometers is that their tips are small and they can provide a quick response time. Within 3 to 5 minutes by manufacture's recommendation, soil matric suction can be determined using T5/T5x sensors, which is especially useful in the field. The consistency of matric suction measurements is always an engineering concern. If multiple tensiometer tests are performed on the same samples that have the same water

content, the question is whether the same matric suction can be obtained for all the samples.

So, this study was undertaken and the objectives of this research are to: 1) study the variability of T5/T5x tensiometer suction measurements by calibrating the tensiometers using uniformly compacted soil samples, 2) provide a reliable equilibrium time for the suction measurements, and 3) Study the short term response of the tensiometer that can be used for the determination of soil suction in the field conditions.

The equilibrium time needed to obtain readings from the T5 and T5x tensiometers was studied by using uniformly compacted A-7-5 (MH) (A-7-5, in AASHTO and MH, in USCS) soil in a standard compaction mold. Tensiometer suction data were obtained using Shelby tube samples (A-7-5/MH and A-5/ML) both in the field and in the laboratory. The suction readings taken in the field were studied since the suction was within a relative short period of time that is less than equilibrium.

3.2. Background

Normally, a tensiometer can measure matric suction only up to 100 kPa due to water cavitation. However, research has been conducted to develop high-suction measurement tensiometers that can measure soil matric suction higher than 100 kPa. Some of these high-section tensiometers can measure suction up to 500 kPa (Guan and Fredlund 1997), and even to 1000 kPa (Ridley and Burland 1996). However, there is no unified response time for the different tensiometers. The time responses of tensiometers developed by different researchers are shown in Figure 3.1.

The response time of a tensiometer is controlled by different factors, such as the system's compressibility, hydraulic conductivity, thickness of the sensor tip, and the

hydraulic conductivity of the soil (Lu and Likos 2004). Also, trying to determine the suction value before the tensiometer equilibrium is established can lead to measurement errors. So, in order to obtain reliable tensiometer suction data, the response time of each tensiometer must be determined before the actual measurement is taken.

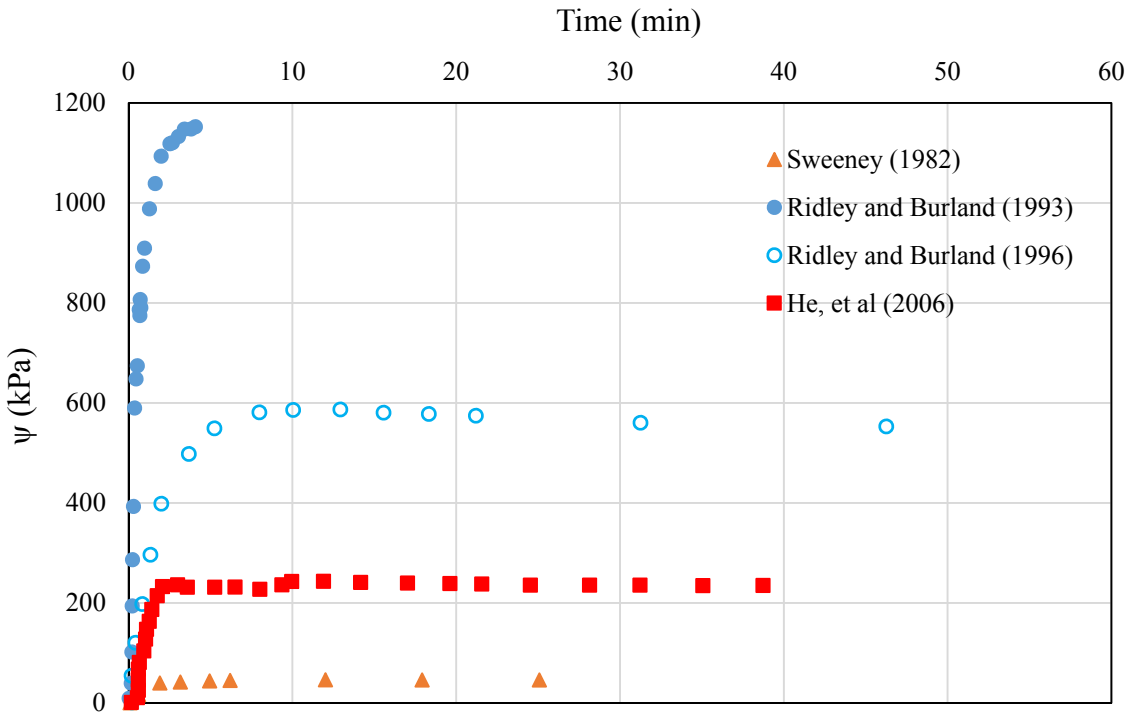

Fig. 3.1 Time responses of different tensiometers

Tensiometers have been used to test soil matric suction for different purposes and they have different response times. Sweeney (1982) used two types of commercially available tensiometers, Quick Draw and a flexible tube tensiometer for *in situ* soil suction measurements taken for Hong Kong residual soil slopes. These types are traditional

tensiometers and their maximum measurable suction is less than 85 kPa. Sweeney observed de-airing of the tensiometer while taking measurements. The response time increased with the increase in the number of readings due to the de-airing of the tensiometer.

A miniature tensiometer developed by Ridley and Burland (1993) can measure suction over 1000 kPa with a response time of less than five minutes. Under laboratory conditions, this miniature tensiometer measured 560 kPa of suction after 45 minutes. The same London clay soil was tested using the filter paper method to calibrate the tensiometer with matric suction of 490 kPa. The tensiometer suction was 15% higher than that obtained using the filter paper method (Ridley and Burland 1996). The uncertainty of this miniature tensiometer was examined by Monroy et al. (2012) and they proposed a ±7% correction to the measured suction. Another miniature tensiometer was developed and tested in a modified triaxial set-up by Meilani et al. (2002). Their results showed that the sensor could measure 100 kPa matric suction accurately and maintain the reading during the shearing process for 130 hours. He et al. (2006) developed a miniature tensiometer as well. They studied the factors that could affect the performance of the sensor in detail; these factors included pre-pressurization, the assembly procedure, pressure reversal, equilibrium time, suction sustaining time, and restoration after suction exceeding the air entry value of the ceramic disk.

The tensiometer was tested using a residual soil sample from the sedimentary Jurong Formation of Singapore. The matric suction measurements were obtained accurately and rapidly within five minutes at 250 kPa suction level.

A high initial degree of saturation is important to providing reliable tensiometer

suction measurements. Take and Bolton (2003) studied the saturation that affects the quality of suction measurements using a high-suction capacity tensiometer. They found that the initial saturation of the tensiometer is important to the quality of the results and "the stepwise pressurization process shows that poor saturation of tensiometer will limit the measurable suction and cause pressure hysteresis" (Take and Bolton 2003).

The literature indicates that most tensiometers can measure soil suction in a relatively short period of time, but the limitations of the measurement range, the cavitation of the water, and the requirement of constantly refilling and resaturating the tensiometer restrict its usage on a regular basis. However, due to developments in technology, the suction measurement range has been greatly improved. For example, the new commercially available T5 tensiometers used in this study are discussed in the following Section 3.3.

3.3. T5 and T5x Tensiometer

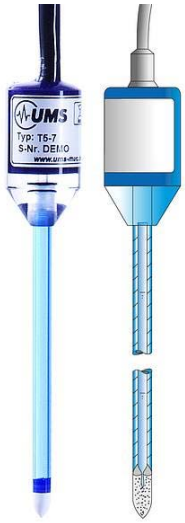

Fig. 3.2 T5 Tensiometer

The T5 Miniature Tensiometer (as shown in Fig. 3.2) is specially designed for taking punctual measurements. With an active surface of only 0.5 cm^2 and a diameter of 5 mm, the ceramic tip has all the advantages of small dimensions: little soil disturbance, punctual pick-up, and fast response. Specifications for both the T5 and the specialized T5x Miniature Tensiometer are presented in Table 3.1. Both tensiometers are used to measure matric suction by insertion directly into the soil. The range of the T5 tensiometer is from +100 kPa (pore water pressure) to -85 kPa (matric suction). The special version T5x can measure a higher range of matric suction to -160 kPa due to the finer pores of the ceramic tip of the sensor.

Table 3.1 T5 and T5x Tensiometer Specifications

Material	Acrylic glass
Shaft length	5 cm for T5(x)-5 and 10 cm T5(x)-10
Shaft diameter	5 mm
Sensor body length	3.5 cm
Sensor body diameter	20 mm
Power supply	10.6VDC/1.3mA
Accuracy	±0.5 kPa
Range	T5: +100 kPa to -85 kPa T5x: +100 kPa to -160 kPa
Advantages	Accurate zero-tension reading Fast response: With sufficient filling, the T5 responds within 5 seconds to an applied air pressure change of 0 kPa to 85 kPa. Most standard T5x reach a range of at least 160 kPa
Limitations	Not for dry soils and not frost resistant

Operation of the tensiometers (testing, precautions, and saturation)

Testing. By using the shaft to drill a hole in the soil, the sensor is installed in the predrilled hole. When the test is performed, the shaft of the sensor must not be twisted or it will loosen the connection between the shaft and the sensor body, which may cause the sensor to become desaturated or give erroneous readings.

Saturation. Before each test, the saturation condition of the sensors must be checked to ensure the accuracy of the tests. If the sensor is desaturated, air bubbles can easily be observed in the transparent shaft.

Sensor operation. The tensiometer needs to be refilled if the curve of the readings becomes flatter and/or if the maximum -85 kPa can no longer be attained. If the soil dries out and reaches the air entry value (-200 kPa for T5 and -500 kPa for T5x), the tension will decrease rapidly as air enters the cup. In order to check if the T5 requires refilling, it should be connected to a voltmeter. Then, a dry paper tissue should be wrapped around the cup to dry the ceramic surface. If the reading rises to -80 kPa within 10 seconds when the T5 tip is waved in the air, then the T5 does not require refilling.

3.4. Reading Duration of T5 and T5x Tensiometers

A calibration study was undertaken for this research to evaluate the performance of the fast-response tensiometers.

Lab set-up and description

Residual soil from Greensboro, NC was chosen as the test material. The properties of this soil are presented in Table 3.2. A detailed description of the test site and sampling is provided in the Chapter2: Wang (2014) "Characterization of suction-related soil properties of residual soils".

Table 3.2 Properties of North Carolina Residual Soil Used as Compacted Samples

Soil type	Specific Gravity	Liquid Limit	Plasticity Index	Percentage Passing #200
A-7-5 (MH)	2.77	59	19	85

The soil aggregate was carefully ground and sieved through a No. 6 sieve to ensure the homogeneity of the sample. Soil samples were stored in plastic wrap for 24 hours to reach sample equilibrium, as shown in Figure 3.3. Then, the soil was compacted in a standard compaction mold. Each compacted sample was 4 inches in diameter and 4.5 inches in height. The compaction effort was 20 blows to ensure the uniformity of the sample. The energy input was one-third the falling height for the denser samples ($\rho_d \geq 1.2$ g/cm^3) and one-twelfth the falling height for the looser samples (1.2 g/cm^3 $\geq \rho_d \geq$ 1.0 g/cm^3) using a standard proctor.

Fig. 3.3 Compacted sample preparation (mixing soil with water and wrapping for equilibrium)

Paired sensors, i.e., the T5x and T5 tensiometers, were used to test the compacted samples; the testing scheme is shown in Figure 3.4. The paired tensiometers were tested at five locations within the footprint of the mold. Ten readings were obtained. At a given specific location, the paired sensors were 2 cm apart from each other. During the testing, the top surface of each sample was sealed with plastic wrap to prevent evaporation.

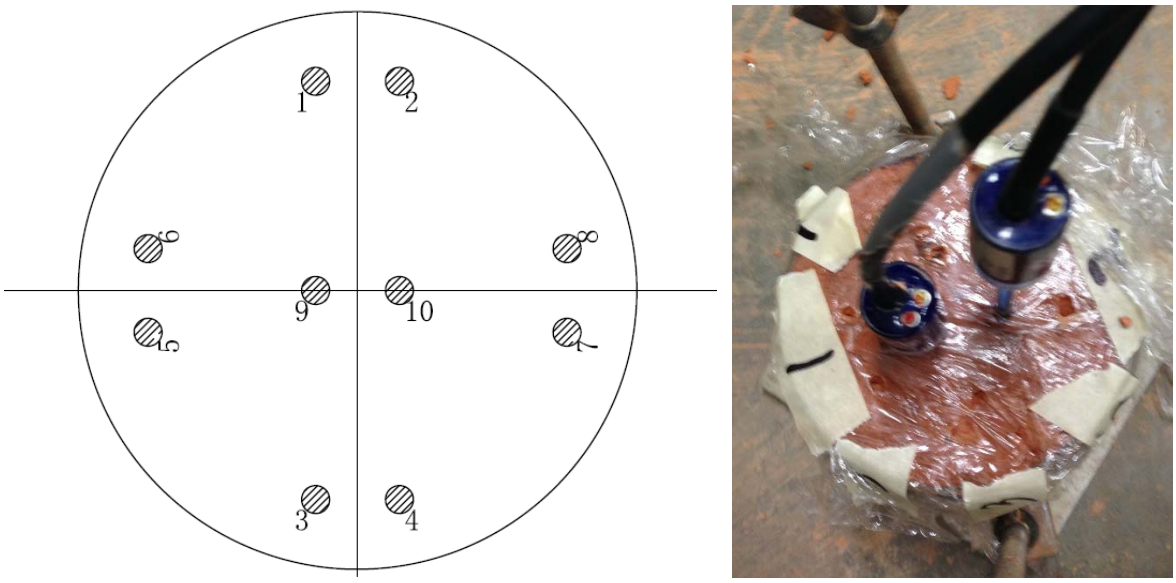

Fig. 3.4 Tensiometer test of compacted samples

Water content and suction of samples

Four soil samples were prepared at different water contents and, therefore, different suction levels, and tensiometers were inserted as described above. A detailed post-test investigation of each of the four test samples (divided into ten sub-domains) produced the water content variation shown in Table 3.3.

Table 3.3 Water Content Variation of Samples

Suction of Samples	11 kPa	23 kPa	35 kPa	68 kPa
μ (%)	36.9	31.7	30	24.4
σ (%)	0.3	0.3	0.6	0.1
COV (%)	0.8	1	2	0.6
ρ_d (g/cm^3)	1.24	1.28	1.04	1.08
S (%)	81.8	74.8	49.7	42.7
θ_w	0.46	0.41	0.31	0.26

Note:
μ: mean water content
σ: standard deviation of water content
COV: coefficient of variation of water content
ρ_d: dry density
S: degree of saturation
θ_w: volumetric water content

Compared with a reported representative coefficient of variation (COV) for water content of 22% (Diaz-Padilla and Vanmarcke 1974), the COV range in this study is 0.6~2. This range reflects a uniform sample.

3.5. Results

The suction level of each sample was determined from the equilibrium readings at 60 minutes. The tensiometer-measured suction data for the samples at 11 kPa, 23 kPa and 35 kPa, and 68 kPa were analyzed to produce the best-fit function. The best-fit curves and their respective R^2 values are shown in Figures 3.5 through 3.8.

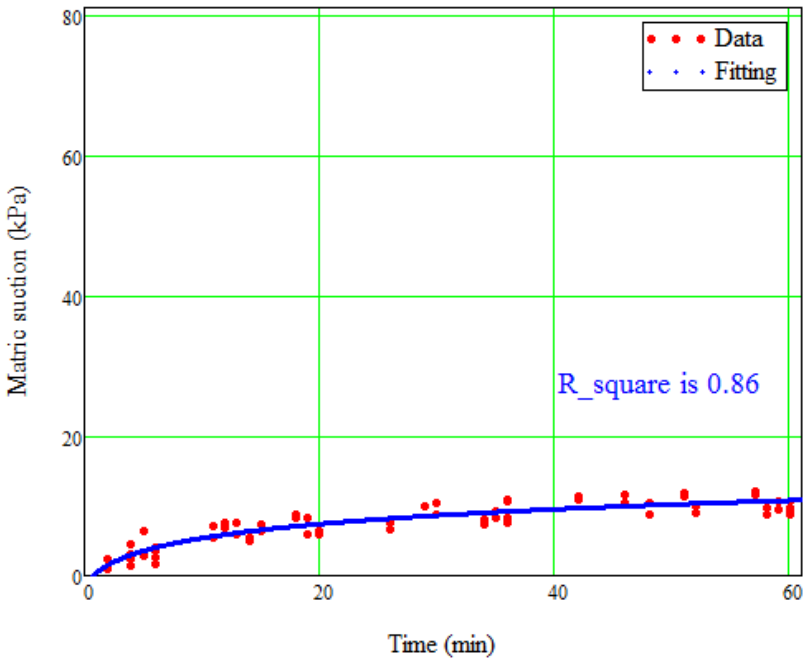

Fig. 3.5 Tensiometer test at 11 kPa suction level

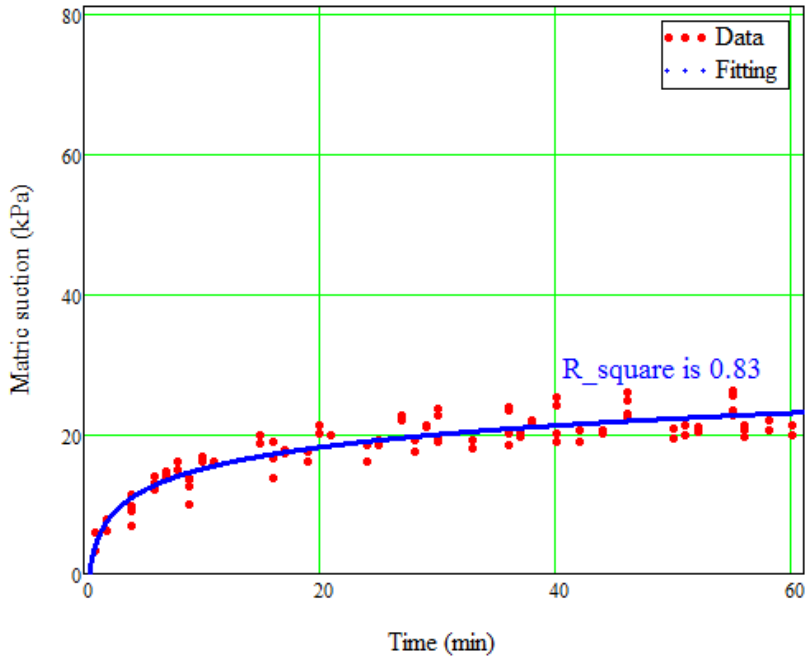

Fig. 3.6 Tensiometer test at 23 kPa suction level

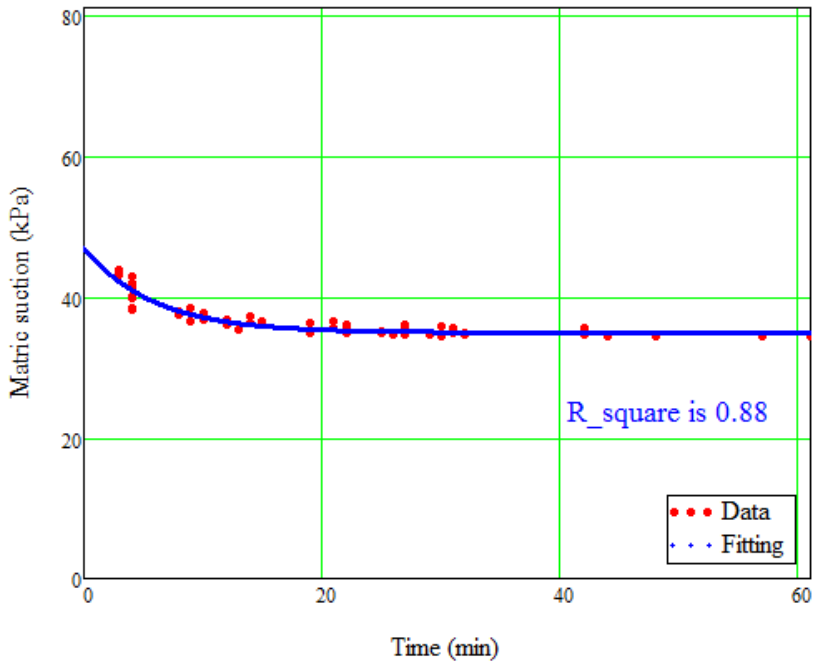

Fig. 3.7 Tensiometer test at 35 kPa suction level

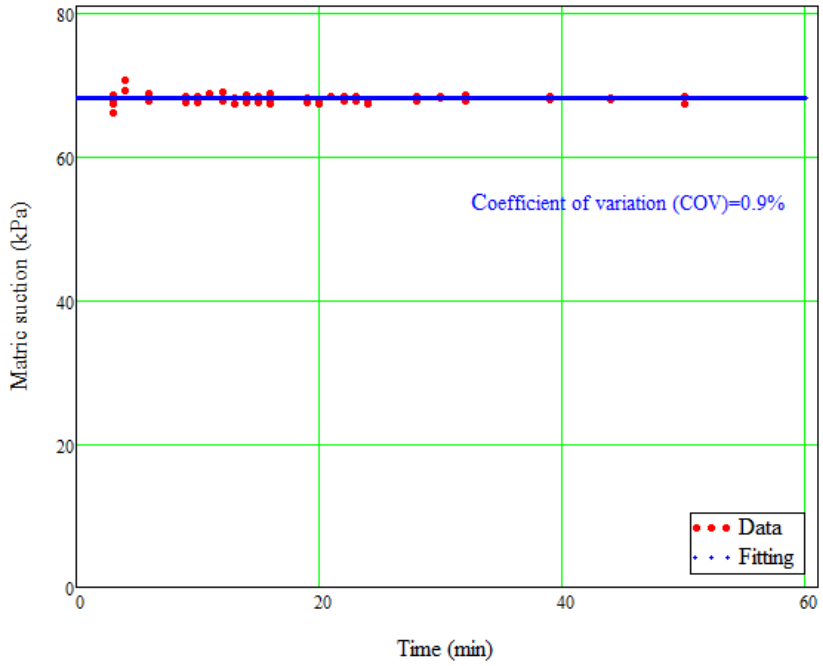

Fig. 3.8 Tensiometer test at 68 kPa suction level

Paired sensors investigation

For each suction level, the ratio between the T5 and T5x tensiometers was plotted, as presented in Figure 3.9, as a function of time. The T5/T5x ratio is seen to be within 0.89 and 1.2 after 20 minutes. The ratio between the T5 and T5x sensors seems not to be affected by the passage of time. That is, no obvious trend or pattern for the readings is evident from the two sensors. The data do not show that T5x provides consistently higher readings than T5. So, both T5 and T5x are seen to generate nearly the same matric suction values (for values lower than 70 kPa) with a COV of 15 percent.

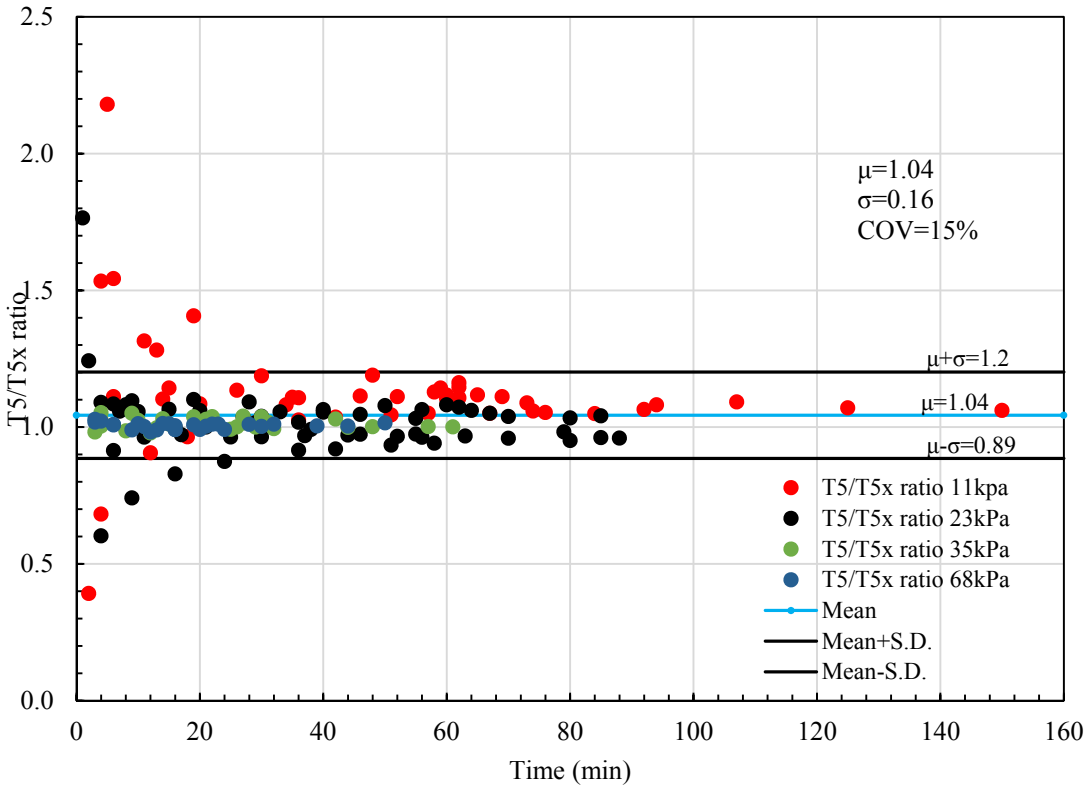

Fig. 3.9 T5/T5x ratio by passage of time

Figure 3.10 shows the same data from Figure 3.9 plotted against the suction of the T5x sensor. For suction levels higher than 20 kPa, both the T5 and T5x tensiometers still show consistent results, and the variation between the two sensors is 0.89 to 1.2. So, T5 and T5x can generate similar matric suction values at different suction levels and times.

The compacted samples indicate that the required equilibrium time can be determined as 20 minutes. For the paired T5 and T5x tensiometers, the variation is 0.89 to 1.2. It appears that neither time nor suction level affects the measuring consistency of the two sensors. One sensor is the same as the other for suction levels higher than 20 kPa and lower than 70 kPa.

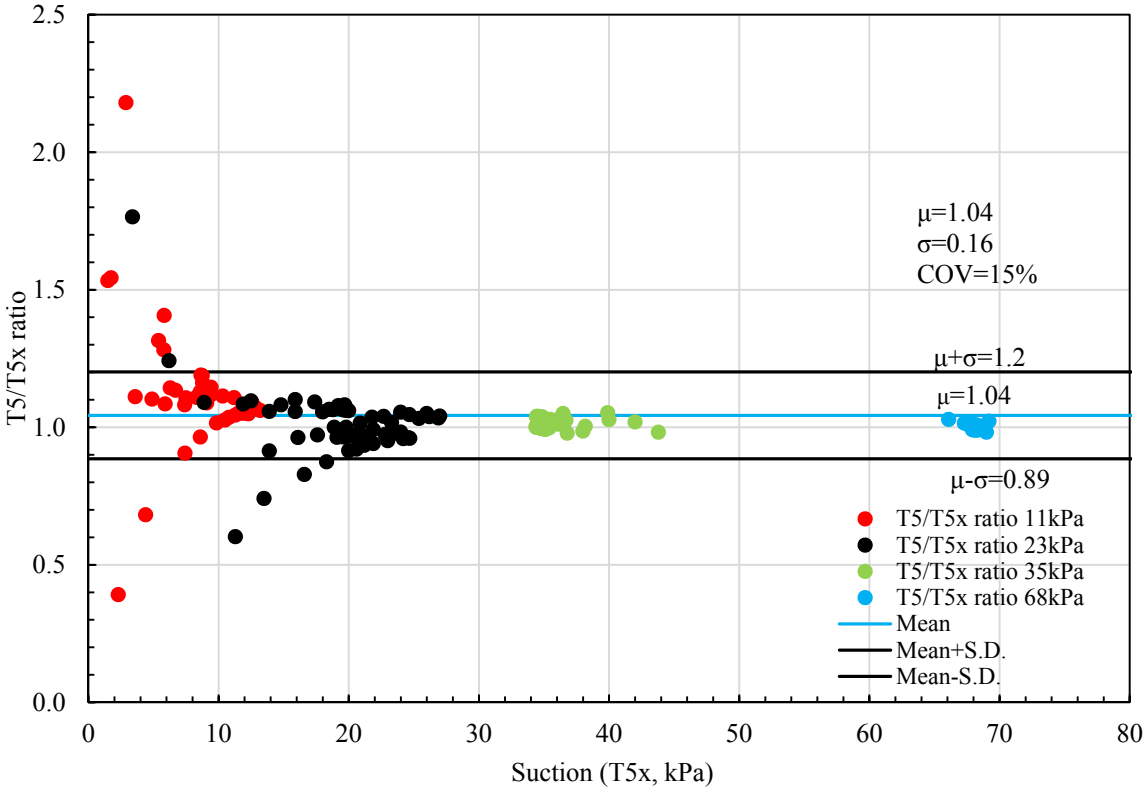

Fig. 3.10 T5/T5x ratio over suction range

Proposed test duration for matric suction determination

Table 3.4 presents the suction readings at 20 minutes and 60 minutes and the ratio of suction at 20 minutes and 60 minutes for each suction level.

Table 3.4 Measured Suction of Compacted Samples: 20 Minutes vs. 60 Minutes

Suction level (kPa)	ψ_{20min} (kPa)	ψ_{60min} (kPa)	$\psi_{20min}/\psi_{60min}$ (%)
11	7.4	10.7	68.6
23	18.1	23.0	78.6
35	35.3	34.9	101.1
68	68.0	68.0	100.0

Note: ψ_{20min}: Suction at 20 minutes
ψ_{60min}: Suction at 60 minutes

For 11 kPa and 23 kPa suction levels, $\psi_{20min}/\psi_{60min}$ are 68.6% and 78.6%, respectively. Therefore, approximately 70% of the suction at 60 minutes can be obtained at 20 minutes. At 35 kPa and 68 kPa, the 20-minute readings are basically the same as the 60-minute readings. For suction levels lower than 20 kPa (which is close to the air entry value of the A-7-5 soil), a longer time is required to reach equilibrium. Therefore, 20 minutes can be considered as a reliable time to determine the equilibrium suction for suction levels higher than 35 kPa.

3.6. Suction readings at 2min

Because suction measurements taken during the thin-walled tube sampling process in the field were obtained over a relatively short time, on the order of a few minutes (between tube extraction and wax-sealing of the tube ends), it was determined that a suction correction factor (*SCF* in figures) was necessary to predict the actual field suction.

Suction correction factor of lab-tested Shelby tube samples

In the lab, readings for both short (on the order of two minutes) and long (on the order of 20 minutes) times were obtained for the tube samples of the A-7-5 (MH) and A-4 (ML) soils. Again, in these tests, the paired sensors, as shown in Figure 3.11, were used to ensure the accuracy of the readings. The number of tube samples tested is shown in Table 3.5. The statistically determined data outliers were excluded from this analysis.

Fig. 3.11 Tensiometer testing in the laboratory

Table 3.5 Number of Samples Tested in Laboratory

Soil Type	A-7-5 (MH)	A-4 (ML)
Number of tubes tested	32	20
Outliers excluded	8	6
Number of data points used	24	14

Based on analysis of the data presented in Figure 3.12, a function for predicting the 20-minute value (believed to be the actual equilibrium value) from the 2-minute value was developed. Knowing the suction at two minutes, the ratio between ψ_{20min} and ψ_{2min} could be calculated as

$$\psi_{20min}/\psi_{2min} = 1.011 - 0.000061\psi_{2min} \tag{3.1}$$

In order to account for the variability (scatter) in the measured data, a lower-bound model, such one that has as a 95% confidence limit (Triola 1998), could be used, as shown in Equation 3.2.

$$\psi_{20min} = \psi_{2min} * \left\{1.011 - 0.000061\psi_{2min} - 0.04\left[0.042 + \frac{(\psi_{2min} - 63.8)^2}{8446}\right]^{0.5}\right\} \tag{3.2}$$

However, instead of using Equation 3.2, a simple suction correction factor of 0.99, based on the lower prediction at the mean of the data, is presented in Figure 3.12. This correction factor can provide a reasonable approximation to the more complex function. Thus, the model in Equation 3.3 can be obtained:

$$\psi_{20\text{min}MH} = 0.99\psi_{2min} \tag{3.3}$$

So, the 2min readings are essentially the same as the 20min readings.

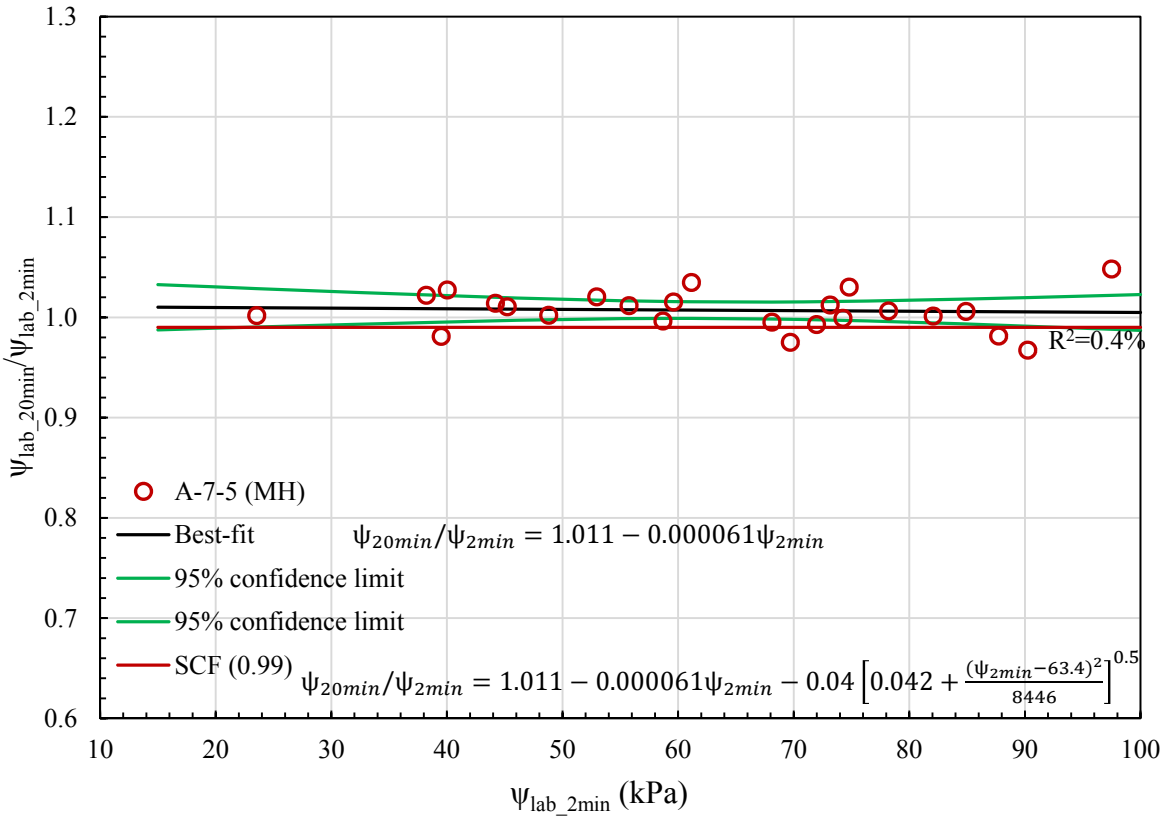

Fig. 3.12 SCF for A-7-5 (MH) soil by using best-fit function and lab tests of tube samples

The same procedures were followed using the data obtained from tests of the A-4 (ML) soil; the results are presented in Figure 3.13 and Equations 3.4, 3.5, and 3.6.

The ratio between ψ_{20min} and ψ_{2min} is

$$\psi_{20min}/\psi_{2min} = 1.052 - 0.0000483\psi_{2min} \quad (3.4)$$

The 95% confidence limit at the lower bound is

$$\psi_{20min} = \psi_{2min} * \left\{1.052 - 0.000483\psi_{2min} - 0.066\left[0.071 + \frac{(\psi_{2min} - 41.8)^2}{8518}\right]^{0.5}\right\} \quad (3.5)$$

The mean suction correction factor based on the mean of the data for the A-4 (ML) soil is

$$\psi_{20\text{min}ML} = 0.99\psi_{2min} \quad (3.6)$$

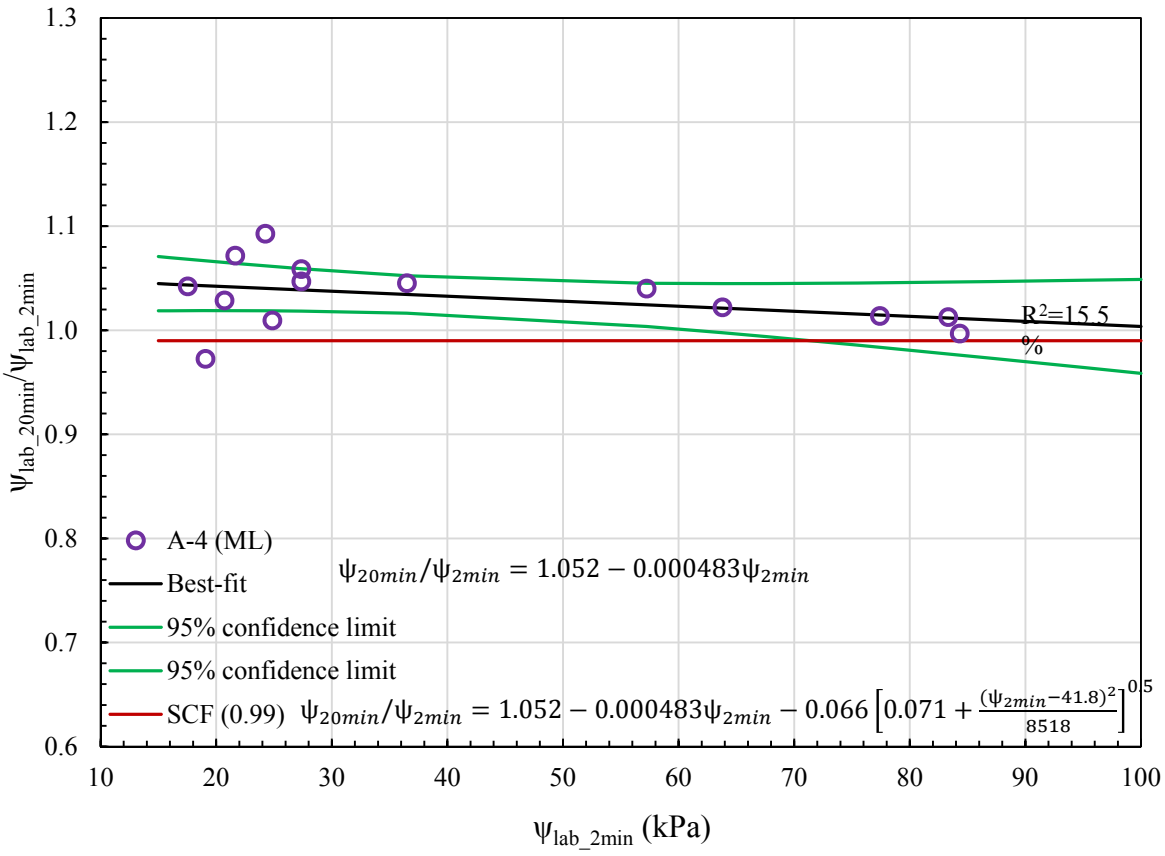

Fig. 3.13 SCF for A-4 (ML) soil by using best-fit function and lab tests of tube samples

The simplified suction correction factor for both the A-7-5 (MH) and A-4 (ML) soils is 0.99. So, for the lab-tested samples, the suction at two minutes essentially can be assumed to be the same as the suction at 20 minutes.

Suction values obtained in the field

A tensiometer also was used for the field suction measurements (Fig. 3.14). Thirty-nine field suction measurements were taken on April 17 2013, February 10 2014, and March 14 2014. The temperature on February 10 2014 was lower than zero Celsius degree, which is out of the working range of the tensiometer. The tensiometer can be used only under frost-free conditions. So, the data for February 10, 2014 were excluded. Thirty-two data points were used in this analysis.

The same group of Shelby tubes was brought back to the lab, and the suction at 20 minutes was determined under laboratory conditions. The ratios between the 20-minute suction in the lab (ψ_{lab_20min}) and the two-minute suction in the field (ψ_{field_2min}) were plotted against the 95% confidence intervals obtained from the previous lab-tested samples, as shown in Figures 3.15 and 3.16.

Fig. 3.14 Tensiometer testing in the field

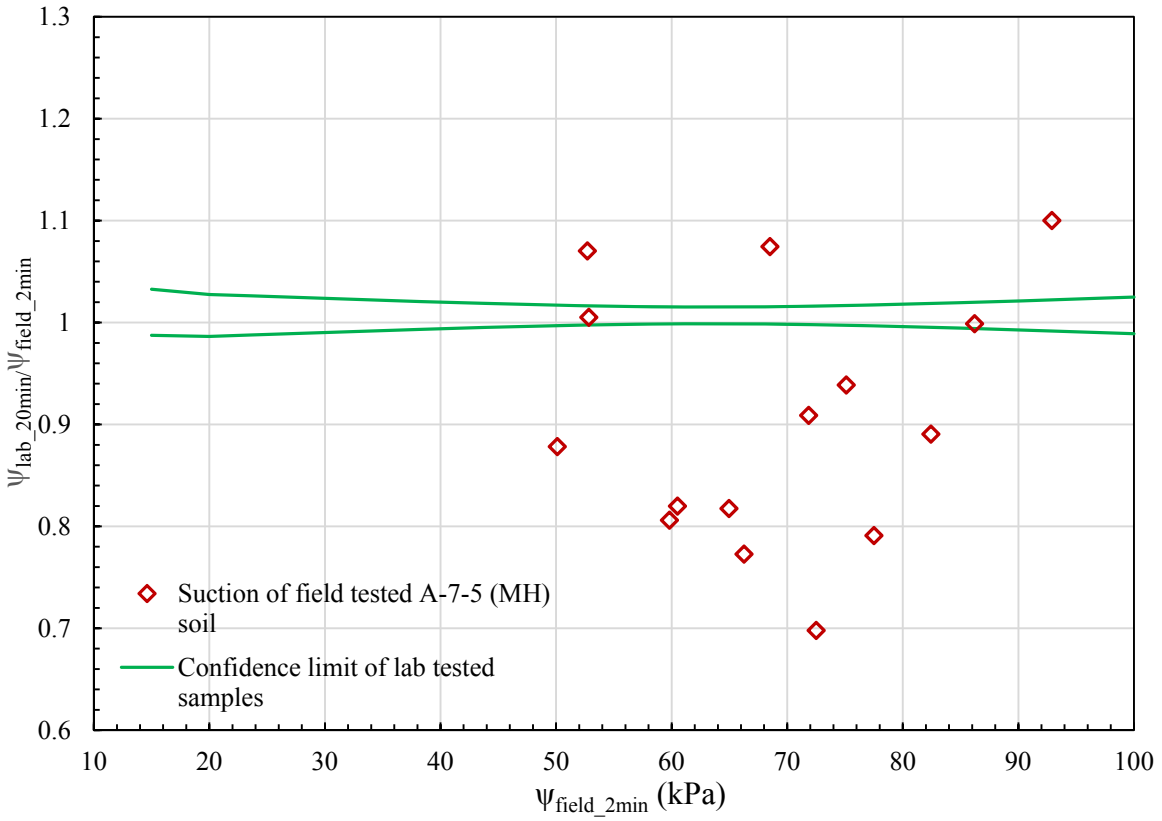

Fig. 3.15 Suction tested in the field at 2 min against confidence intervals of lab-tested A-7-5 (MH) soil

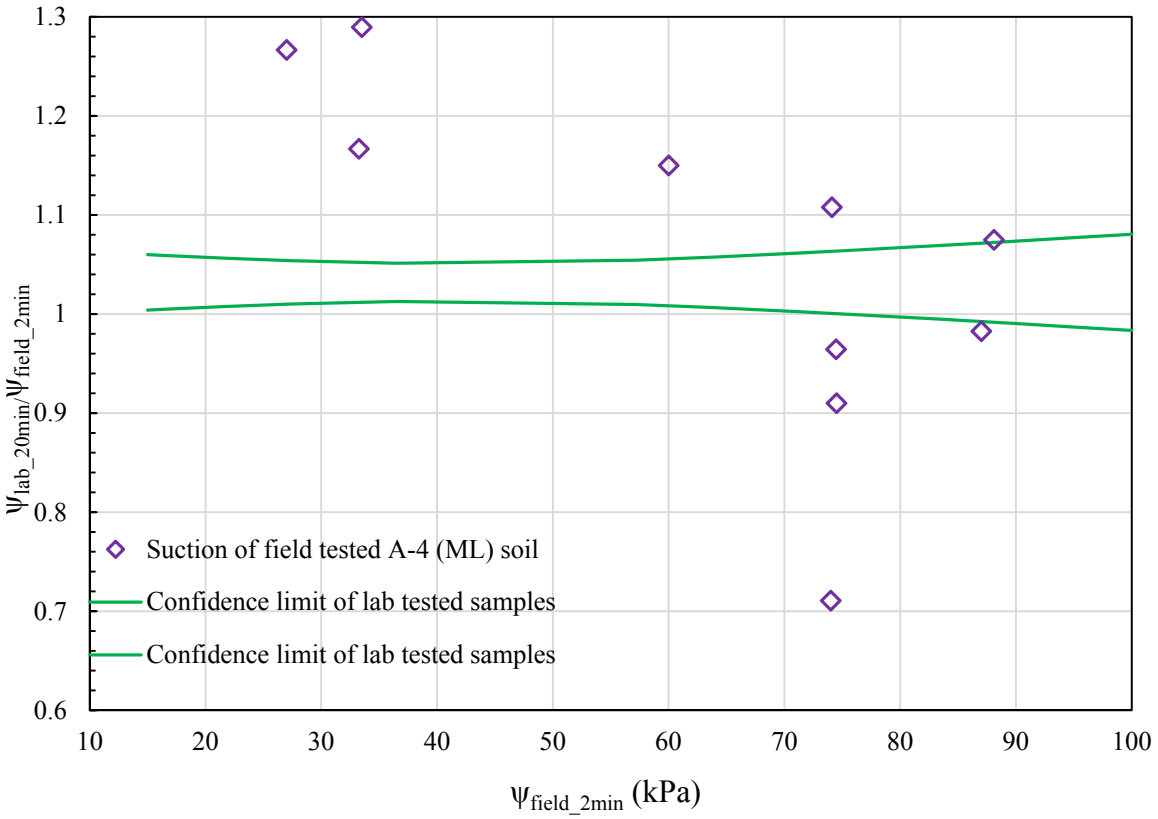

Fig. 3.16 Suction tested in the field at 2 min against confidence intervals of lab-tested A-4 (ML) soil

Figures 3.15 and 3.16 show that the 95% confidence intervals developed from the lab tests do not fit the field-tested soils particularly well. The suction values determined in the field show more variability than those determined under laboratory conditions.

The reasons for the field readings having more variability may be because the field suction readings were taken before the samples reached equilibrium. The field suction by the tensiometers was taken during the thin-walled tube sampling process in the field which is over a relatively short time. But in the laboratory condition, the sample has been staying for several days and the Shelby tube samples have already reached equilibrium and the

tensiometer readings taken in the lab can reach equilibrium in a relatively short period of time compared with the field condition. Fig. 3.17 shows the different equilibrium time for the tensiometer suction.taken in the field and lab.

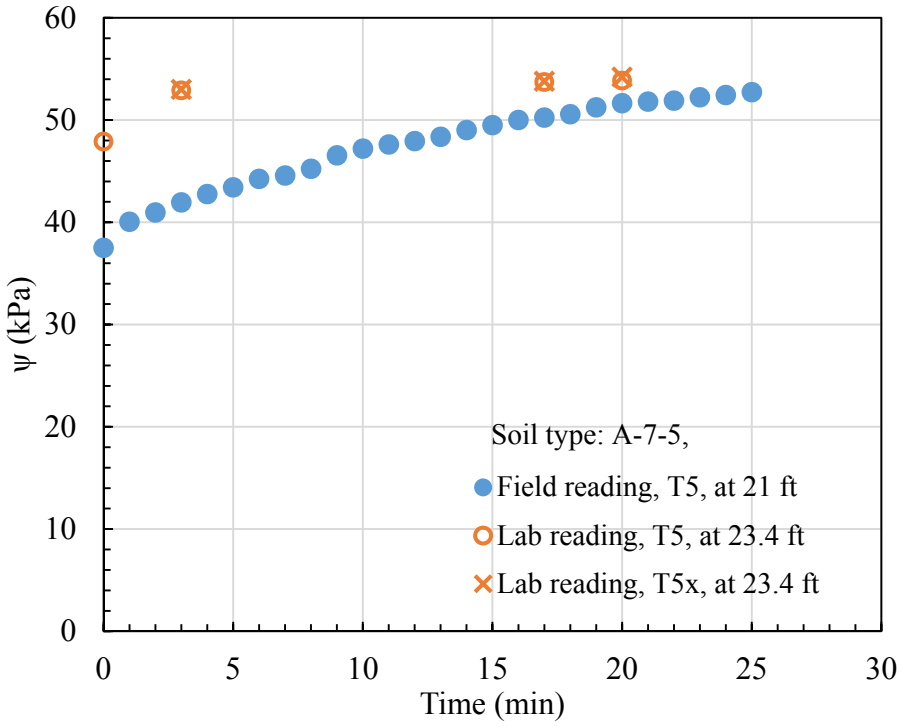

Fig. 3.17 Equilibrium time for the suction by tensiometer in lab and field conditions

The field tested sample reached 52 kPa after 25 min. But for the same type of sample at the same depth and suction level, the suction reading reached 52 kPa at 3 minutes. This is consistent with the results from the compacted sample that at the same suction level, the sample can reach equilibrium within 5 minutes. So, for the tensiometer tests performed at the field, it may requires certain amount of time for the sample to reach equilibrium state.

3.7. Conclusions

Commercially available paired T5 and T5x tensiometers were used in this study for obtaining suction measurements due to their advantages of creating little soil disturbance and offering punctual pick-up and fast responses. The reliability and variability of the paired T5 and T5x tensiometers were investigated using relatively uniformly compacted soil samples at four different suction levels: 11 kPa, 22 kPa, 35 kPa, and 68 kPa. Because suction measurements that were taken during the thin-walled tube sampling process in the field were obtained over a relatively short time, the short-term readings, which were the readings obtained after a two-minute duration, were examined under both laboratory and field conditions. Certain suction correction factors are proposed based on statistical analysis.

The following conclusions were drawn from this tensiometer study:

1. Twenty minutes is a reasonable duration for obtaining reliable suction readings.
2. The paired sensors, T5 and T5x, can provide consistent results for suction tests. No obvious trends were found between the readings from these two types of sensors. Likewise, no time or suction effects were observed regarding measurement consistency for the two sensors. The two types of sensors, T5 and T5x, can be treated as independent sensors for suction levels that are higher than 20 kPa and lower than 70 kPa.
3. Under laboratory conditions, two minutes of suction appears to provide a reliable estimate for the 20-minute suction value.
4. T5 and T5x tensiometers can be used as reliable tools to measure soil suction.

4. SUCTION PREDICTION MODEL FOR RESIDUAL SOILS

4.1. Introduction

The soil water characteristic curve (SWCC) expresses the relationship between the volumetric water content and matric suction. The SWCC provides basic information for obtaining other unsaturated soil properties, shear strength (Vanapalli et al. 1996), and permeability (Mualem 1976). Typically, SWCCs are obtained using the pressure plate test, but this test is time-consuming. For each data point on the SWCC, at least 48 hours of soil water equilibrium is required by ASTM D6836. Moreover, the equilibrium time is expected to be longer for some high plasticity clay due to the clay's low permeability. So, from a practical point of view, when considering soil suction in engineering design, it is necessary to construct an empirical correlation between routinely tested basic soil indices, i.e., grain size distribution, Atterberg limits, etc., and the SWCC. Knowing the established correlation, and without the need for the time-consuming pressure plate test, the suction values can be extrapolated based on a predicted SWCC.

The objectives of this study are to: 1) study the unsaturated residual soil properties by determining SWCCs, 2) test the predictive ability of the current existing suction prediction models, 3) investigate the effects of basic soil properties on soil suction via statistical analysis, and 4) propose a new model based on the unsaturated properties of residual soils using multivariate analysis.

4.2. Background

In soil science, the SWCC is also called the *soil water retention curve* (SWRC). This

curve is used routinely to check soil water storage and soil permeability. In geotechnical engineering applications, such as the design of dams, landfills, and pavement, permeability and soil water potential is important to the design and therefore requires soil water relationships, as expressed by SWCCs. The curves typically are tested using an axis translation technique. Under natural conditions, the atmosphere pressure is constant. The soil water potential is changed by the fluctuation of the water content, which normally is induced by rainfall or air-drying. For the actual measurement of SWCCs, by using the axis translation technique, the applied air pressure on top of the soil is controlled and changed. Due to changes in the applied air pressure, the water content in the soil sample will decrease (expressed as a desorption curve) or increase (adsorption curve). Normally, the desorption curve, or drying curve, can be derived using a pressure plate extractor, or pressure membrane. The adsorption curve can be derived from hanging column tests (ASTM D6836).

In order to apply SWCCs to numerical simulations, an integral function must be used. So, a reasonable curve-fitting equation must be applied to the laboratory data. Two main SWCC curve-fitting models are widely used and are known as the Van Genutchen and Fredlund-Xing models.

Van Genuchten (1980) proposed a closed form to describe a soil water retention curve, which is commonly used in soil science.

$$\theta = \theta_r + \frac{(\theta_s - \theta_r)}{[1 + (a\psi)^n]^m} \tag{4.1}$$

where

$$m = 1 - {}^{1}/_{n}$$

Similar to the form of the Van Genuchten model, Fredlund and Xing (1994) proposed a general form of the SWCC best-fit function:

$$\theta(\psi, a, n, m) = C(\psi) \frac{\theta_s}{\left\{ln\left[e + \left(\psi/a\right)^n\right]\right\}^m} \tag{4.2}$$

where $C(\psi)$ is a correction function defined as

$$C(\psi) = \frac{\ln(1 + \psi/\psi_r)}{\ln\left[1 + \left(10^6/\psi_r\right)\right]}$$

This equation can fit the entire suction range from 0 kPa to 10^6 kPa reasonably well. In this equation, *a* is related to the air entry value, *n* reflects the slope of the curve, and *m* represents the slope of the curve within the high-suction range.

Leong and Rahardjo (1997) reviewed both of these models for describing SWCCs and found that both the Van Genutchen and Fredlund-Xing models provide good fitness for SWCCs compared to other curve-fitting models. Zapata et al. (2000) showed that the Fredlund-Xing curve-fitting model gives the best fitting results compared with other curve-fitting functions. Sillers and Fredlund (2001) used the so-called Akaike Information Criterion to compare the fitness of different SWCC fitting models, and Fredlund and Xing (1994) presented the lowest number of the Akaike Information Criterion, which means that the Fredlund-Xing equation provides the best fit for experimental data when compared with other models. Regardless of the method or test set-up that is used to determine SWCCs, it is generally a time-consuming process due to the low permeability of the soil and slow soil-water equilibrium process. Practical engineers are always inclined to use easily-accessible soil parameters to correlate with other more complex soil properties, so a faster and efficient model is needed.

Matric suction is determined by the surface tension at the soil-water interface, so it is related directly to the pore size distribution of the soil. The pore size distribution is linked to the grain size distribution. Based on these linkages, numerous research studies have been conducted using basic soil properties, such as grain size distribution, to predict SWCCs. In soil science areas, the predictions of SWCCs or SWRCs based on soil properties are called pedo-transfer functions, which are predictive functions of certain properties using data from soil surveys (Bouma 1989). These prediction methods can be separated into the following three categories. These categories also have been addressed by Cornelis et al. (2001), Johari et al. (2006), Zapata et al. (2000) and Fredlund et al. (2012).

The three prediction approaches are:

1. Direct correlation between volumetric water content and matric suction using basic soil properties and statistical regression analysis.
2. Empirical correlation between basic soil properties (grain size distribution, Atterberg limits, etc.) and SWCC fitting parameters.
3. Conceptual physical model with correlation between grain size and SWCC.

First approach: Empirical correlation between measured suction and soil properties

Gupta and Larson (1979) developed a model based on the SWRC of 43 soils. They correlated the volumetric water content of each soil at a certain matric suction level with different soil properties using multivariate regression. The form of the equation is

$$\theta_p = a \times (\%\text{sand}) + b \times (\%\text{silt}) + c \times (\%\text{clay}) + d \times (\%\text{organic matter}) + e \times \text{bulk density } (g/cm^3) \quad (4.3)$$

where θ_p is the predicted volumetric water content at a given matric suction, and *a*, *b*, *c*, *d* and *e* are the regression coefficients. The twelve given matric suction values range from 0.04 bar to 15 bars.

Rawls et al. (1982) used data from 1,323 soils and generated an equation similar to that of Gupta and Larson (1979), but they included two more components: volumetric water content at 0.33 bar and 15 bars.

$$\theta_p = a + b \times (\%\text{sand}) + c \times (\%\text{silt}) + d \times (\%\text{clay}) + e \times (\%\text{organic matter}) + f \times \text{bulk density}\left(\frac{g}{cm^3}\right) + g \times 0.33 \text{ bar moisture}\left(\frac{cm^3}{cm^3}\right) + h \times 15 \text{ bar moisture}\left(\frac{cm^3}{cm^3}\right) \quad (4.4)$$

Second approach: Correlation between soil properties and SWCC parameters

This second approach uses the soil properties to correlate the curve-fitting parameters of SWCCs.

Saxton et al. (1986) proposed a generalized form of a function to estimate soil potential using the volumetric water content and soil texture as a percentage clay and sand. The relationship between the soil water and its potential is continuous and nonlinear from 10 kPa to 1500 kPa, is linear from 10 kPa to the air entry value, and is constant below the air entry potential. The equations are:

From 10 kPa to 1500 kPa:

$$\psi = A\theta^B \quad (4.5)$$

$$A = \exp[-4.396 - 0.0715 * (\%\text{clay}) - 4.88 \times 10^{-4} * (\%\text{sand})^2 - 4.285 \times 10^{-5} * (\%\text{sand})^2 * (\%\text{clay})] * 100.0 \quad (4.6)$$

$$B = -3.14 - 0.00222 * (\%\text{clay})^2 - 3.484 \times 10^{-5} * (\%\text{sand})^2 * (\%\text{clay}) \quad (4.7)$$

From 10 to ψ_e (air entry value):

$$\psi = 10.0 - (\theta - \theta_{10})(10.0 - \psi_e)/(\theta_s - \theta_{10}) \quad (4.8)$$

$$\theta_{10} = \exp[(2.302 - \ln A)/B] \quad (4.9)$$

$$\psi_e = 100.0 * [-0.108 + 0.341 * \theta_s] \quad (4.10)$$

$$\theta_s = 0.332 - 7.251 \times 10^{-4} * (\%\text{sand}) + 0.1276 * \log_{10}(\%\text{clay}) \quad (4.11)$$

From ψ_e to 0.0:

$$\theta = \theta_s \quad (4.12)$$

Vereecken et al. (1989) proposed a model to estimate the soil moisture retention curve from the soil's texture, bulk density, and carbon content. Scheinost et al. (1997) proposed a new pedo-transfer function to correlate the Van Genuchten (1980) curve-fitting parameters, *a*, *n*, θ_s and θ_r. For *a* and *n*, the geometric mean particle diameters were used as the regression variables, and for θ_s and θr, the prediction correlation from Vereecken et al. (1989) was used. Compared with Vereecken's model, this newer model of Scheinost et al. improved the prediction substantially, and the average error was reduced by twice.

Cornelis et al. (2001) evaluated nine pedo-transfer functions and found that the Vereecken model provided the most accurate results. Zapata et al. (2000) investigated the variability of measured SWCCs and found that the variability of SWCCs caused by different operators can lead to significant differences. Zapata et al. (2000) also found that the variation can be 47% in the low-suction range (air entry region) for sandy material, 55% for silty material, and 54% for clayey material. The soil suction values and SWCCs could not be

obtained with precision due to the variability inherent of suction testing. She also proposed a model that can predict SWCCs based on soil index properties. In this model, the Fredlund-Xing SWCC parameter can be correlated to D60 for non-plastic soil (PI = 0) and wPI, the product of the percentage of soil finer than the #200 sieve (0.075 mm) and the PI for plastic soil (PI > 0). The database used is from the SoilVison program, which is embedded with the published data.

The equations for plastic soil (PI > 0) by Zapata et al. (2000) are:

$$\mathrm{a} = 0.00364(wPI)^{3.35} + 4(wPI) + 11 \tag{4.13}$$

$$\frac{n}{m} = -2.313(wPI)^{0.14} + 5 \tag{4.14}$$

$$\mathrm{m} = 0.0514(wPI)^{0.465} + 0.5 \tag{4.15}$$

$$\frac{\psi_r}{a} = 32.44e^{0.0186(wPI)} \tag{4.16}$$

Perera et al. (2005) improved the Zapata et al. (2000) model and proposed a revised model by including more pressure plate tests. The new model improved the Zapata (2000) model errors from 88.5% to 8.6% for non-plastic soils and 20.4% to 0.1% for plastic soils. This model also was included in work by Zapata and Houston (2008).

The equations (for plastic soil) are:

$$a = 32.835[\ln(wPI)] + 32.438 \tag{4.17}$$

$$\mathrm{b} = 1.421(wPI)^{-0.3185} \tag{4.18}$$

$$\mathrm{c} = -0.2154[\ln(wPI)] + 0.7245 \tag{4.19}$$

$$\psi_r = 500\ in\ psi \tag{4.20}$$

Third approach: Using physical model to construct SWCCs

Arya and Paris (1981) proposed a physico-empirical model to predict SWCCs based on particle size distribution and soil density information. By dividing the particle size distribution into a number of segments, the pore radius of a unit soil sample can be expressed as:

$$r_i = R_i\left[4en_i^{(1-\alpha)}/6\right]^{1/2} \tag{4.21}$$

where R_i is the mean particle radius, e is the void ratio, n_i is the number of particles, and α is an empirical constant ranging in value from 1.35 to 1.40. The soil suction value is obtained using the equation to calculate the capillary force:

$$\psi_i = 2\gamma cos\theta/\rho_w g r_i \tag{4.22}$$

where ψ_i is the soil suction, γ is the surface tension of water, θ is the contact angle,

ρ_w is the density of water, g is the gravity acceleration, and r_i is the pore radius.

By using the grain size distributions and SWCCs from the published literature, Fredlund et al. (1997) proposed a SWCC prediction model based on volume-mass properties and grain size distribution. The concept is to divide the grain size distribution into many small groups that have the same uniform size of soil particles. The SWCC of each group is known, and the incremental SWCCs are combined into a final SWCC. This prediction model is incorporated into the SoilVision program.

Thakur et al. (2007) examined some published pedo-transfer functions and compared the predicted suction with measured data using a tensiometer and chill-mirrored hygrometer.

The predictions from Fredlund et al. (1997) matched the experimental results.

Summary of three suction prediction approaches

Using the first approach, the relationship between volumetric water content and suction at a certain level can be obtained. This approach is convenient from the practical point of view, but if the relationship at an arbitrary suction level is required, this approach would not be taken because a non-monotonic soil water retention function may occur when the water contents are calculated from different regression variables at different suction ranges (Tietje and Tapkenhinrichs 1993) and the curve-fitting parameters cannot be obtained. So, if SWCCs are used for numerical analysis, this method is not applicable.

The second approach can easily be incorporated into numerical modeling and is generally applicable for most soils. A predicted integral SWCC can be obtained, and this SWCC then can be used as an input for future shear strength, seepage, and deformation applications. This second approach is adopted for this study.

The third approach requires detailed information regarding grain size distribution and density. Other soil information that may affect soil suction, such as PI, plasticity index and organic matter, is not included in the models.

4.3. Experimental Program

4.3.1. Laboratory set-up and pressure plate test procedures

The same soil sample from chapter one is used here for study purposes. For suction characterization purposes, twelve pressure plate tests were performed, and the tested results were curve-fitted using the Fredlund-Xing equation. Two existing suction prediction models

that are widely used, i.e., the Zapata and Houston (2008) and Fredlund et al. (1997) models, were applied to predict North Carolina residual soil suction.

Sample preparation

An undisturbed sample was extruded from a Shelby tube into a standard consolidation ring with dimensions of 5 cm in diameter and 2.5 cm in height. The sample was sandwiched and stabilized using filter paper and porous stone in a perforated disk-shaped clamp. The sample was immersed in a plastic cell with sufficient de-aired water. A vacuum was applied on top of the cell for at least 48 hours. If air bubbles still escaped from the sample, a longer time of saturation was required until no air bubbles were observed. The target sample mass at 100% saturation was calculated before the sample was saturated. The sample mass at post-saturation was measured and compared with the target mass at 100% saturation. If 99% saturation was not reached, the saturation process was repeated.

Before the saturation of the soil sample, a 5-bar ceramic stone (air entry value of the ceramic stone is 500 kPa) was saturated, and the ceramic stone was kept in the pressure plate extractor filled with de-aired water to maintain the saturation level. Once the sample was placed on top of the ceramic stone, it was rotated about 180 degrees to ensure close attachment to the stone. Air pressure was applied from a compressed air tank and controlled by air pressure regulators. A stepwise increasing air pressure supply was used from 10 kPa to 480 kPa, and each air pressure increment doubled the previous air pressure, i.e., 10 kPa to 20 kPa, 20 kPa to 40 kPa, until reaching the maximum 480 kPa, which is close to the air entry value of 500 kPa of the ceramic stone. At each pressure level before increasing to next

pressure level, 48 hours of equilibrium (as recommended in ASTM) was applied to establish the soil-air-water equilibrium for the system. The water that was squeezed out from the sample was collected in a pair of transparent plastic tubes with diameters of 1 cm each. By applying different air pressures, the decreasing water content of the soil sample was reflected in the increasing water level in the tubes. Based on the recorded water level in the tubes, the water content that corresponded to the applied air pressure could be back-calculated.

4.3.2. Grain size distribution and SWCCs of tested samples

Sample information

Two general types of soil were tested: low plasticity silt, i.e., ML (A-4), and high plasticity silt, i.e., MH (A-7-5). Twelve samples were tested, and the soil properties are shown in Table 4.1. The grain size distribution of both the A-7-5 (MH) and A-4 (ML) soils were curve-fitted using the Fredlund and Xing (1994) model, as shown in Figures 4.1 and 4.2. At the tail of the grain size distribution curve, where the particle diameters are smaller than 0.005 mm, the curves do not fit the hydrometer data well. So, for the data at the tail, the interpolated values were obtained by arithmetic average.

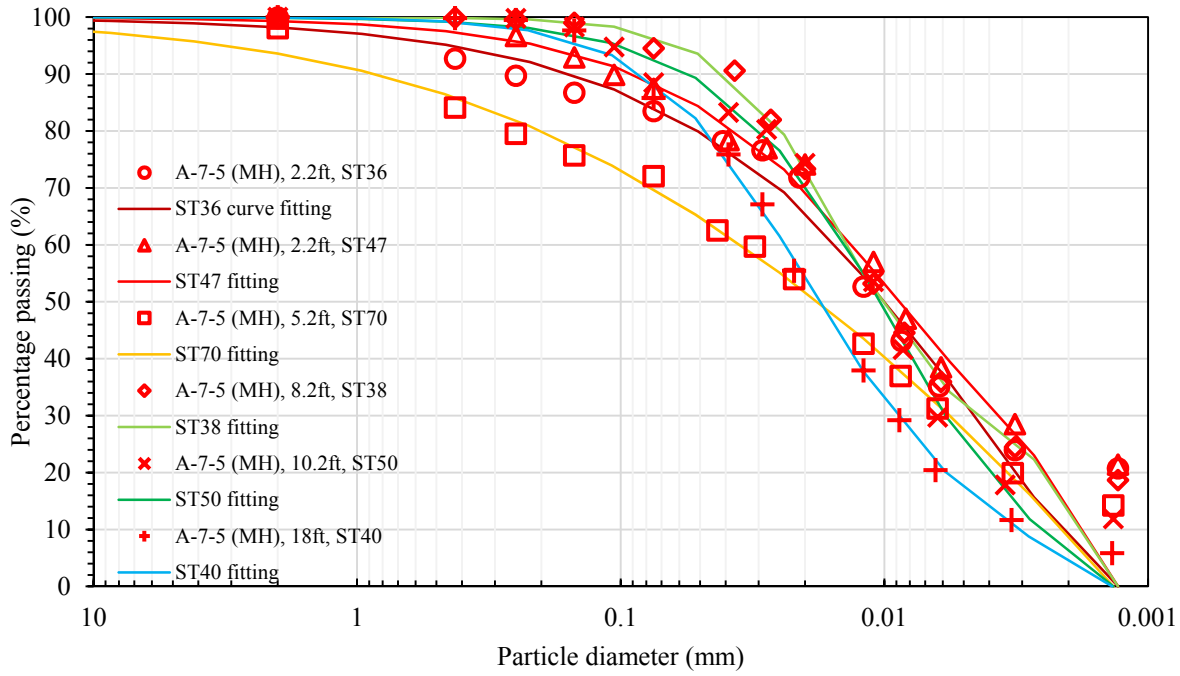

Fig. 4.1 Grain size distribution of A-7-5 (MH) soil

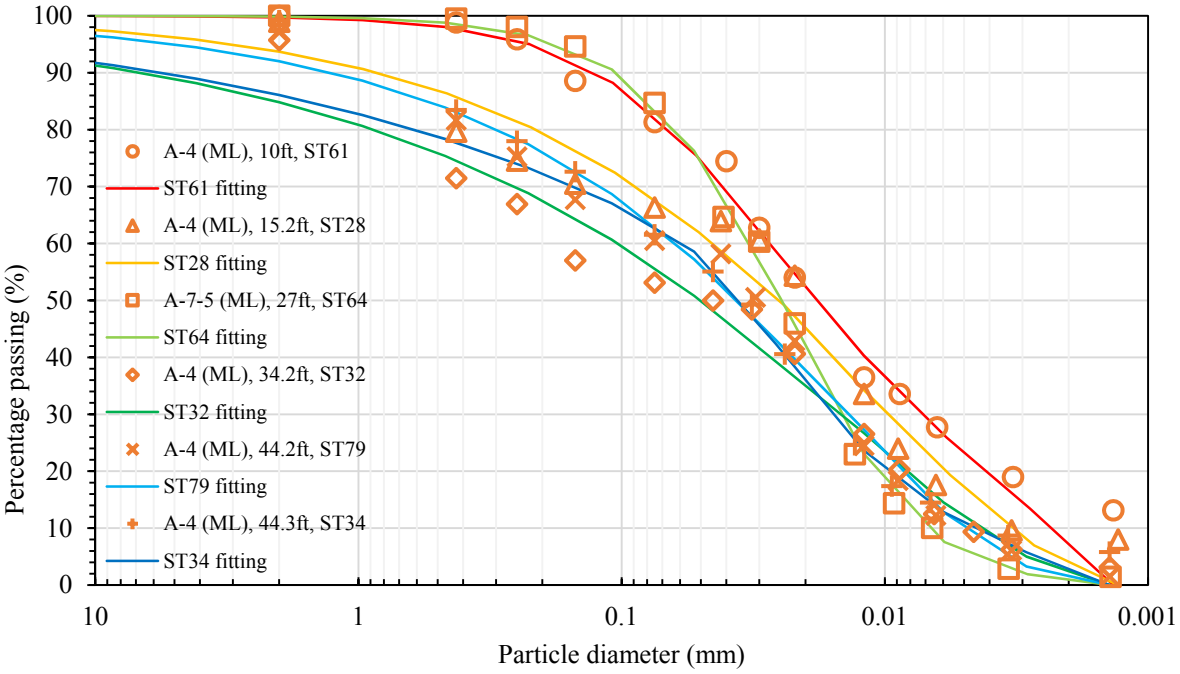

Fig. 4.2 Grain size distribution of A-4 (ML) soil

Table 4.1 Summary of sample properties

#	Depth (ft)	Type (USCS)	P200 (%)	P2 μm (%)	Cu	Cc	LL	PI	θ_s	Gs	ρ_d (g/cm^3)
ST36	2.2	MH	83.5	22.3	30	2.8	50	16	0.541	2.69	1.235
ST47	2.2	MH	87.4	25.0	13	1.1	61	22	0.615	2.75	1.058
ST70	5.2	CL	72.1	17.1	32	0.8	45	19	0.533	2.70	1.262
ST38	8.2	MH	94.6	21.5	14	1.5	61	21	0.611	2.72	1.060
ST50	10.2	MH	88.5	14.9	12	2.4	59	23	0.594	2.79	1.133
ST40	18.0	MH	85.8	8.8	8	1.1	58	16	0.580	2.74	1.150
ST61	10.0	ML	81.3	16.1	12	0.8	34	8	0.422	2.78	1.608
ST28	15.2	ML	66.3	8.8	9	0.9	36	7	0.435	2.69	1.521
ST64	27.0	ML	84.7	2.2	4	1.1	45	12	0.442	2.81	1.569
ST32	34.2	ML	53.1	4.7	32	0.3	38	8	0.509	2.77	1.360
ST79	44.2	ML	60.5	3.8	14	0.6	28	3	0.456	2.83	1.540
ST34	44.3	ML	61.5	7.3	14	0.8	38	10	0.490	2.79	1.425

Curve-fitting the experimental data

The experimental data of the SWCCs were curve-fitted using the Fredlund and Xing (1994) model. The upper bound used in the pressure plate test was 500 kPa. The residual matric suction was pre-designated as 3000 kPa. Fredlund and Xing (1994) found that the ψ_r, residul matric suction is generally in the range of 1500 kPa to 3000 kPa and that it will normally generate satisfactory approximation. Also, Vanapalli et al. (1996) used 3000 kPa as the ψ_r for estimating unsaturated shear strength from SWCCs.

These studies provide the basis for using 3000 kPa as the residual matric suction in the curve fitting in this study.

The SWCCs of the two soil types are shown in Figure 4.3 and Figure 4.4. The parameters *a*, *n*, and *m* in the Fredlund-Xing model are shown in Table 4.2. Some variability in the measured SWCCs is evident for the same type of soils. This variability of the tested SWCCs also was noted by Zapata et al. (2000).

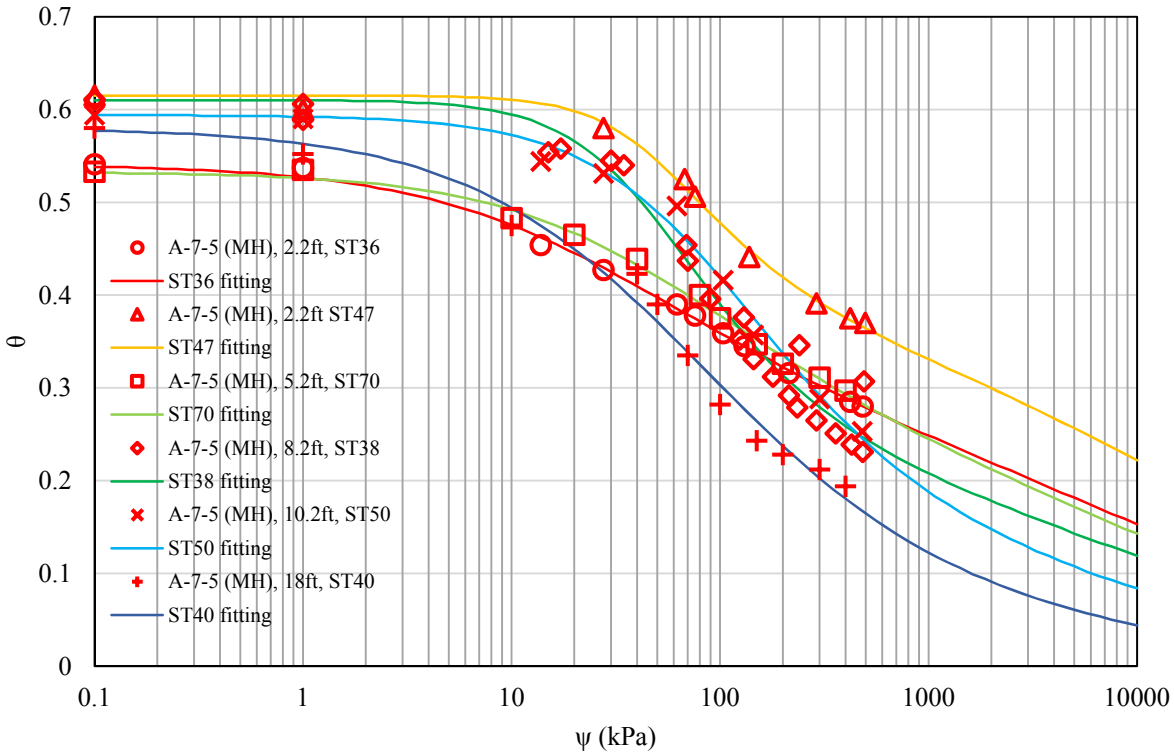

Fig. 4.3 Soil water characteristic curves of A-7-5 (MH) soil samples

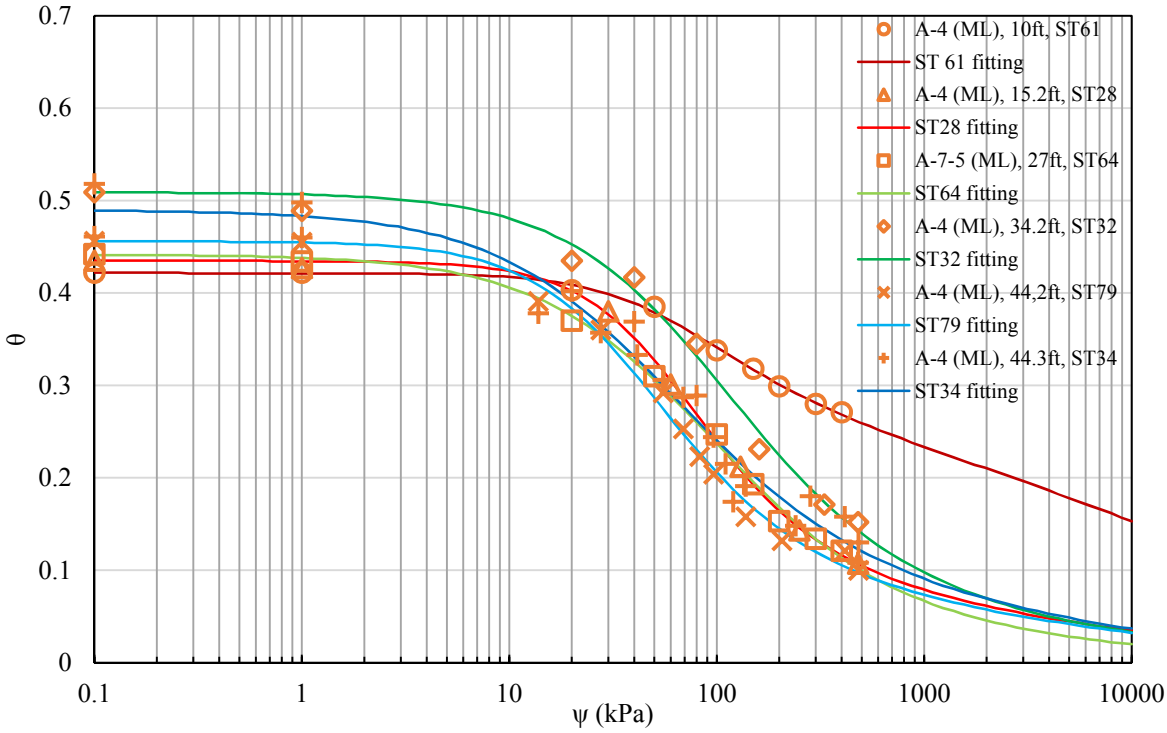

Fig. 4.4 Soil water characteristic curves of A-4 (ML) soil samples

Table 4.2 Fredlund-Xing Parameters of Tested SWCCs

#	Depth (ft)	a	n	m
ST36	2.2	14.9	0.78	0.60
ST47	2.2	38.5	2.04	0.30
ST70	5.2	30.9	0.85	0.64
ST38	8.2	36.3	1.64	0.61
ST50	10.2	72.4	1.14	0.97
ST40	18.0	49.8	0.76	1.63
ST61	10.0	44.6	1.65	0.33
ST28	15.2	49.9	1.66	1.03
ST64	27.0	69.2	1.03	1.73
ST32	34.2	73.6	1.1	1.45
ST79	44.2	33	1.42	1.12
ST34	44.3	36.3	1.01	1.32

4.3.3. Applying Existing Models to Soil Being Tested

Two existing suction prediction models, Zapata et al. (2000) and Fredlund et al. (1997), were used to predict the suction of North Carolina residual soil. In the model proposed by Zapata, a weighted plasticity index (PI), i.e., wPI, was used as the main variable to correlate the SWCC parameters. wPI is expressed as the percentage passing the #200 sieve (as a decimal) multiplied by the PI, which is also a percentage. The equations for the wPI and (Fredlund and Xing 1994) SWCC parameters are:

$$\mathrm{a} = 0.00364(wPI)^{3.35} + 4(wPI) + 11 \tag{4.23}$$

$$\frac{n}{m} = -2.313(wPI)^{0.14} + 5 \tag{4.24}$$

$$\mathrm{m} = 0.0514(wPI)^{0.465} + 0.5 \tag{4.25}$$

$$\frac{\psi_r}{a} = 32.44e^{0.0186(wPI)} \tag{4.26}$$

Fredlund et al. (1997) model was used to estimate the SWCCs using grain size distribution data and volume-mass properties. The grain size distribution of the soil was divided into small groups of uniform particles. The SWCCs of each soil particle were summed to generate the final SWCC. The predicted SWCCs were generated by inputting the grain size distribution data and volume-mass properties into SoilVision software.

The suction values determined from the twelve pressure plate tests were compared to those predicted from the Zapata model and SoilVision, as shown in Figure 4.5 and Figure 4.6, respectively. The results from both the Zapata model and SoilVision software show a significant amount of deviation from the measured data, which have coefficients of determination R^2, 51% and 48 percent. These two methods do not generate satisfactory predicted suction data for North Carolina residual soil. Because these existing models could not provide enough confidence in the suction predictions, an empirical model based on grain size distribution and a soil volume-mass relationship is proposed in this study. That is, a new model specifically designed for North Carolina residual soil is proposed here.

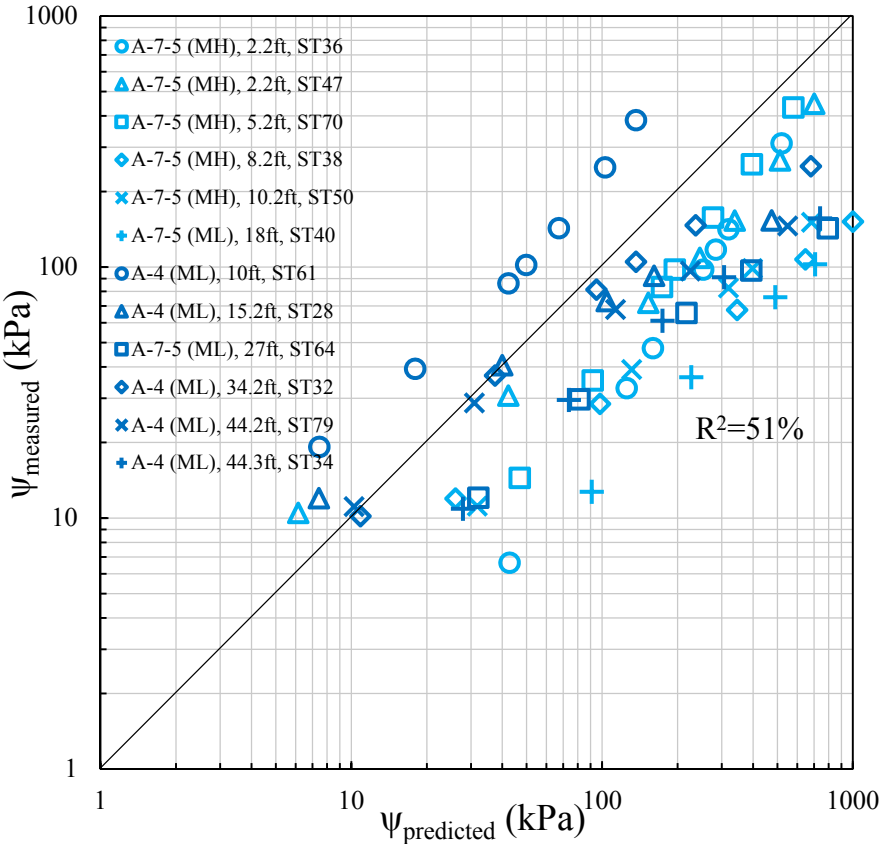

Fig. 4.5 Measured vs predicted suction by Zapata model

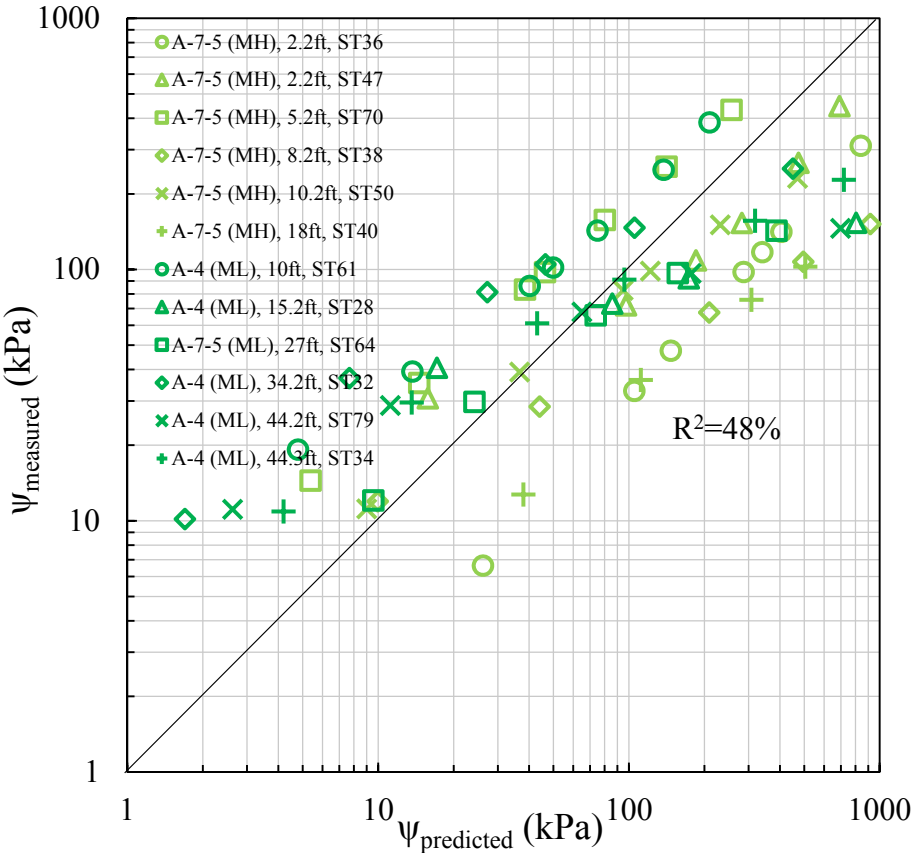

Fig. 4.6 Measured vs predicted suction by SoilVision

4.3.4. New Model Development Using Multivariate Regression Analysis

For the new model development, SWCCs of twelve samples were determined: six high plasticity and six low plasticity silty soils. The corresponding soil properties also were tested. The first step was to include as many properties as possible in the statistical analysis because no physical theory was available to support which properties should be included or excluded. Also, some of the possible parameters might have an effect on the curvature of the SWCCs. So, the rule of thumb principle was employed to include as many soil index

properties as possible. Three categories of soil properties were included for the new model development: grain size distribution, Atterberg limits, and volume-mass relationships.

The SWCCs were determined using pore size distribution, which correlates directly with grain size distribution. The included parameters are: P200, P5 μm (percentage passing 5 μm), P2 μm (percentage passing 2 μm), D10, D30, D60, Cu, Cc, LL, PI, Gs, and ρd.

The so-called 'Best' subsets algorithm (a built-in block in MINITAB) was used to determine the necessary variables for the model. A group of 'Best' subsets, which included different independent variables, was correlated with the response variable in the form of

$$Y = \beta_0 + \beta_1 X_1 + \cdots$$

$$Y = \beta_0 + \beta_1 X_1 + \beta_2 X_2 + \cdots$$

$$Y = \beta_0 + \beta_1 X_1 + \beta_2 X_2 + \beta_3 X_3 + \cdots$$

These subsets were generated by the MINITAB program. The detailed theory and procedures are explained in Neter et al. (1996). Three criteria were used to determine the best-fit function: R^2, adjusted-R^2, and predicted-R^2. R^2 is the percentage of the response variable variation that is explained by the predictor variables. The adjusted-R^2 criterion is the R^2 value adjusted for the number of predictors in the model. The predicted-R^2 can prevent over-fitting the models. In general, R^2 and adjusted-R^2 will be higher if more predictor variables are included, even when some variables are not necessary. Over-fitted models will give better R^2 and adjusted- R^2 values, but fail to generate valid predictions for future data (Ryan et al. 1982). The results of the best subsets analysis from MINITAB are presented in Table 4.3.

Table 4.3 Example of Best Subsets Analysis for *a* Values

Vars	R-Sq	R-Sq (adj)	R-Sq (pred)	Mallows Cp	S	P200	5μm	1/D10	1/D30	1/D60	Cu	Gs	ρd	D30	D60
1	33.5	26.8	9.6	2.8	15.552			X							
1	23.0	15.3	0.0	4.5	16.733		X								
2	44.2	31.8	0.6	3.0	15.015			X		X					
2	39.6	26.2	0.0	3.8	15.621	X		X							
3	60.9	46.3	0.0	2.3	13.324			X		X					X
3	60.3	45.4	0.0	2.4	13.431			X		X	X				
4	86.5	78.8	50.0	0.2	8.3740			X	X	X	X				
4	83.8	74.6	33.8	0.6	9.1659		X	X		X	X				
5	**92.3**	**85.8**	**69.3**	**1.3**	**6.8418**			**X**	**X**	**X**	**X**		**X**		
5	89.5	80.7	54.5	1.7	7.9832		X	X		X	X		X		
6	92.9	84.4	0.0	3.1	7.1797			X	X	X	X		X		X
6	92.7	84.0	60.2	3.2	7.2801		X	X	X	X	X		X		
7	93.7	82.8	0.0	5.0	7.5463		X	X	X	X	X		X		X
7	93.3	81.6	0.0	5.1	7.7992			X	X	X	X		X	X	X
8	93.8	77.3	0.0	7.0	8.6586		X	X	X	X	X	X	X		X
8	93.7	77.0	0.0	7.0	8.7133		X	X	X	X	X		X	X	X
9	93.8	66.0	0.0	9.0	10.601	X	X	X	X	X	X	X	X		X
9	93.8	66.0	0.0	9.0	10.602		X	X	X	X	X	X	X	X	X
10	93.8	32.1	0.0	11.0	14.986	X	X	X	X	X	X	X	X	X	X

The best subsets analysis indicates that the related soil properties with *a*, *n*, and *m* can be considered as the following general forms of functions:

$$a = f(\frac{1}{D_{10}}, \frac{1}{D_{30}}, \frac{1}{D_{60}}, \frac{D_{60}}{D_{10}}, \rho_d) \tag{4.27}$$

$$n = f(P200, \frac{1}{D_{30}}, \frac{D_{60}}{D_{10}}, \rho_d, D_{30}, D_{60}) \tag{4.28}$$

$$m = f(P200, 5\mu m, G_s, \rho_d) \tag{4.29}$$

Next, multivariate linear regression analysis was performed to determine which explanatory variables should be incorporated into the function. The criterion to determine the

significance of each explanatory variable is the P-value. A hypothesis test was performed to determine the coefficient of each explanatory variable. If the P-value for the coefficient of one explanatory variable was higher than 0.05, this coefficient was considered as zero, and the corresponding explanatory variable was considered insignificant and was excluded from the model. So, after the first-step refinement, the insignificant variable, D_{30} in the equation 4.24 with P-value = 0.165, was excluded from the model. The P-value of each term is shown in Table 4.4.

Table 4.4 P-values for Choosing the Terms in Prediction Model

a		n		m	
Term	P-value	Term	P-value	Term	P-value
$\frac{1}{D_{60}}$	0.001	P200	0.049	P200	0.036
$\frac{1}{D_{30}}$	0.008	D_{60}	0.000	5μm	0.000
$\frac{1}{D_{10}}$	0.002	$\frac{1}{D_{30}}$	0.000	G_s	0.012
$\frac{D_{60}}{D_{10}}$	0.004	$\frac{D_{60}}{D_{10}}$	0.012	ρ_d	0.000
		ρ_d	0.006		

The prediction models for each Fredlund-Xing *a*, *n*, and *m* parameter are

$$a = 17.2 + \frac{1.89}{D_{60}} - \frac{0.363}{D_{30}} - \frac{0.063}{D_{10}} + 2.5 * \frac{D_{60}}{D_{10}} \quad (4.30)$$

$$n = -0.105 - 0.018 * P200 + 9.55 * D_{60} + \frac{0.012}{D_{30}} - 0.057 * \frac{D_{60}}{D_{10}} + 9.55 * \rho_d \quad (4.31)$$

$$m = 11.24 + 0.0074 * P200 - 0.075 * 5\mu m - 2.665 * G_s - 1.452 * \rho_d \quad (4.32)$$

Due to the limitation of the data used for generating the model, the bounds for the parameter are designated and the correlation coefficients used to quantify the fitness of the model are shown in Table 4.5.

Table 4.5 Correlation Coefficients to Quantify Fitness of Proposed Model

	R^2 (%)	Adjusted- R^2 (%)	Predicted-R^2 (%)	Bound
a	86.5	78.8	50	(14, 74)
n	93.7	88.4	67.4	(0.7, 2.1)
m	97.6	96.2	93.9	(0.3, 1.8)

The predicted suction values determined by the model were compared to the measured suction values, as shown in Figure 4.7. The figure indicates that most of the data points for predicted suction versus measured suction fall on the 1:1 ratio line and that the R-square value is 93%, which indicates a better fit than both the Zapata model (R^2 is 51%) and SoilVision (R^2 is 48%).

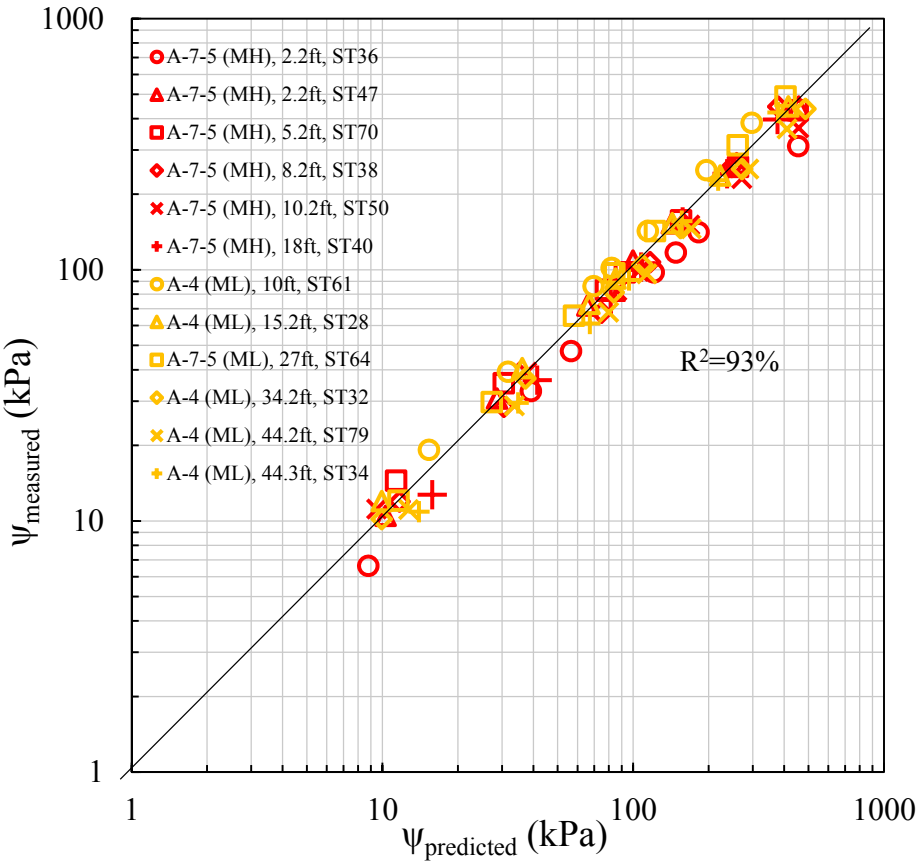

Fig. 4.7 Measured vs predicted suction using suction prediction model

4.4. Testing New Model Using Data from Rahardjo et al. (2012)

The proposed model was tested using the unsaturated properties tested by Rahardjo (2012) who had studied residual soils in Singapore. The soil water characteristic curve of residual soils were obtained from soils at three locations: sedimentary Jurong Formation, Bukit Timah Granite and Old Alluvium in Singapore. The silty material from Bukit Timah Granite was used for testing the model here since it is similar to the soil in this study.

The grain size distribution from Rahardjo (2012) is presented in Fig. 4.8. But the specific gravity and dry density information at this location wasn't explicitly mentioned in Rahardjo (2012). So, the specific gravity and dry density is respectively set to be default values of 2.7 and 1.2 g/cm^3, respectively, both believed to be reasonable assumptions for residual soils. The predicted SWCC by the proposed model is compared with the measured data in Fig. 4.9.

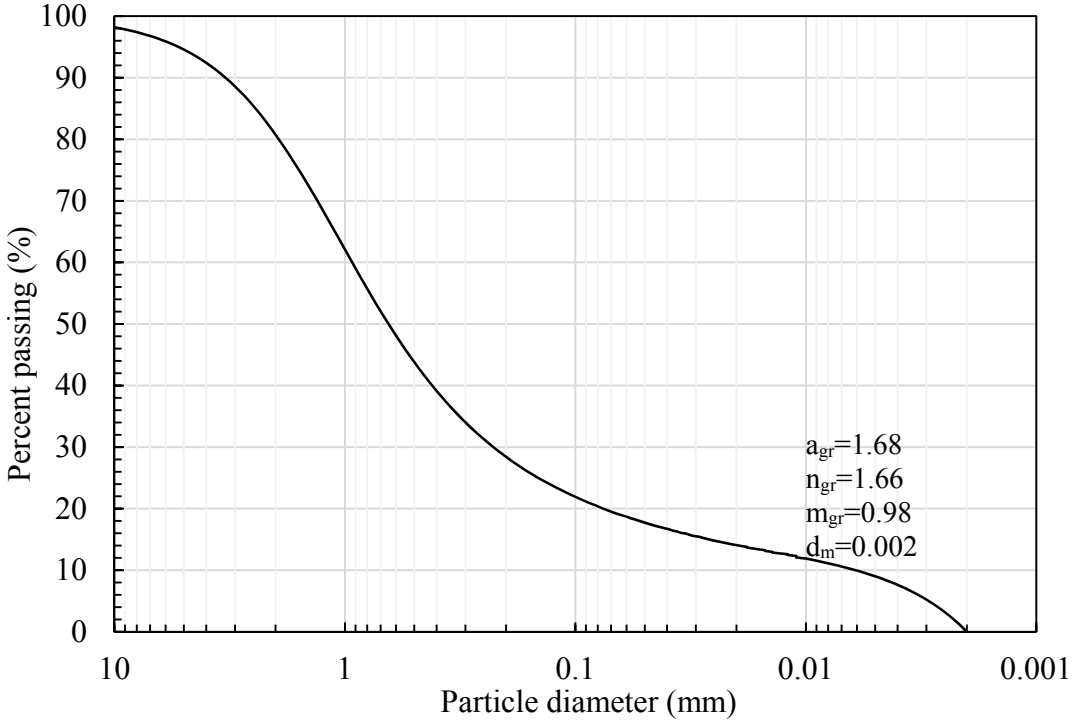

Fig. 4.8 Grain size distribution of residual soil from Bukit Timah Granite (Rahardjo, 2012)

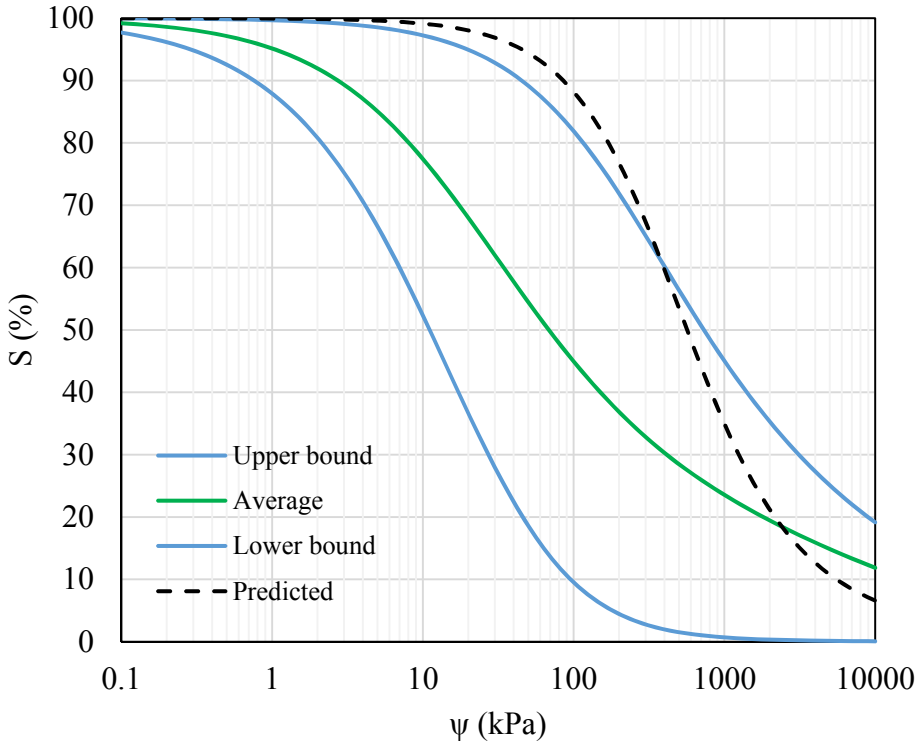

Fig. 4.9 Drying SWCC of residual soil from Bukit Timah Granite vs the predicted SWCC

The predicted SWCC from the proposed model shows a reasonably good agreement with the upper bound of SWCC from Bukit Timah Granite. And this also suggests that without the specific data of specific gravity and dry density, the default values of specific gravity, 2.7 and dry density, 1.2 g/cm^3 be used for predicting SWCCs.

4.5. Suggested correction for design purpose

In order to consider the variability of the data from an engineering design point of view, a suggested correction factor based on 95% confidence limit of the data should be applied to the predicted suction values.

The comparison of the suction values obtained by the prediction model and the actual measurements, as shown in Figure 4.7, is transposed to Figure 4.10. Knowing the predicted suction values from the previous analysis, the best-fit function of the actual suction can be expressed as

$$\psi_{\text{measured}} = 3.572 - 0.972\psi_{\text{predicted}} \tag{4.33}$$

In order to account for the variability (scatter) in the measured data, a lower bound model, such as one that includes a 95% confidence limit, could be used:

$$\psi_{measured} = 3.57 + 0.97\psi_{predicted} - 59.4\left[0.012 + \frac{\left(\psi_{predicted} - 146.5\right)^2}{10^6}\right]^{0.5} \tag{4.34}$$

However, instead of using Equation (4.34), a simple correction factor of 0.94 that is based on the lower prediction at the mean of the data is shown in Figure 4.10 to provide a very reasonable approximation of the more complex function. Thus, the following model is derived:

$$\psi_{measured} = 0.94\psi_{predicted} \tag{4.35}$$

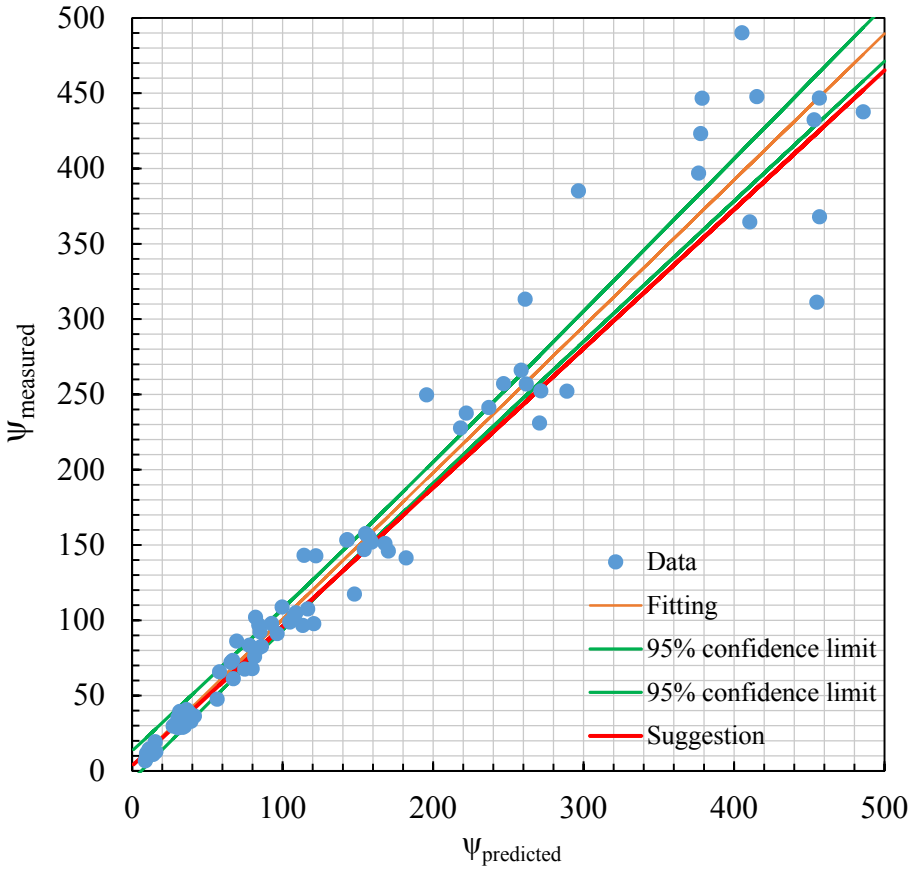

Fig. 4.10 Suggested correction for the predicted suction

4.6. Conclusions

Twelve SWCCs were obtained from pressure plate test results. The corresponding basic soil properties, i.e., grain size distribution, specific gravity, dry density and Atterberg limits, also were determined to investigate the soil properties which may be influencing the suction. The SWCCs were curve-fitted using Fredlund-Xing (1994) equations. Systematic multivariate analysis was performed to correlate the Fredlund-Xing parameters with the basic soil properties. As a result, if the water content of the soil is known, the suction can be predicted by testing the basic soil properties, which are easy to perform. The conclusions drawn from this study are as follows.

1. Using SWCCs and statistical analysis, an empirical model to predict suction in residual soils is proposed that can correlate basic soil properties, i.e. grain size distribution, density, and specific gravity, with the fitting parameters in the Fredlund-Xing equations.
2. Compared to existing suction prediction models, Zapata (R^2 = 51%) and SoilVision (R^2 = 48%), the proposed model provides much better fitness (93% R^2) to the tested data. The proposed model also was tested using the published Rahardjo (2012) data. The predicted SWCC obtained using the proposed model show reasonably good results when compared to actual measured data.
3. Considering the variability of the tested data, a suction correction factor of 0.94 is recommended and should be applied to the predicted suction at 95% confidence limit.

5. FIELD MONITORING OF THE RESIDUAL SOIL SUCTION AND MOISTURE PROFILES

5.1. Introduction

A field monitoring program (mentioned in Chapter 2) was undertaken to study the effects of infiltration on the changes in suction and moisture profiles. Sixteen suction sensors and sixteen moisture sensors were installed to monitor the changes in the water content and suction of the soil. Three slopes (0.5:1, 0.25:1, and 1:1) and one cantilever sheet pile wall were monitored both during staged-excavation and after 22 feet of excavation. After the excavation, an infiltration state was initiated by ponding water on top of the slopes. Data from the monitoring sensors were collected during the project. At the end of the project, 30 Shelby tube samples were obtained for testing the suction and water content of the soil at the post-infiltration stage and for checking the accuracy of the data monitored by the suction and moisture sensors.

The objectives of this field monitoring study were to:

1. Monitor the performance of three slopes and one sheet pile wall under the effect of water infiltration.
2. Study the movement of the suction and moisture profiles under the effect of infiltration.
3. Propose suggestions for the future use of the sensors by comparing the data obtained from the field-installed sensors with the measurements taken under laboratory conditions.

5.2. Background

Field matric suction measurements are critical for evaluating the unsaturated strength of the soil for many geotechnical projects, such as those that involve embankments and slopes. The Fredlund thermal conductivity (FTC) sensor is applicable for long-term field matric suction monitoring and was used in this study for taking field suction measurements.

Principles of thermal conductivity sensors

The thermal diffusivity of the ceramic tip of a thermal conductivity sensor is driven mostly by water content. A heater and a temperature sensor are located inside the sensor. Constant heat that is applied to the ceramic tip will either dissipate or not dissipate. The thermal diffusivity of water is much higher than that of air; therefore, a ceramic tip with high water content will lead to more dissipated heat and vice versa. The heat that does not dissipate will be reflected by the temperature sensor. When the sensor is working, the actual results indicate a relationship between the sensor temperature (converted into voltage) and the water content of the ceramic tip. The water content that is absorbed by the ceramic tip then is related to the matric suction in the soil (Perera and Fredlund 2004). That is, the rise in temperature of the sensor is a function of the water content of the ceramic, which, in turn, is a function of the matric suction of the soil. A calibration curve (i.e., the temperature and matric suction relationship) is predetermined in the lab and is referred to as the indirect matric suction measurement.

Before thermal conductivity sensors can be commercialized, the effects of calibration, hysteresis, temperature, etc. must be investigated. Sattler and Fredlund (1989) introduced a calibration procedure for thermal conductivity sensors whereby the thermal conductivity

sensor can measure reasonable matric suction values under laboratory conditions. Feng (1999) focused on the capillary hysteresis of thermal conductivity sensors. Based on Feng's research, the capillary hysteresis of a thermal conductivity sensor is crucial. When a sensor is installed in the field, it experiences wet-dry cycles. The drying and wetting processes may begin or end at any suction value following a primary or secondary scanning curve or a main wet-dry curve, depending on the direction of the water movement in the surrounding soil. Feng et al. (2002) observed that the effects of capillary hysteresis on measurements of matric suction are significant when using thermal conductivity suction sensors. They used an analytical model to adjust the measured suction by taking into account the capillary hysteresis. Hysteresis and temperature correction were applied to the data analysis, which clearly showed the difference between uncorrected and corrected suction. Shuai et al. (2002) found that matric suction readings obtained from sensors are subject to environmental effects, including temperature changes and wet-dry cycles. Feng and Fredlund (2003) proposed a revised calibration procedure that takes into consideration the capillary hysteretic effects based on laboratory test results. Leong et al. (2012) investigated another type of thermal conductivity sensor and noted that heat transfer in the ceramic tip is highly pressure-dependent due to latent heat transfer.

Tan et al. (2007) investigated the installation of thermal conductivity sensors. They used an auger with a slightly larger diameter than the sensor to drill a hole. Then, another auger with the same diameter as the sensor was inserted to provide good soil-to-sensor contact for the entire circumference of the sensor. Once the sensor was installed (still dry), the readings were taken and compared to the dry calibration curve. Nichol et al. (2003) also

performed field installation and monitoring. They found that correcting for the hysteresis and changing the ambient temperature is important prior to the installation of a thermal conductivity sensor.

Conclusions: FTC suction sensors can be used for taking long-term field suction measurements. They are installed to monitor the suction changes that are due to the movement of moisture in the soil profile. Once an FTC sensor is installed, it is stable. However, it requires temperature, hysteresis, and input voltage correction.

5.3. Field instrumentation

In order to accomplish the stated objectives, an experimental program was developed using a North Carolina Department of Transportation (NCDOT) Geotechnical Unit test site in Greensboro, North Carolina. The Project No. 39406.1.1 highway construction site is located at Alamance Road, Greensboro, Guilford County, North Carolina. Three slopes (0.5:1 at 405+70, 0.25:1 at 404+50 and 1:1 at 403+45) and one sheet pile wall (at 404+50 94'RT) are located in the field. Three stages of soil excavation have been completed. The excavation depth is 22 feet to the ground surface (Fig. 5.1). The slopes were infiltrated using ponded water after the excavation (Fig. 5.2).

In order to monitor the suction and moisture movement in the soil profile, sixteen FTC-100 sensors were installed for taking the matric suction measurements (Fig. 5.3) and sixteen 10HS moisture sensors were installed for taking the volumetric water content measurements (Fig. 5.4).

The suction and moisture sensors were installed on June 13, 2013. The initial readings were taken on June 27, 2013, which was two weeks after the installation to give the

sensors a sufficient amount time to reach equilibrium.

The monitoring schedule incorporated every two weeks from June 27, 2013 to March 10, 2014. The suction and moisture profile changes over time were monitored using instrumentation. Man-made infiltration by ponding water on top of the slopes was maintained from February 6, 2014 to the end of monitoring.

Fig. 5.1 View of site after 22-ft excavation

Fig. 5.2 Infiltration on top of slopes

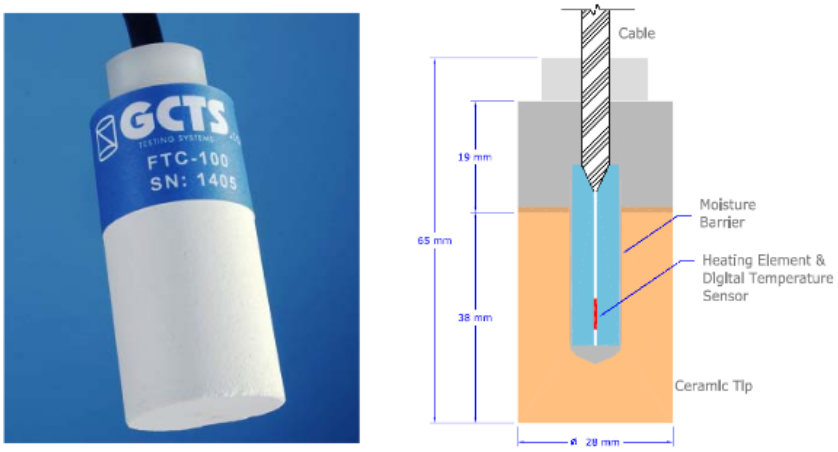

Fig. 5.3 FTC-100 sensor from GCTS Co.

Fig. 5.4 Moisture sensor from Decagon Co.
(Dimensions: 14.5 cm x 3.3 cm x 0.7 cm)

Table 5.1 presents information about the installed matric suction and volumetric water content measuring sensors. Good contact between the sensors and soil was ensured upon installation. The readings of the matric suction sensors were taken in conjunction with the moisture sensors.

Table 5.1 Installed Sensors Information

Slope	Station	FTC Sensor (depth, ft)	Quantities	Moisture Sensor (depth, ft)	Quantities
1:1	403+45	3, 6, 10, 20	4	2, 4, 6, 8	4
0.25:1	404+50	3, 6, 10, 20	4	2, 4, 7	3
0.5:1	405+70	3, 6, 10	3	2, 4, 8	3
Sheet pile wall	404+50	3, 6, 10, 14, 20	5	2, 2.6, 4, 5, 6, 14	6

Figures 5.5 through 5.16 show the suction and moisture profiles at various points in time, and the plan view of the installed sensors and borings. The solid squares and crosses

(from light to dark colors) represent the data obtained from the field-installed sensors from the beginning to the end of the monitoring process. To verify the actual state of the field soil, the initial state (hollow red circles) and final state (solid black circles) of the soil profiles were determined by testing the bored samples. The initial and final suction states were determined from the suction of each Shelby tube using tensiometers. The water contents of the Shelby tube samples were determined by oven drying each sample over 24 hours.

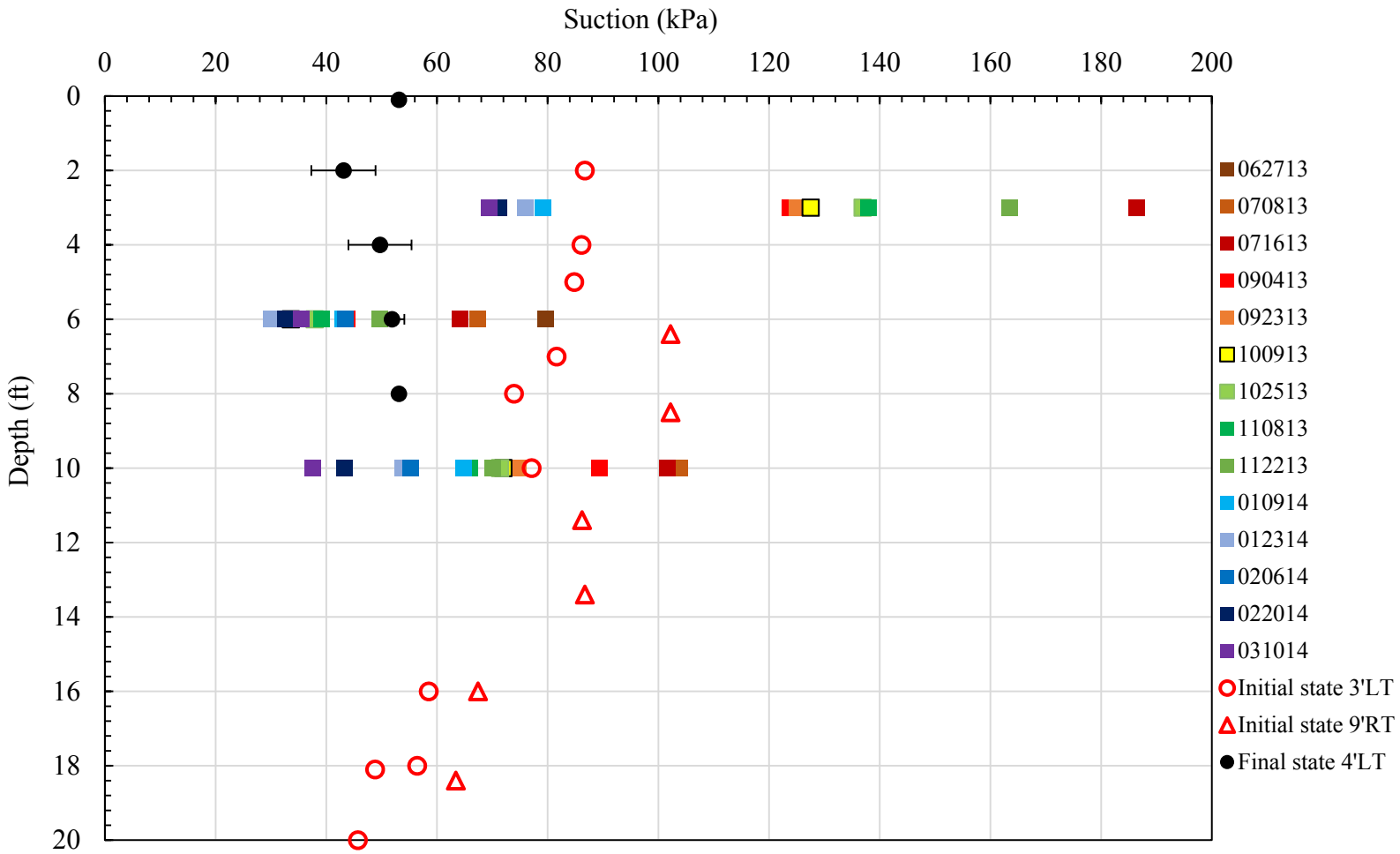

Fig. 5.5 Suction profile of 0.5:1 slope

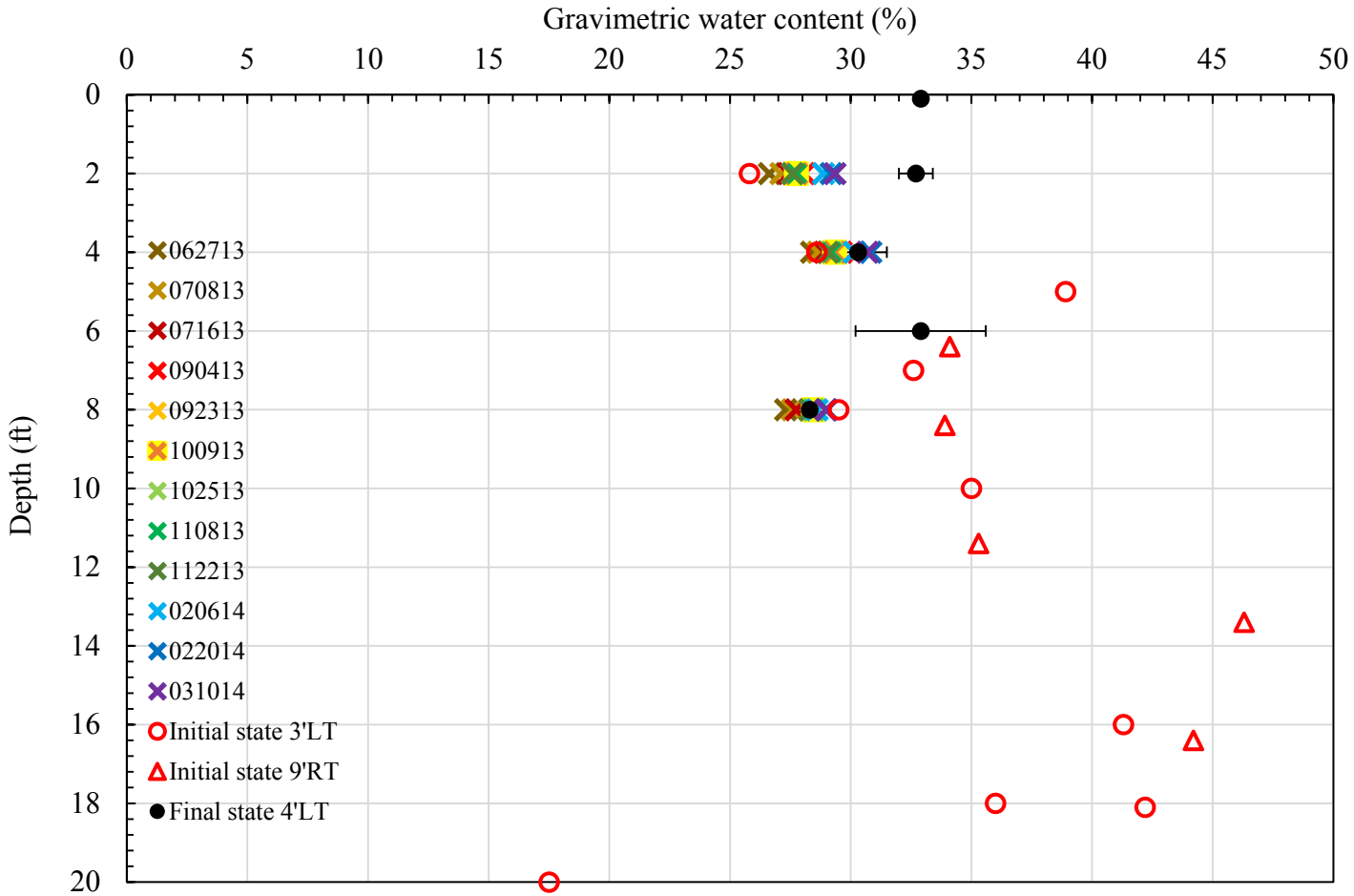

Fig. 5.6 Moisture profile of 0.5:1 slope

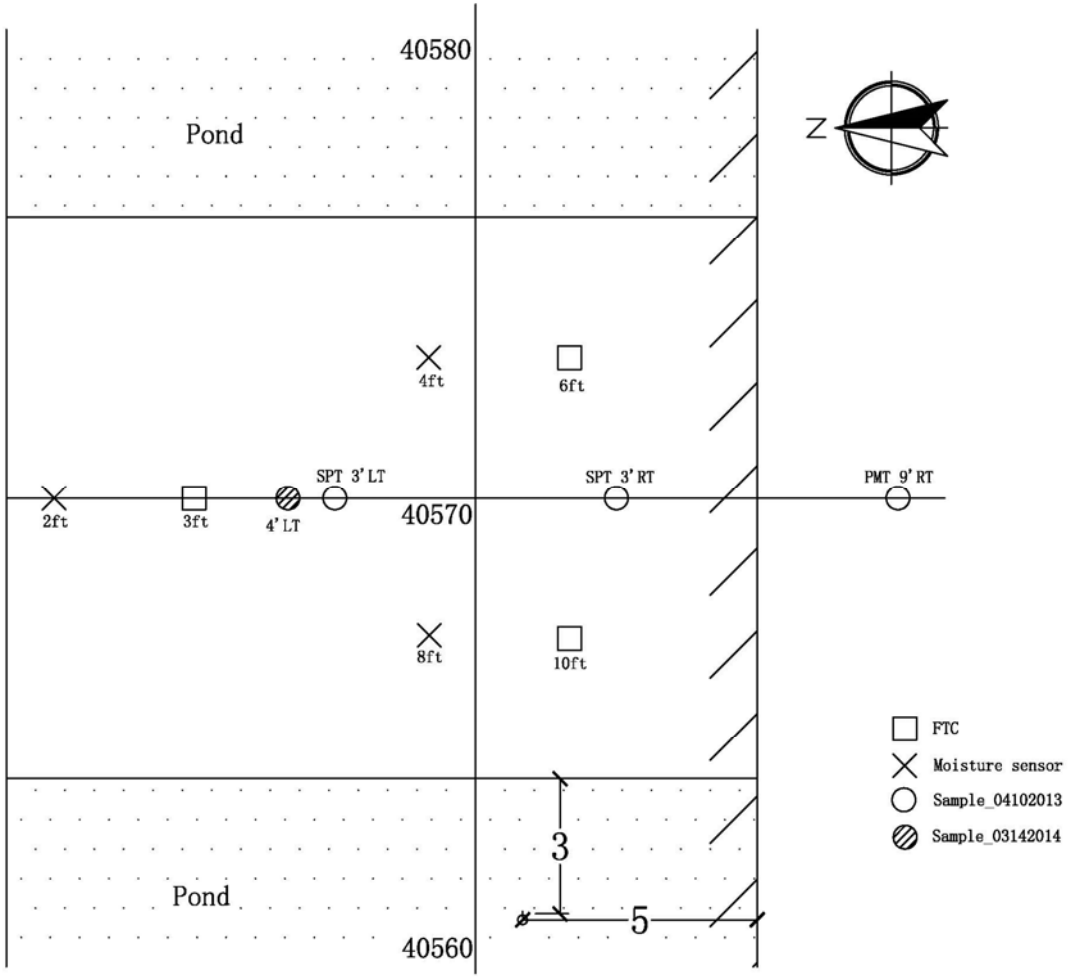

Fig. 5.7 Plan view of the installed sensors and borings at 0.5:1 slope area

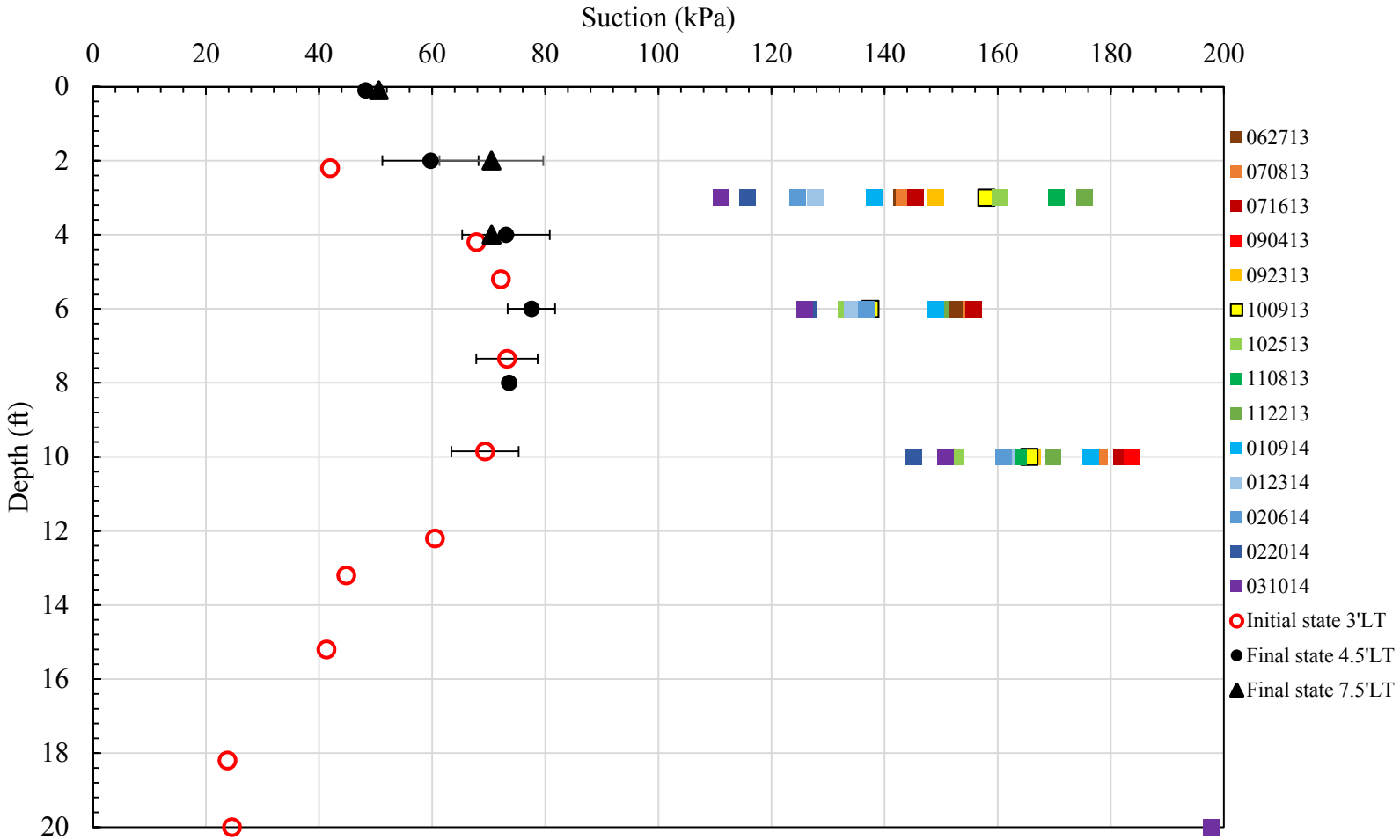

Fig. 5.8 Suction profile of 0.25:1 slope

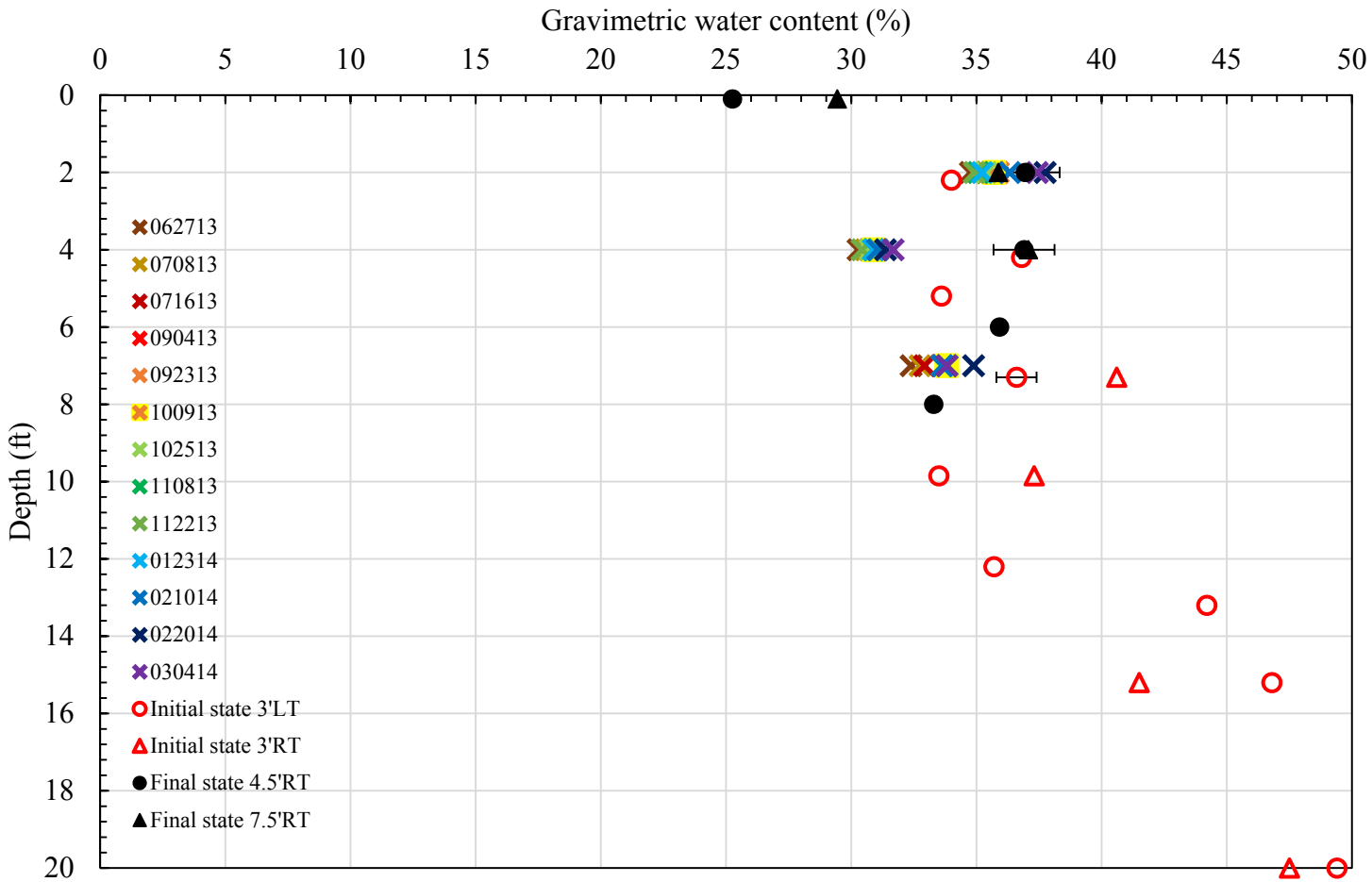

Fig. 5.9 Moisture profile of 0.25:1 slope

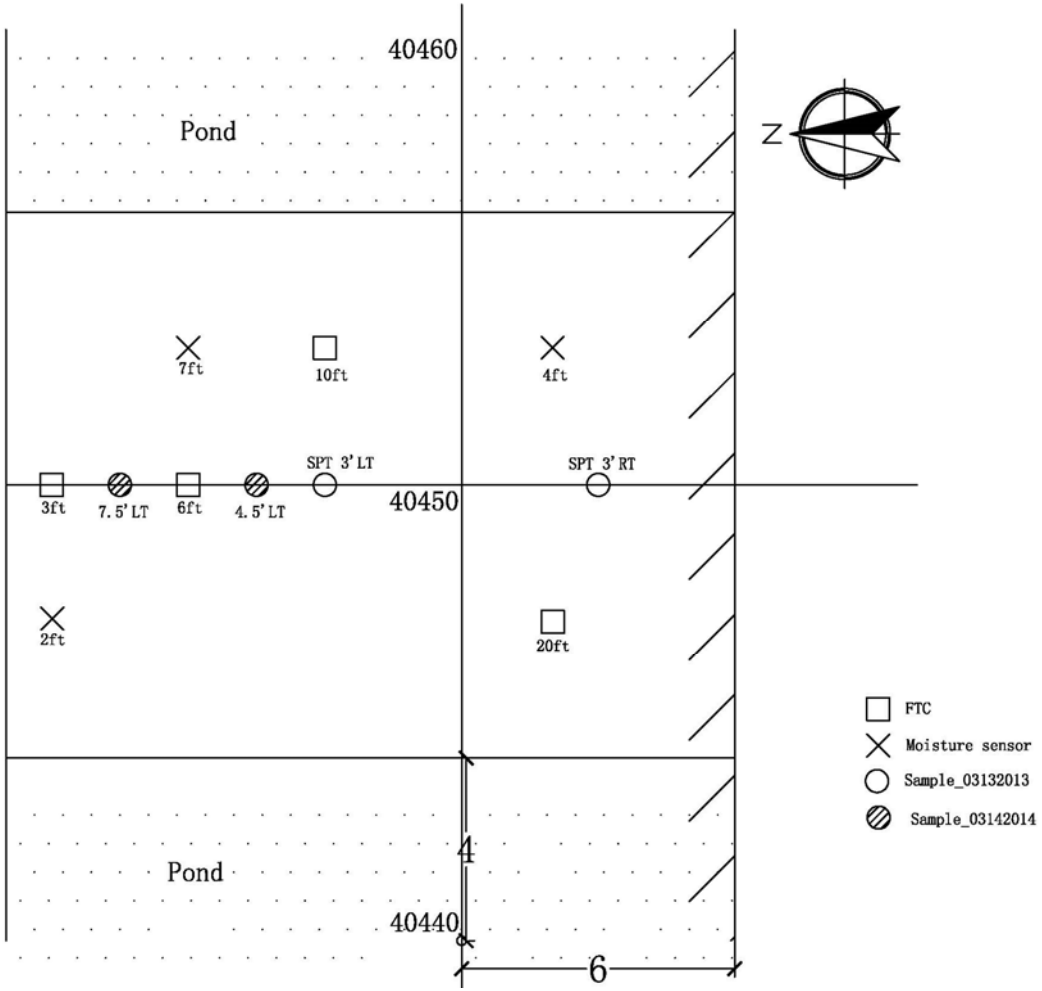

Fig. 5.10 Plan view of the installed sensors and borings at 0.25:1 slope area

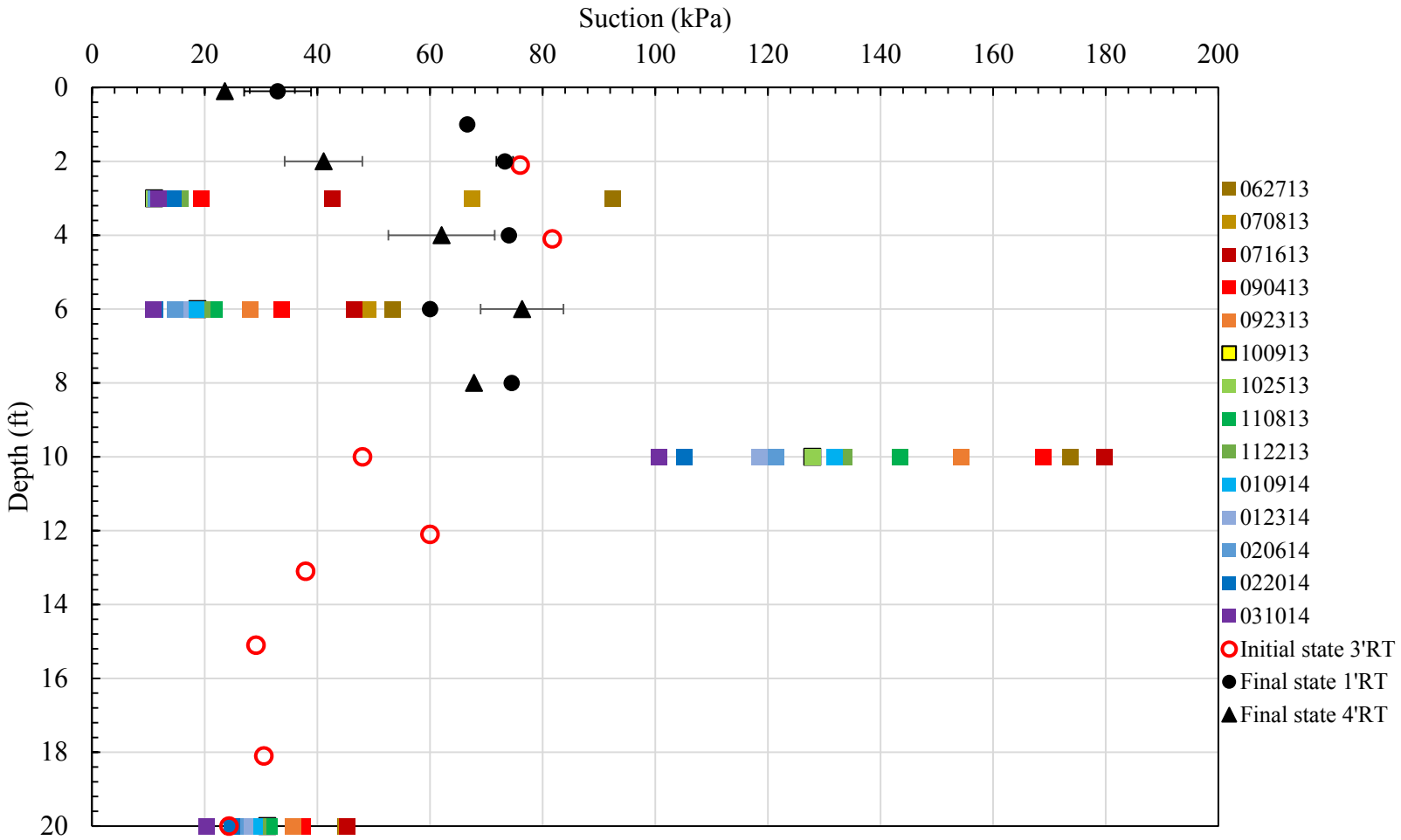

Fig. 5.11 Suction profile of 1:1 slope

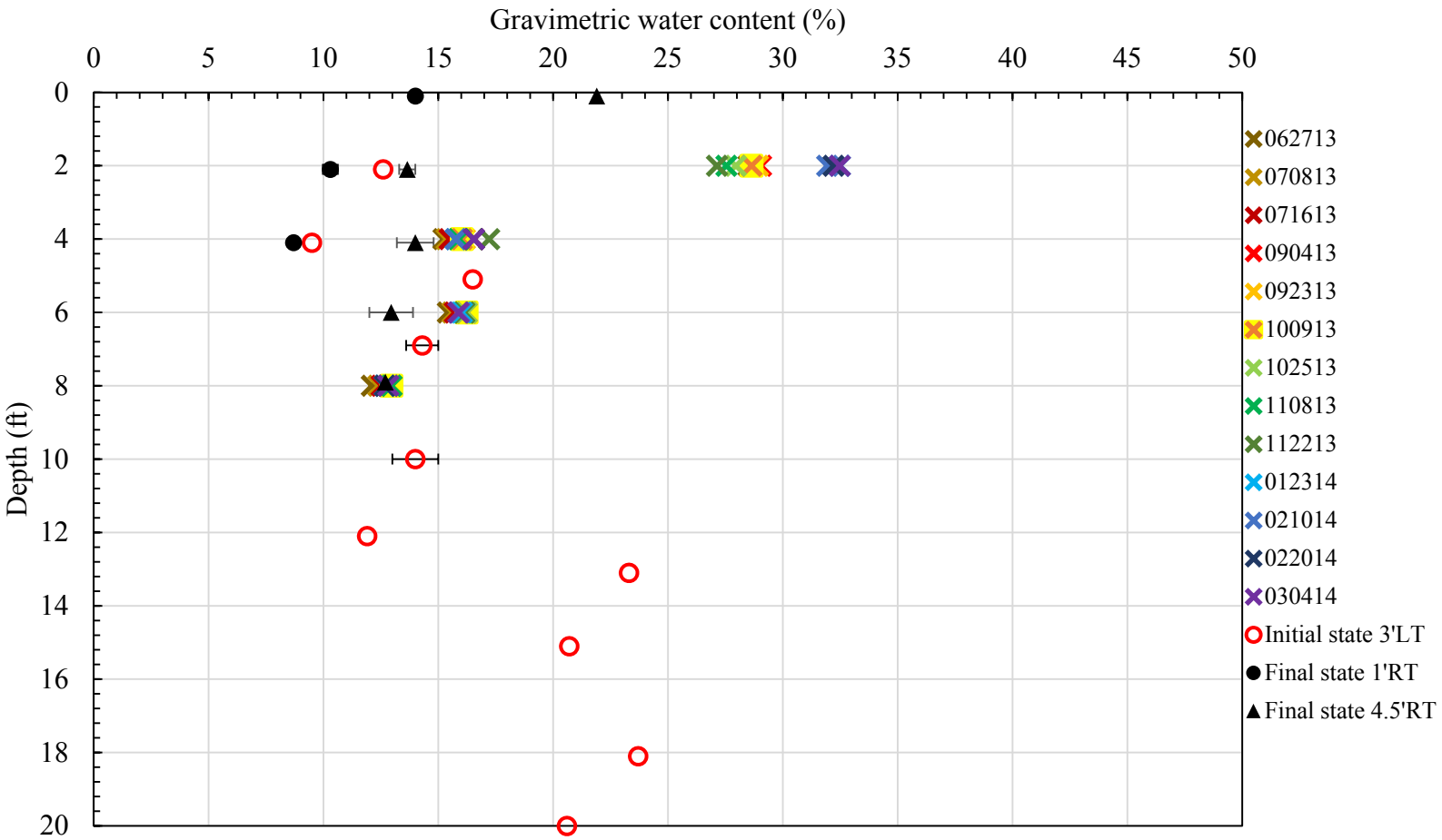

Fig. 5.12 Moisture profile of 1:1 slope

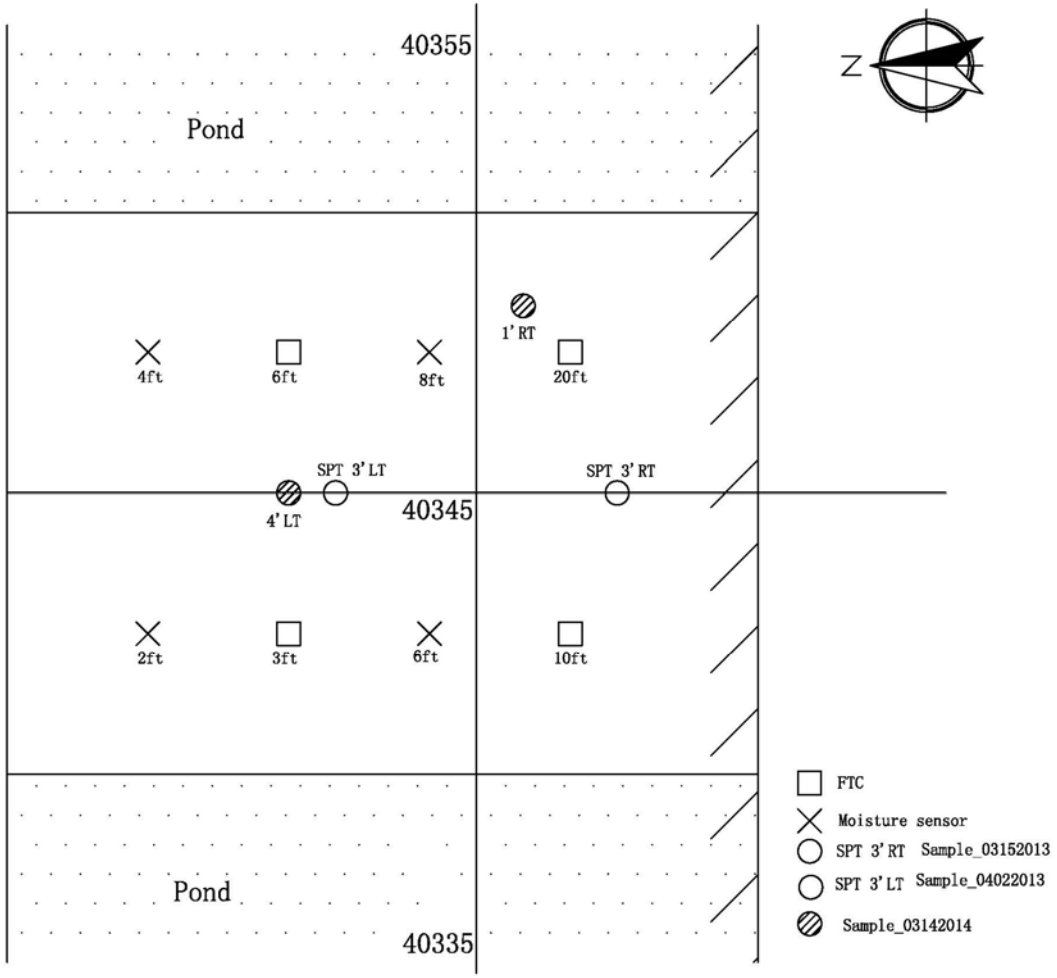

Fig. 5.13 Plan view of the installed sensors and borings at 1:1 slope area

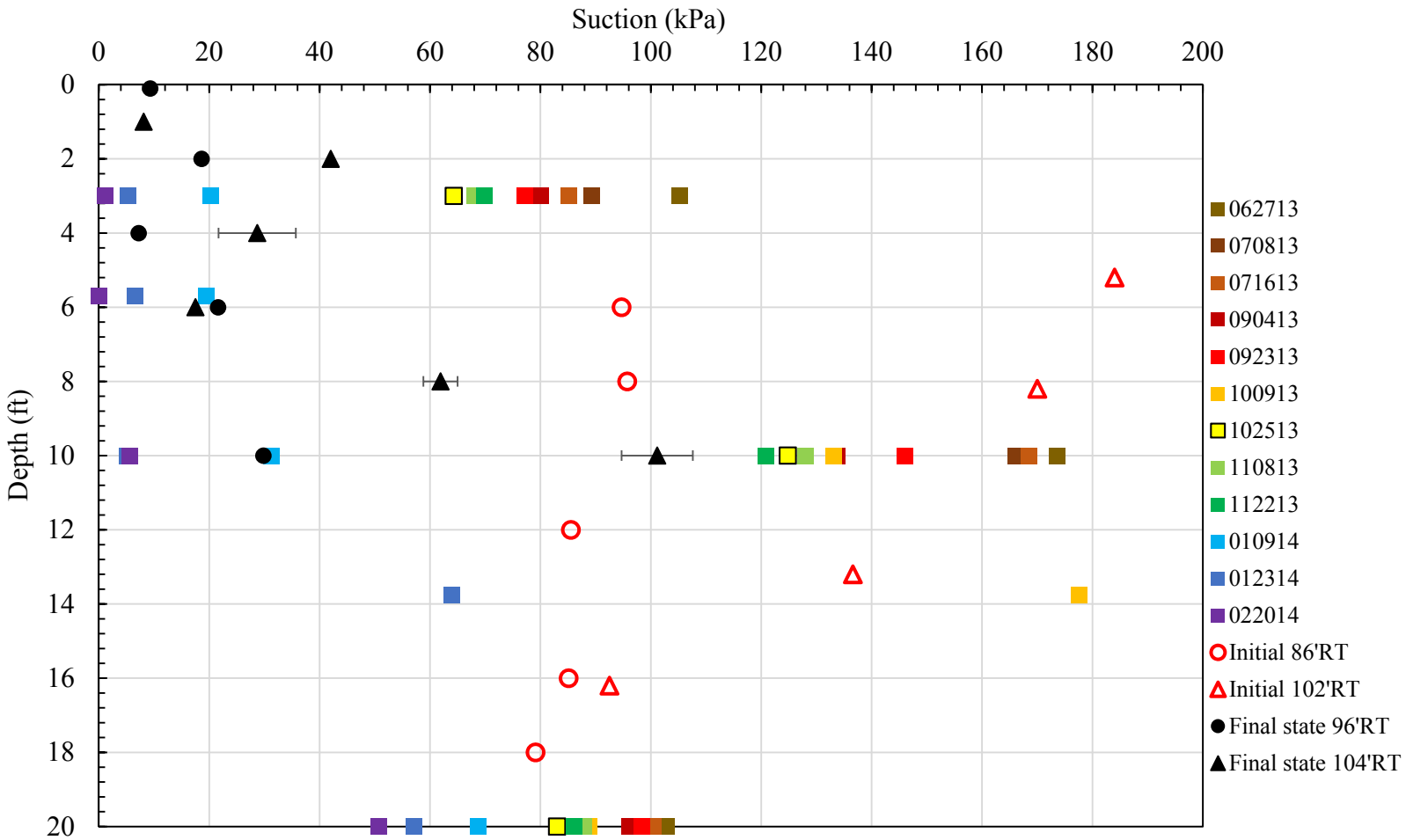

Fig. 5.14 Suction profile of sheet pile wall

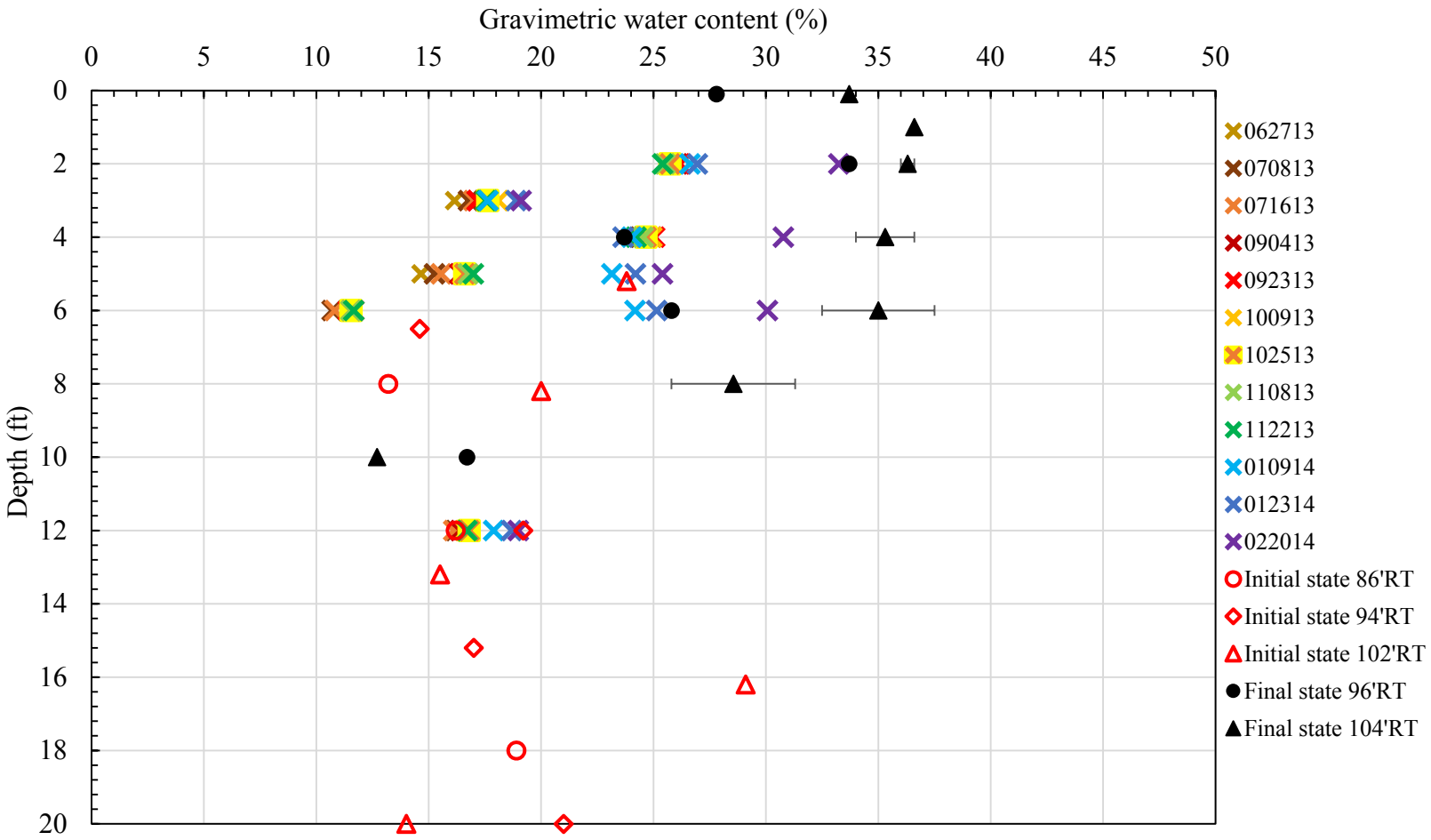

Fig. 5.15 Moisture profile of sheet pile wall

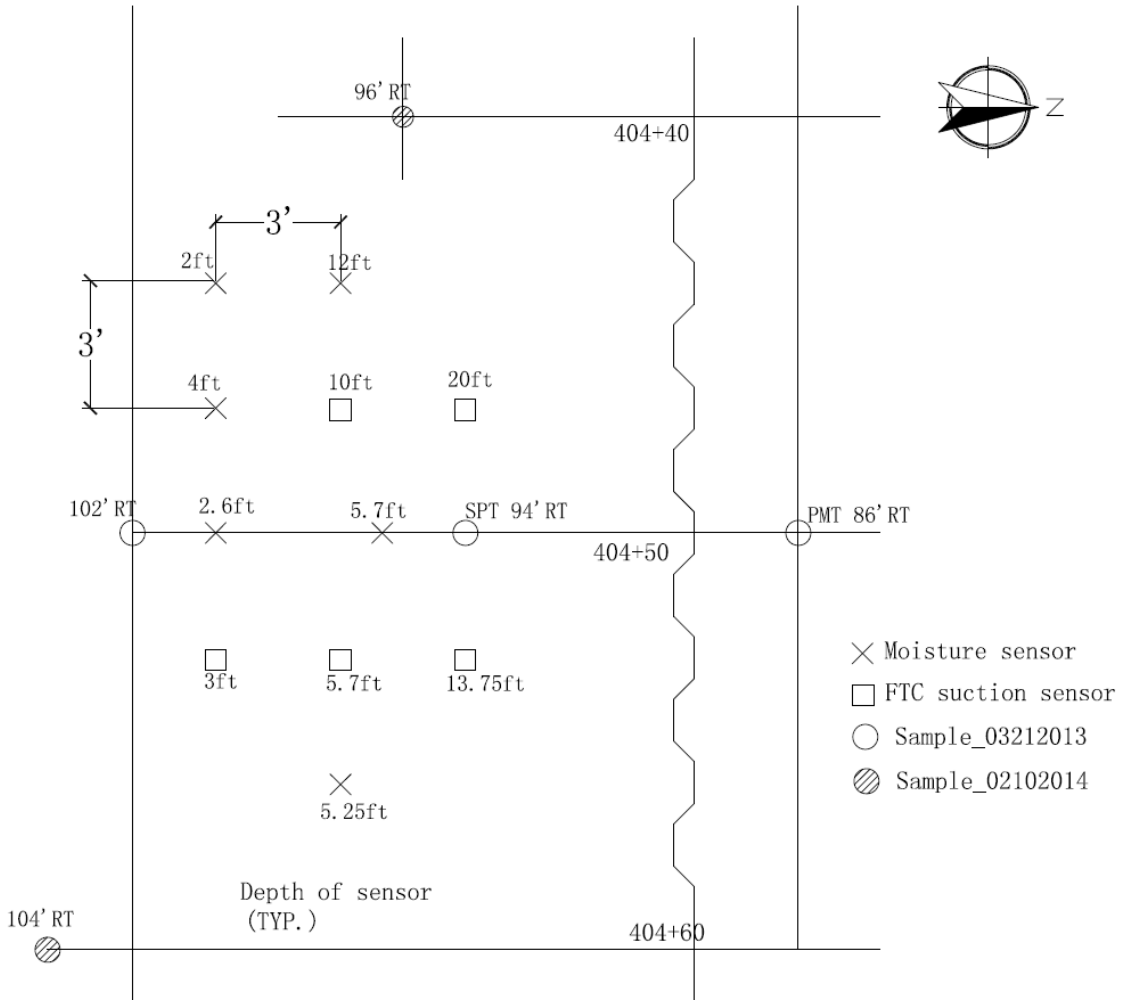

Fig. 5.16 Plan view of the installed sensors and borings at sheet pile wall area

5.4. Presentation and Discussion of Data: Changes in Soil Suction and Moisture Profiles

Infiltration effects observed on 0.5:1 slope

Figures 5.5 and 5.6 indicate the general trend of movement; that is, the soil suction decreased and correspondingly the water content increased. The initial state of the suction profile was nearly constant, about 85 kPa, from 0 feet to 10 feet. At the final state, the suction at the top of ground surface decreased to 20 kPa, and the distribution of the suction profile was stepwise and convergent to the initial state at the depth of 8 feet. Meanwhile, the incremental increase in water content could be observed at 2 feet and 4 feet. The stepwise distribution of the water content profile was also obvious. The distribution of the suction and water content profiles confirms the effect of infiltration at the top of the slope. Also, due to the limited period of time of the infiltration and the permeability of the soil, the infiltration seems to have had less effect on the soil below 8 feet compared with the upper 4 feet.

The phenomenon of the stepwise decrease of the suction profile and increase of the water content profile also was observed in the results obtained by the field-installed suction and moisture sensors. However, some inconsistency in the results was found. Figure 5.5 indicates that the magnitude of the decreasing suction was greater than the actual measurements. Meanwhile, Figure 5.6 shows that the increasing water content determined by the moisture sensors was not exactly the same as the water content of the actual samples. No clear reasons were found for this discrepancy between the monitoring results from the sensors and the actual measurements.

In general, for the 0.5:1 slope, the water in the infiltration ponds was fully absorbed into the soil. This finding is consistent with the actual measured data.

0:25:1 and 1:1 slopes

Suction sensors

Figures 5.8 and 5.11 indicate the inconsistency between the actual measurements and the suction measured by the sensors. For the 0.25:1 and 1:1 slope areas, the actual measurements of the tube samples suggest that the suction and moisture profiles did not move. However, for the 0.25:1 slope, the suction value measured by the FTC suction sensor (Fig. 5.8) was higher than 100 kPa, and the measurement results were lower than 80 kPa. On the other hand, for the 1:1 slope (Fig. 5.11), the sensor-measured suction values were lower than 20 kPa, but the actual measurements taken by the tensiometer were around 60 kPa to 80 kPa.

Moisture sensors

The moisture sensors generally provided satisfactory and expected results at the 4-ft depth of the 0.25:1 slope (Fig. 5.9) and 2-ft depth of the 1:1 slope (Fig. 5.12). The water content measured by the sensors showed consistent results with the measured water content.

Significant drop of suction and increase of water content at the sheet pile wall

Figures 5.14 and 5.15 indicate significant amounts of decreasing suction and increasing water content for the sheet pile wall. The actual measurements show that the decreasing magnitude of suction is about 100 kPa, from close to 130 kPa to 30 kPa. The installed suction sensor readings suggest that the suction at the end of the monitoring is nearly 0 kPa from a depth of 3 feet to 10 feet. The actual water content increased from 16%

to 35%, which was an increase of 16% to 30% from the water content sensor readings. This noteworthy drop in suction and increase in water content are consistent with the actual field conditions.

When the excavation reached a depth of 22 feet from the ground surface, the sheet pile wall moved due to active earth pressure at the back of the wall. A 7-inch gap, as shown in Figure 5.17, appeared between the sheet pile wall and the soil. The water continued to infiltrate the gap and accumulated in the gap. So, instead of a uniformly vertical movement of water from the ground surface to the bottom of the excavated area, there was horizontal water movement due to the water that ponded in the gap. This occurrence explains the significant decrease in soil suction and increase in water content for the sheet pile wall.

Fig. 5.17 Gap between sheet pile wall and the soil

5.5. Initial and final stage suction by using SWCC from the measured water content

The measured suction changes at the initial and final stages were also predicted by using the SWCCs at 4ft depth of 0.5:1 slope area. Knowing the water content at the initial and final stage, the suction values can also be calculated accordingly and the results were also compared with the measured suction as shown in Table 5.2.

Table 5.2 Predicted suction vs measured suction

	Water content (%)	Predicted suction by SWCC (kPa)	Measured suction (kPa)	Difference (%)
Initial stage	28.6	78.1	86.1	-9.3
Final stage	30.3	44.4	49.7	-10.7

The difference between the predicted and measured suction is -9.3% and -10.7%. This can verify the reliability of the actual suction change from the beginning to the end of the project.

5.6. Prediction of the change in the suction profile by the proposed model

Since the suction profiles were monitored, the proposed suction prediction model in section 4 is used here to produce the predicted change of suction profiles. Since the changed of suction at sheet pile wall and 0.5:1 slope area is obvious, the soil properties at those two locations were used here to produce the predicted suction profiles in order to study the predictive ability of the model. By using the measured soil properties, such as grain size

distribution, specific gravity and density information, the SWCC parameters can be predicted by the proposed model which was expressed as equation 4.30, 4.31 and 4.32. The soil properties and predicted SWCC parameters is shown in Table 5.2 and 5.3. This analysis only used the soil properties above upper 10 ft since the monitored change of suction profiles was only at upper 10ft of soil layers. The predicted SWCCs for the soils at sheet pile wall and 0.5:1 slope area are shown in Fig. 5.18-5.21.

Table 5.3 Soil properties at sheet pile wall and predicted SWCC parameters by the proposed model

Depth (ft)	#	D60 (mm)	D30 (mm)	D10 (mm)	5μm (%)	ρd (g/cm^3)	Gs	θs	a	n	m
5.2	70	0.035	0.006	0.001	27.7	1.26	2.7	0.51	29.8	0.74	0.67
13.2	72	0.039	0.014	0.002	16.2	1.73	2.71	0.61	54.6	0.9	0.85

Table 5.4 Soil properties at 0.5:1 slope and predicted SWCC parameters by the proposed model

Depth (ft)	#	D60 (mm)	D30 (mm)	D10 (mm)	5μm (%)	ρd (g/cm^3)	Gs	θs	a	n	m
4	36	0.015	0.005	0.0005	32.5	1.24	2.69	0.54	12.9	0.91	0.46
7	37	0.013	0.003	0.002	35.9	1.15	2.72	0.58	30.9	3.12	0.29

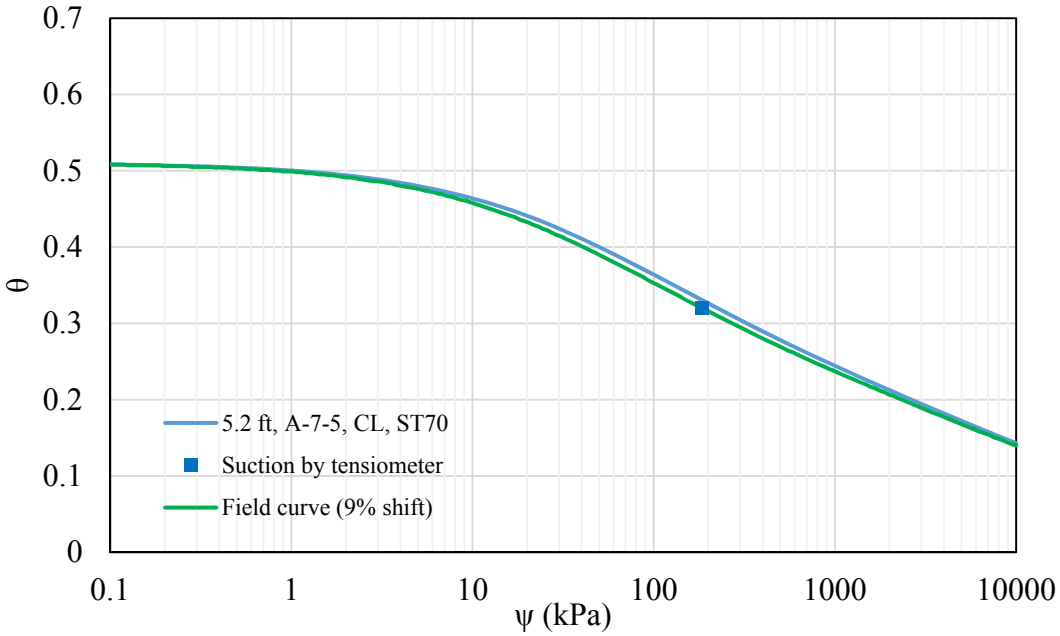

Fig. 5.18 Predicted SWCC and field curve at 5.2 ft of sheet pile wall area

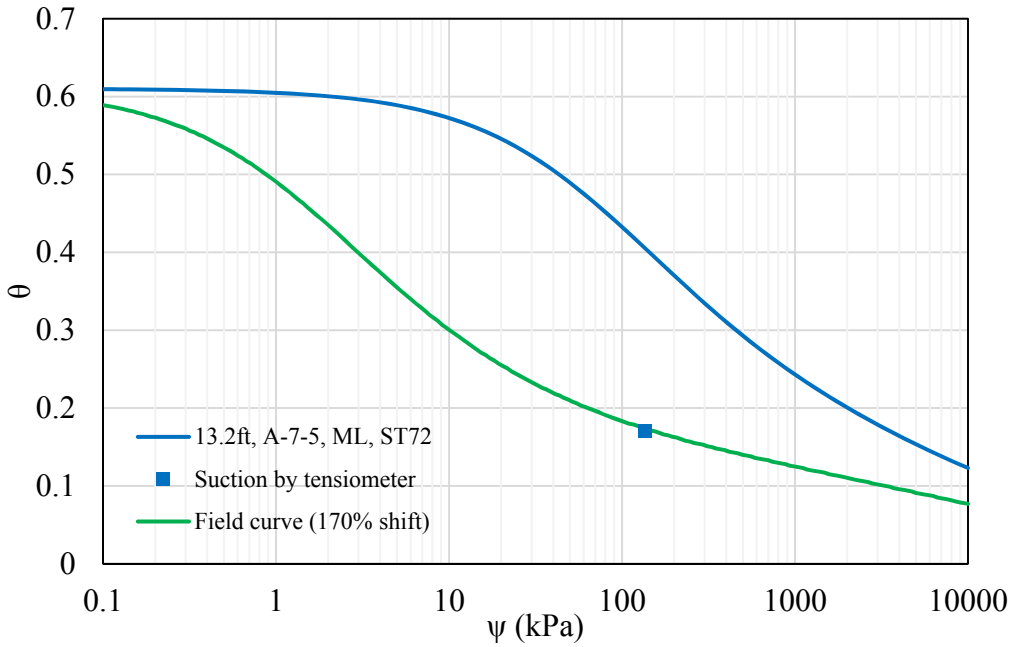

Fig. 5.19 Predicted SWCC and field curve at 13.2 ft of sheet pile wall area

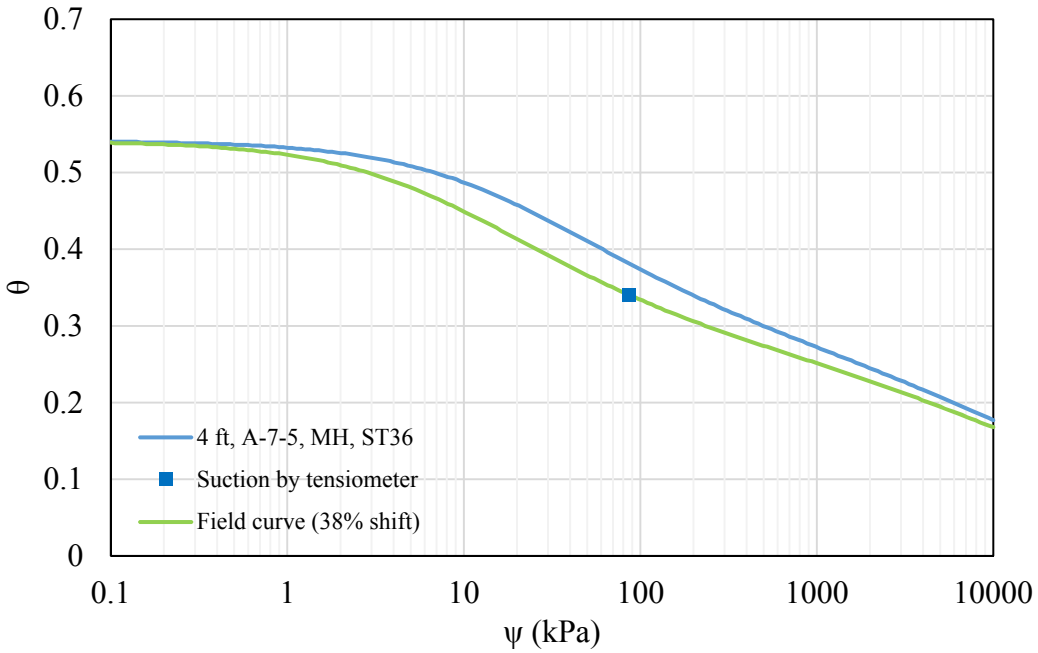

Fig. 5.20 Predicted SWCC and field curve at 4 ft of 0.5:1 slope area

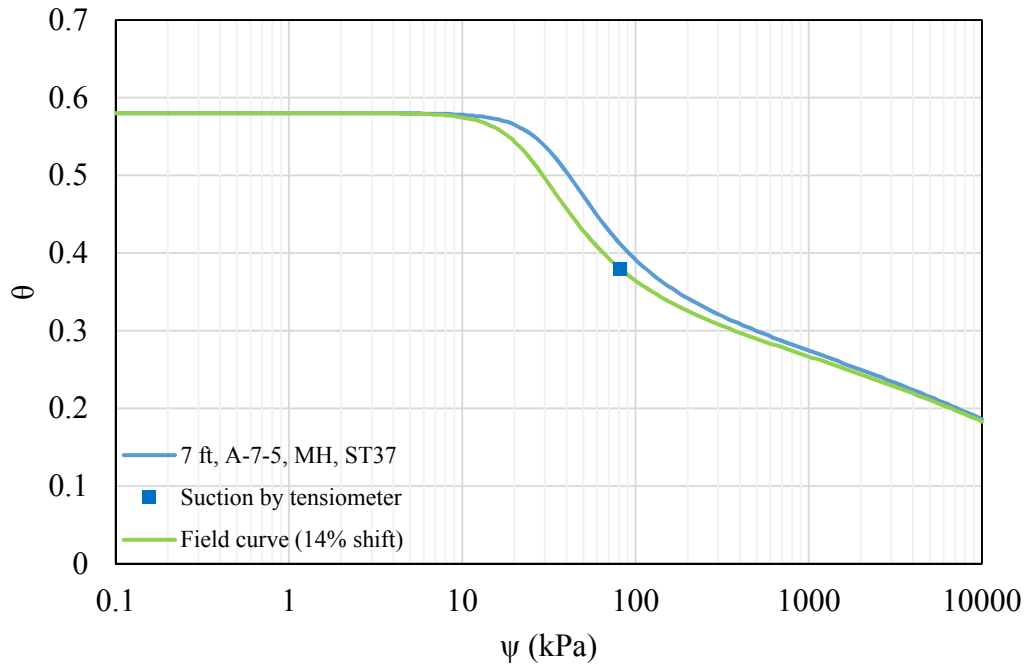

Fig. 5.21 Predicted SWCC and field curve at 7 ft of 0.5:1 slope area

The SWCCs obtained from the suction prediction model were shifted to the point where the suction of soil is tested by tensiometer. So, the field curves were generated for a more precise suction prediction by considering the actual suction condition in the soil. Fig. 18 to 21 also show the corresponding field curves with the predicted drying curves at sheet pile wall and 0.5:1 slope area.

Discussion on predicted suction profiles

Based on the measured water content at the initial and final state of the monitoring process, the suction profiles were predicted and plotted against the actual measured suction as shown in Fig. 5.22 and Fig, 5.23.

Predicted suction profiles at sheet pile wall area

From Fig. 5.22, the predicted suction is reasonable compared with the actual measured suction. For the initial suction state, the predicted suction seems not quite consistent with the measured data. At 5.2 ft, the measure suction is 175 kPa and the predicted suction is 270kPa which is nearly 50% higher. But the actual suction was reaching the maximum measurable range of the tensiometer (85kPa for T5 and 160 kPa for T5x). The actual suction of the soil could have a higher suction potential and the predicted suction might be reasonable from that perspective. At 13.2 ft, the predicted suction is 13kPa and this is lower than the actual measured suction of 130 kPa. This will give a more conservative value from the design point of view.

For the final suction state, the predicted suction is quite close to the measured suction from 0 to 6 ft. But at 10 ft, the predicted suction is 40 kPa which is 60% lower than the actual measured 100kPa.

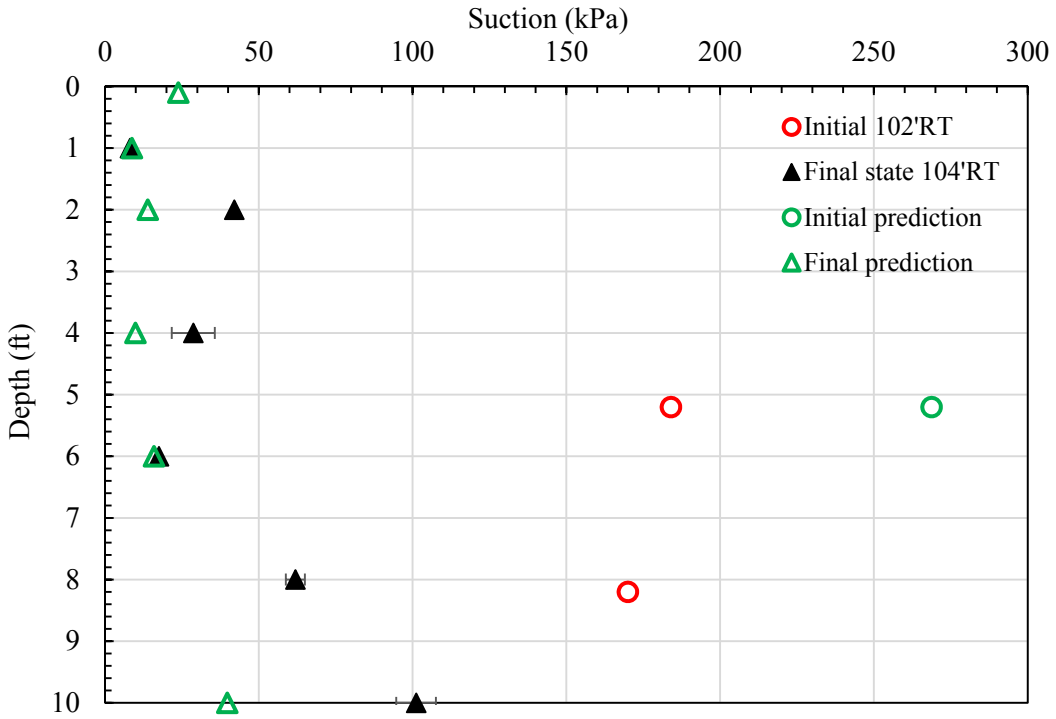

Fig. 5.22 Predicted suction profiles by the proposed model vs measure suction profiles at sheet pile wall area (160kPa is the upper bound of the tensiometer)

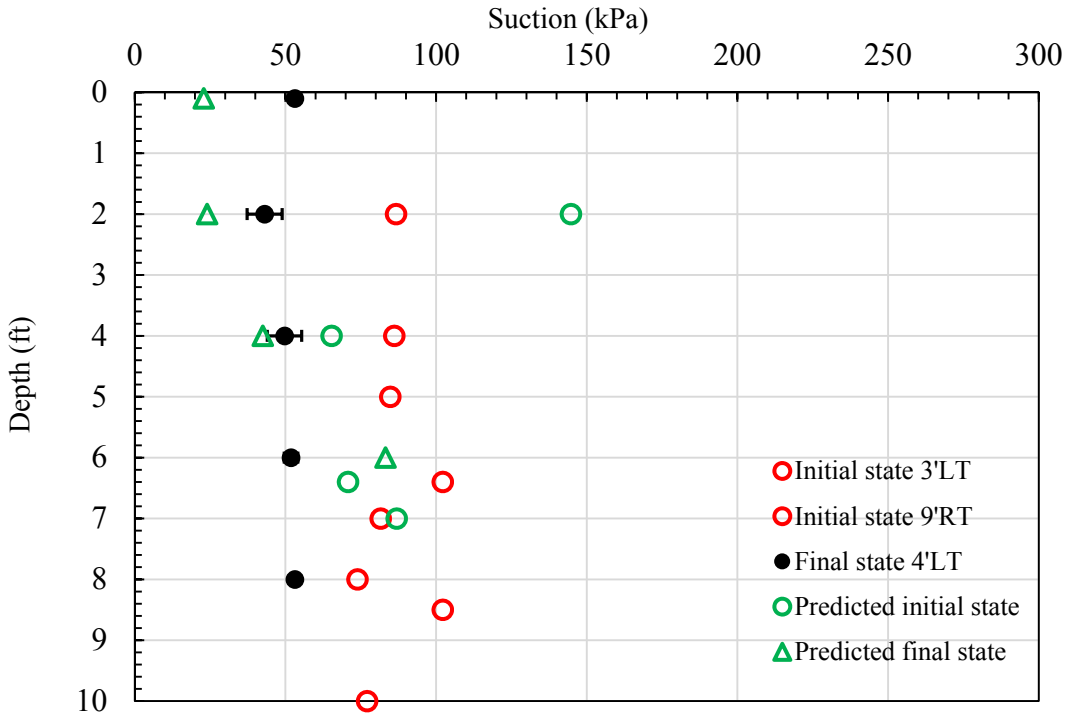

Fig. 5.23 Predicted suction profiles by the proposed model vs measure suction profiles at 0.5:1 slope area

Predicted suction profiles at 0.5:1 slope area

Similar to the results of sheet pile wall area, the predicted suction at initial state was not quite consistent with the measured initial state. At 2 ft, the predicted suction is 140 kPa which is about 50% higher than the measured 90 kPa suction values. But again, over 85 kPa is above the measurable range of tensiometer. So, the actual suction of soil might be higher than the measured suction by tensiometer. At final state, the predicted suction was close to the measured suction from 0 to 4 ft which is consistent with the result in sheet pile wall area.

5.7. Conclusions

A field monitoring program was undertaken to investigate variations in the movement of the suction and moisture profiles over time by monitoring the installed FTC suction sensors and 10HS moisture sensors. The infiltration process could be monitored by the installed sensors. The following conclusions were drawn:

1. The changes in the suction and moisture profiles under the effect of water infiltration were monitored successfully.
2. FTC suction sensors can give inappropriate suction values; nonetheless, the trend of the decrease in suction can still be captured.
3. The moisture sensors can give reasonably satisfactory results and are recommended for future use.
4. The proposed suction prediction model can capture the change of the suction for residual soil and shows reasonable results compared with the measured suction.

6. SUMMARY AND CONCLUSIONS

The objectives of this study were to characterize the suction-related properties of North Carolina residual soils and propose an empirical model to predict soil suction based on basic soil indices. A comprehensive experimental program was designed to study the unsaturated properties of residual soil at a Greensboro test site. A summary of the tests and the major conclusions drawn from this study are presented briefly in the following sections.

6.1. Summary of Tests Performed

Three suction measurement techniques, i.e., tensiometer, filter paper method, and pressure plate tests, were employed in the laboratory to determine soil suction. The corresponding basic soil properties also were investigated to determine the degree to which different factors might affect soil suction. Field instrumentation and monitoring also were employed to study the changes in soil suction due to infiltration. The following steps were taken to perform the tests.

- A test site was selected in Greensboro, North Carolina. Three different slopes (0.25:1, 0.5:1, and 1:1) and a sheet pile wall were constructed, and a 22-ft stage excavation was completed.
- Sixty-four Shelby tube samples were obtained from the test site. For all the undisturbed samples, the soil suction was tested using a tensiometer and the filter paper method. The corresponding basic soil properties, including natural water content, grain size distribution, specific gravity, and Atterberg limits, were investigated. A comprehensive database that incorporated all the tested

suction-related soil properties was developed.

- Tensiometer suction measurements were made on Shelby tube samples taken in the field. The reliability and variability of the T5 and T5x tensiometers were subsquently investigated by testing uniformly compacted soil samples at suction levels of 11 kPa, 23 kPa, 35 kPa, and 68 kPa.
- Twelve SWCCs were determined from pressure plate tests for two soil types: high plasticity silt (MH in USCS and A-7-5 in AASHTO) and low plasticity silt (ML in USCS and A-4 in AASHTO).
- Sixteen FTC suction sensors and 16 moisture sensors were installed in the field. The monitoring process was from June 27, 2013 to March 10, 2014. The slope areas were under man-made infiltration by ponding water on the top of the slopes from February 6, 2014 to the end of monitoring. At the end of the project, 30 Shelby tube samples were obtained to test the soil suction at the post-infiltration stage and to ensure the accuracy of the sensor readings.

6.2. Observations and Conclusions

Based on the results of the pressure plate tests, tensiometer, and filter paper tests, and the statistical analysis of the basic soil properties and the SWCCs, as well as the suction values and water contents obtained from the sensors during field monitoring, the following observations and conclusions are noted in four categories.

1. Characterization of suction-related residual soil properties
    - The suction range of the soil profile was shown to be from 60 kPa to 100 kPa

for the upper 30 feet of the clayey silty zone. Once the material transitions to the sandy silty zone, the suction drops to below 50 kPa. Based on the suction-related soil properties profile, it can be concluded that the soil type, water content, and volume-mass relationship affects the changes in the suction profile.

- The matric suction measured by the filter paper method was seen to be 50% to 150% higher than that measured using the tensiometer. This discrepancy could be due to the fact that the tested material was a silty soil and the contact area between the filter paper and soil sample was not 100% ensured, which may have caused the actual measured matric suction to be a combination of both matric suction and total suction. Other reasons, such as the heterogeneity of the soil, the calibration used for the filter paper method, and the operation during the filter paper test, could also affect the results.
- The tensiometer is recommended as a direct suction measurement tool for future use because of its advantages of quick results and ease of operation.
- A field curve concept is demonstrated to correct the suction value that is obtained from the drying curve. This concept is based on the idea developed by (Fredlund et al. 2011) that the wetting curve can be obtained by shifting the drying curve and that the percentage shift is related to the soil type. By measuring the suction of the Shelby tube samples, which reflects the field condition of the soil, a field curve can be used to correct the suction value obtained from the drying curves.

2. Reliability and variability of tensiometer
    - The duration required for obtaining reliable suction readings was shown to be 20 minutes.
    - Paired sensors, T5 and T5x tensiometers, can provide consistent results for suction testing. No obvious trends were found in the readings between these two types of sensors. No effects of time or suction were found in terms of measurement consistency of the two sensors. These two types of sensors, T5 and T5x, can be treated as independent sensors for pressure levels that are higher than 20 kPa and lower than 70 kPa.
    - For laboratory conditions, two minutes of suction can be considered as a reliable estimate for the 20-minute suction value. In the field condition, the suction tested by tensiometer can be variable due to the insufficient sample equilibrium time.
    - T5 and T5x tensiometers can be used as reliable tools to measure soil suction.

3. Proposed suction prediction model for North Carolina residual soils
    - An empirical model to predict residual soil suction is proposed to correlate the basic soil properties, i.e., grain size distribution, density, and specific gravity, with the parameters of the Fredlund-Xing equation.
    - Compared with the published suction prediction models, Zapata (R^2 = 51%) and SoilVision (R^2 = 48%), the proposed model provides much better fitness, i.e., 93% R^2, to the tested data. The model was verified using the published

data. The predicted suction values derived using the proposed model correlate reasonably well with the actual measured values.

- Considering the variability of the tested data, a suction correction factor of 0.94 should be applied to the predicted suction values at 95% confidence limit for engineering design.

4. Field instrumentation for monitoring the changes in the suction and moisture profiles
    - The changes in the suction and moisture profiles under the effect of infiltration were monitored successfully.
    - FTC suction sensors can give inappropriate suction values; nonetheless, the trend of a decrease in suction can be captured.
    - Moisture sensors can give reasonably satisfactory results and are recommended for future use.
    - Predicted suction profiles by the proposed model can give reasonable results.

6.3. Recommendations for Future Research

Based on the conclusions from this research, the future recommendations are proposed:

1) To improve the predictive ability of the proposed model, more pressure plate tests can be performed. Because the proposed suction prediction model is based on statistical analysis, more samples included in the model will allow better representation and prediction ability.
2) For studying the infiltration effect on the suction change, the wetting soil water characteristic curve is necessary to be tested. Since the drying curve is the upper bound of the suction at a given volumetric water content, the actual in situ suction would be located on a certain scanning curve in between the drying and wetting curves. Knowing the wetting curve which is the lower bound of the SWCCs, the tests of the wetting curves are very necessary.
3) To incorporate the suction predicted by the proposed model into shear strength analysis and slope stability analysis. Based on the basic soil properties (GSD characterization, dry density and specific gravity), the soil suction can be easily predicted. It will be very helpful to understand the influence of the suction on the shear strength if the predicted suction can be used in strength analysis.

7. REFERENCES

Anderson, M. G., and Richards, K. S. (1987). *Slope stability: geotechnical engineering and geomorphology.* John Wiley & Sons.

Arya, L. M., and Paris, J. F. (1981). "A physicoempirical model to predict the soil moisture characteristic from particle-size distribution and bulk density data." *Soil Sci.Soc.Am.J.,* 45(6), 1023-1030.

Au, S. (1998). "Rain-induced slope instability in Hong Kong." *Eng.Geol.,* 51(1), 1-36.

Bittelli, M., and Flury, M. (2009). "Errors in Water Retention Curves Determined with Pressure Plates." *Soil Science Society of America Journal,* 73(5), 1453-1460.

Bouma, J. (1989). "Using soil survey data for quantitative land evaluation." *Advances in soil science,* Springer, 177-213.

Chandler, R. J., and Gutierrez, C. I.,. (1986). "Filter-paper method of suction measurement." *Géotechnique,* 36(2), 265-268.

Chin, K., Leong, E., and Rahardjo, H. (2010). "A simplified method to estimate the soil-water characteristic curve." *Canadian Geotechnical Journal,* 47(12), 1382-1400.

Cornelis, W. M., Ronsyn, J., Van Meirvenne, M., and Hartmann, R. (2001). "Evaluation of pedotransfer functions for predicting the soil moisture retention curve." *Soil Sci.Soc.Am.J.,* 65(3), 638-648.

Cui, Y. J., Tang, A. M., Mantho, A. T., and De Laure, E. (2008). "Monitoring field soil suction using a miniature tensiometer." *Geotechnical Testing Journal,* 31(1), 95-100.

Diaz-Padilla, J., and Vanmarcke, E. H. (1974). *Settlement of Structures on Shallow Foundations: A Probabilistic Analysis.* Department of Civil Engineering, Massachusetts Institute of Technology.

Feng, M. (1999). "The effects of capillary hysteresis on the matric suction measurement using themral conductivity sensors". Maser of science. Department of Civil Engineering, University of Saskatchewan.

Feng, M., Fredlund, D. G., and Shuai, F. (2002). "A Laboratory Study of the Hysteresis of A Thermal Conductivity Soil Suction Sensor." *Geotechnical Testing Journal,* 25(3), 1-12.

Feng, M., and Fredlund, D. G. (2003). "Calibration of thermal conductivity sensors with consideration of hysteresis." *Canadian Geotechnical Journal,* 40(5), 1048-1055.

Fredlund, D. G., Rahardjo, H., and Fredlund, M. D. (2012). *Unsaturated Soil Mechanics in Engineering Practice.* Wiley, New Jersey.

Fredlund, D. G., and Morgenstern, N. R. (1977). "Stress state variables for unsaturated soils." *J.Geotech.Geoenviron.Eng.,* 103.

Fredlund, D. G., Rahardjo, H., and Fredlund, M. D. (2012). *Unsaturated soil mechanics in engineering practice.* Wiley.

Fredlund, D. G., Sheng, D., and Zhao, J. (2011). "Estimation of soil suction from the soil-water characteristic curve." *Canadian Geotechnical Journal,* 48(2), 186-198.

Fredlund, D. G., and Xing, A. (1994). "Equations for the soil-water characteristic curve." *Canadian Geotechnical Journal,* 31(4), 521-532.

Fredlund, D., Morgenstern, N., and Widger, R. (1978). "The shear strength of unsaturated soils." *Canadian Geotechnical Journal,* 15(3), 313-321.

Fredlund, M. D., Fredlund, D. G., and Wilson, G. (1997). "Prediction of the soil-water characteristic curve from grain-size distribution and volume-mass properties." *Proc., 3rd Brazilian Symp. on Unsaturated Soils,* Rio de Janeiro, 13-23.

Fredlund, M. D., Fredlund, D., and Wilson, G. W. (2000). "An equation to represent grain-size distribution." *Canadian Geotechnical Journal,* 37(4), 817-827.

Guan, Y., and Fredlund, D. (1997). "Use of the tensile strength of water for the direct measurement of high soil suction." *Canadian Geotechnical Journal,* 34(4), 604-614.

Gupta, S., and Larson, W. (1979). "Estimating soil water retention characteristics from particle size distribution, organic matter percent, and bulk density." *Water Resour.Res.,* 15(6), 1633-1635.

He, L., Leong, E. C., and Elgamal, A. (2006). "A miniature tensiometer for measurement of high matric suction." *Geotech Spec Publ,* 147(2), 1897.

Heartz, William. (1986). "Properties of a Piedmont residual soil". PhD. North Carolina State University, Raleigh, N.C.

Houston, S. L., Houston, W. N., and Wagner, A. M. (1994). "Laboratory Filter Paper Suction Measurements." *Geotechnical Testing Journal,* 17(2), 185-194.

Houston, W., Dye, H., Zapata, C., Perera, Y., and Harraz, A. (2006). "Determination of SWCC using one point suction measurement and standard curves." *Unsaturated Soils 2006,* ASCE, 1482-1493.

Iyer, K., Jayanth, S., Gurnani, S., and Singh, D. (2012). "Influence of initial water content and specimen thickness on the SWCC of fine-grained soils." *International Journal of Geomechanics,* 13(6), 894-899.

Johari, A., Habibagahi, G., and Ghahramani, A. (2006). "Prediction of soil–water characteristic curve using genetic programming." *J.Geotech.Geoenviron.Eng.,* 132(5), 661-665.

Leong, E. C., He, L., and Rahardjo, H. (2002). "Factors Affecting the Filter Paper Method for Total and Matric Suction Measurements." *Geotechnical Testing Journal,* 25(3), 322-333.

Leong, E. C., and Rahardjo, H. (1997). "Review of soil-water characteristic curve equations." *J.Geotech.Geoenviron.Eng.,* 123(12), 1106-1117.

Leong, E. C., Zhang, X. -., and Rahardjo, H. (2012). "Calibration of a thermal conductivity sensor for field measurement of matric suction." *Geotechnique,* 62(1), 81-85.

Likos, W. J., and Lu, N. (2002). "Filter paper technique for measuring total soil suction." *Transportation Research Record: Journal of the Transportation Research Board,* 1786(1), 120-128.

Lu, N., and Likos, W. J. (2004). *Unsaturated soil mechanics.* Wiley.

Mahler, C. F., and Mendes, C. A. R. (2005). "Measurement of Suction of Thick Textured Soil using Filter Paper Method and Equivalent Tensiometer - EQT." *Proceedings of the International Conference" From Experimental Evidence towards Numerical Modeling of Unsaturated Soils,",* Springer, Weimar, Germany, 183-192.

Marinho, F., and da Silva Gomes, J. E. (2012). "The Effect of Contact on the Filter Paper Method for Measuring Soil Suction." *Geotechnical Testing Journal,* 35(1), 1-10.

Meilani, I., Rahardjo, H., Leong, E., and Fredlund, D. G. (2002). "Mini suction probe for matric suction measurements." *Canadian Geotechnical Journal,* 39(6), 1427-1432.

Monroy, R., Zdravkovic, L., and Ridley, A. (2012). "Random Uncertainty in the Measurement of Matric Potential Using the Miniature Tensiometer." *ASTM Geotechnical Testing Journal,* 35(1), 41-49.

Mualem, Y. (1976). "A new model for predicting the hydraulic conductivity of unsaturated porous media." *Water Resour.Res.,* 12(3), 513-522.

Mundorff, M. J. (1948). *Geology and ground water in the Greensboro area, North Carolina.* North Carolina, Department of Conservation and Development.

Neter, J., Kutner, M. H., Nachtsheim, C. J., and Wasserman, W. (1996). "Applied linear regression models, 1996." *Irwin, Chicago, USA.p,* 1050.

Nichol, C., Smith, L., and Beckie, R. (2003). "Long-term measurement of matric suction using thermal conductivity sensors." *Canadian Geotechnical Journal,* 40(3), 587-597.

Noguchi, T., Mendes, J., and Toll, D. G. (2011). "Comparison of soil water retention curves obtained by filter paper, high capacity suction probe and pressure plate." *Unsaturated soils : theory and practice : proceedings of the 5th Asia-Pacific Conference on Unsaturated Soils,* Pattaya, Thailand, 409414.

Perera, Y., Zapata, C., Houston, W., and Houston, S. (2005). "Prediction of the soil–water characteristic curve based on grain-size-distribution and index properties." *Advances in Pavement Engineering (Ed.EM Rathje), Geotechnical Special Publication,* 130 49-60.

Perera, Y. Y., and Fredlund, D. G. (2004). "Measurement of Soil Suction In Situ Using the Fredlund Thermal Conductivity Sensor." *Presentation Material for Mining and Waste Management Short Course,* 1-17.

Pham, H. Q. (2002). "An engineering model of hysteresis fro the soil-water characteristic curve". Master. University of Saskatchewan, Saskatoon, SK.

Pham, H., Fredlund, D., and Barbour, S. (2003). "A practical hysteresis model for the soil-water characteristic curve for soils with negligible volume change." *Géotechnique,* 53(2), 293-298.

Power, K. C., Vanapalli, S. K., and Garga, V. K. (2008). "A Revised Contact Filter Paper Method." *Geotechncial Testing Journal,* 31(6), 461-469.

Rahardjo, H., Satyanaga, A., Leong, E. C., Ng, Y. S., and Tam, H. (2012). "Variability of residual soil properties." *Engineering Geology,* 141-142 124-140.

Rahardjo, H., Satyanaga, A., and Leong, E. C. (2011). "Unsaturated soil mechanics for slope stabilization." .

Randy Rainwater, N., Mcdowell, L. A., and Drumm, E. C. (2001). "Measurement of total soil suction using filter paper: investigation of common filter papers, alternative media, and corresponding confidence." *Geotechncial Testing Journal,* 35(2), 295-304.

Rawls, W., Brakensiek, D., and Saxton, K. (1982). "Estimation of soil water properties." *Trans.ASAE,* 25(5), 1316-1320.

Ridley, A., and Burland, J. (1996). "A pore water pressure probe for the in situ measurement of a wide range of soil suctions." *ADVANCES IN SITE INVESTIGATION PRACTICE. PROCEEDINGS OF THE INTERNATIONAL CONFERENCE HELD IN LONDON ON 30-31 MARCH 1995.* .

Ridley, A., and Burland, J. (1993). "A new instrument for the measurement of soil moisture suction." *Géotechnique,* 43(2).

Ryan, T. A., Joiner, B. L., and Ryan, B. F. (1982). *Minitab reference manual.* Pennsylvania State University, Statistics Department..

Sattler, P., and Fredlund, D. G. (1989). "Use of thermal conductivity sensors to measure matric suction in the laboratory." *Canadian Geotechnical Journal,* 26 491-498.

Saxton, K., Rawls, W., Romberger, J., and Papendick, R. (1986). "Estimating generalized soil-water characteristics from texture." *Soil Sci.Soc.Am.J.,* 50(4), 1031-1036.

Scheinost, A., Sinowski, W., and Auerswald, K. (1997). "Regionalization of soil water retention curves in a highly variable soilscape, I. Developing a new pedotransfer function." *Geoderma,* 78(3), 129-143.

Shuai, F., Clements, C., Ryland, L., and Fredlund, D. G. (2002). "Some factors that influence soil suction measurements using a thermal conductivity sensor." *UNSAT 2002, Proceedings of the 3rd international conference on unsaturated soils,* Recife, Brazil, 325-329.

Sillers, W. S., and Fredlund, D. G. (2001). "Statistical assessment of soil-water characteristic curve models for geotechnical engineering." *Canadian Geotechnical Journal,* 38(6), 1297-1313.

Sowers, G., and Richardson, T. (1983). "Residual Soils of Piedmont and Blue Ridge." *Transp.Res.Rec.,* (919),.

Sweeney, D. (1982). "Some in situ soil suction measurements in Hong Kong's residual soil slopes." *Proceedings of the 7th Southeast Asian Geot. conference, Hong Kong,* 91-106.

Take, W. A., and Bolton, M. D. (2003). "Tensiometer saturation and the reliable measurement of soil suction." *Géotechnique,* 53(2), 159-172.

Tan, E., Fredlund, D. G., and Marjerison, B. (2007). "Installation procedure for thermal conductivity matric suction sensors and analysis of their long-term readings." *Canadian Geotechnique Journal,* 44(2), 113-125.

Tarantino, A., and De Col, E. (2008). "Compaction behaviour of clay." *Géotechnique,* 58(3), 199-213.

Tarantino, A., Gallipoli, D., Augarde, C. E., De Gennaro, V., Gomez, R., Laloui, L., Mancuso, C., El Mountassir, G., Munoz, J. J., Pereira, J. -., Peron, H., Pisoni, G., Romero, E., Raveendiraraj, A., Rojas, J. C., Toll, D. G., Tombolato, S., and Wheeler, S. (2011). "Benchamark of experimental technique for measuring and controlling suction." *Geotechnique,* 61(4), 303-312.

Thakur, V. K., Sreedeep, S., and Singh, D. N. (2007). "Evaluation of various pedo-transfer functions for developing soil-water characteristic curve of a silty soil." *Geotech Test J,* 30(1), 25.

Tietje, O., and Tapkenhinrichs, M. (1993). "Evaluation of pedo-transfer functions." *Soil Sci.Soc.Am.J.,* 57(4), 1088-1095.

Townsend, F. C. (1985). "Geotechnical characteristics of residual soils." *J.Geotech.Eng.,* 111(1), 77-94.

Triola, M. F. (1998). *Elementary Statistics, School Version.* Addison-Wesley. .

Van Genuchten, M. T. (1980). "A closed-form equation for predicting the hydraulic conductivity of unsaturated soils." *Soil Sci.Soc.Am.J.,* 44(5), 892-898.

Vanapalli, S. K., Fredlund, D. G., and Pufahl, D. E. (1999). "The influence of soil structure and stress history on the soil-water characteristics of a compacted till." *Géotechnique,* 49(2), 143-159.

Vanapalli, S. K., Fredlund, D. G., Pufahl, D. E., and Clifton, A. W. (1996). "Model for the prediction of shear strength with respect to soil suction." *Canadian Geotechnical Journal,* 33(3), 379-392.

Vereecken, H., Maes, J., Feyen, J., and Darius, P. (1989). "Estimating the soil moisture retention characteristic from texture, bulk density, and carbon content." *Soil Sci.,* 148(6), 389-403.

Wang, C. E., and Borden, R. H.,. (1996). "Deformation characteristics of piedmont residual soils." *Journal of of Geotechnical Engineering,* 122(10), 822-830.

Wang, X., and Benson, C. (2004). "Leak-Free Pressure Plate Extractor for Measuring the Soil Water Characteristic Curve." *Geotechncial Tesing Journal,* 27(2), 1-10.

Yang, H., Rahardjo, H., Leong, E., and Fredlund, D. G. (2004). "Factors affecting drying and wetting soil-water characteristic curves of sandy soils." *Canadian Geotechnical Journal,* 41(5), 908-920.

Zapata, C. E., and Houston, W. N. (2008). *Calibration and validation of the enhanced integrated climatic model for pavement design.* Transportation Research Board..

Zapata, C. E., Houston, W. N., Houston, S. L., and Walsh, K. D. (2000). "Soil-water characteristic curve variability." *Geotech Spec Publ,* (99), 84-124.

Zhai, Q., and Rahardjo, H. (2012). "Determination of soil–water characteristic curve variables." *Comput.Geotech.,* 42 37-43.

APPENDICES

APPENDIX A: PROFILES OF SUCTION-RELATED SOIL PROPERTIES

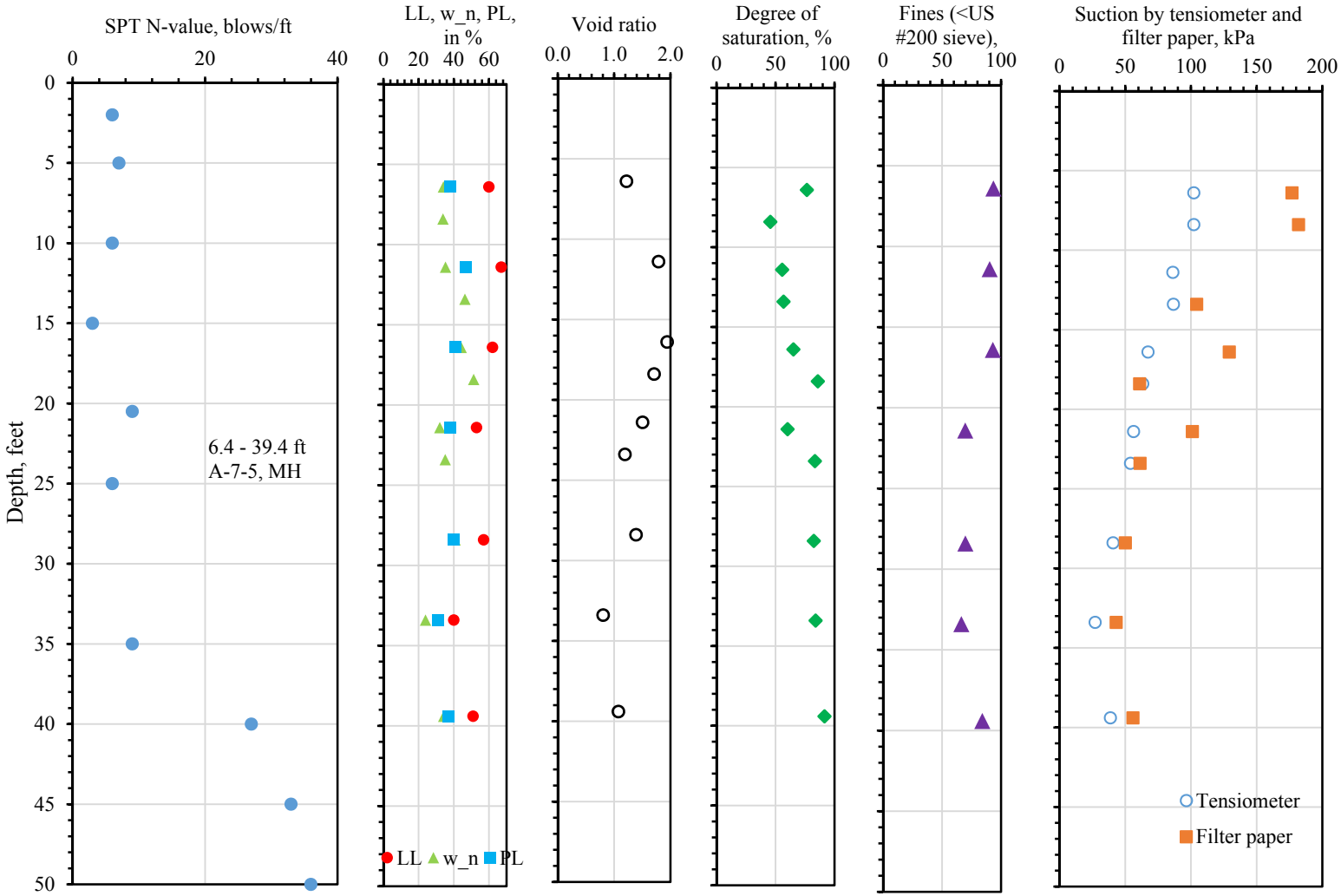

Profile of SPT N-value, moisture content, void ratio, degree of saturation, fines, and suction for 405+70 9’RT

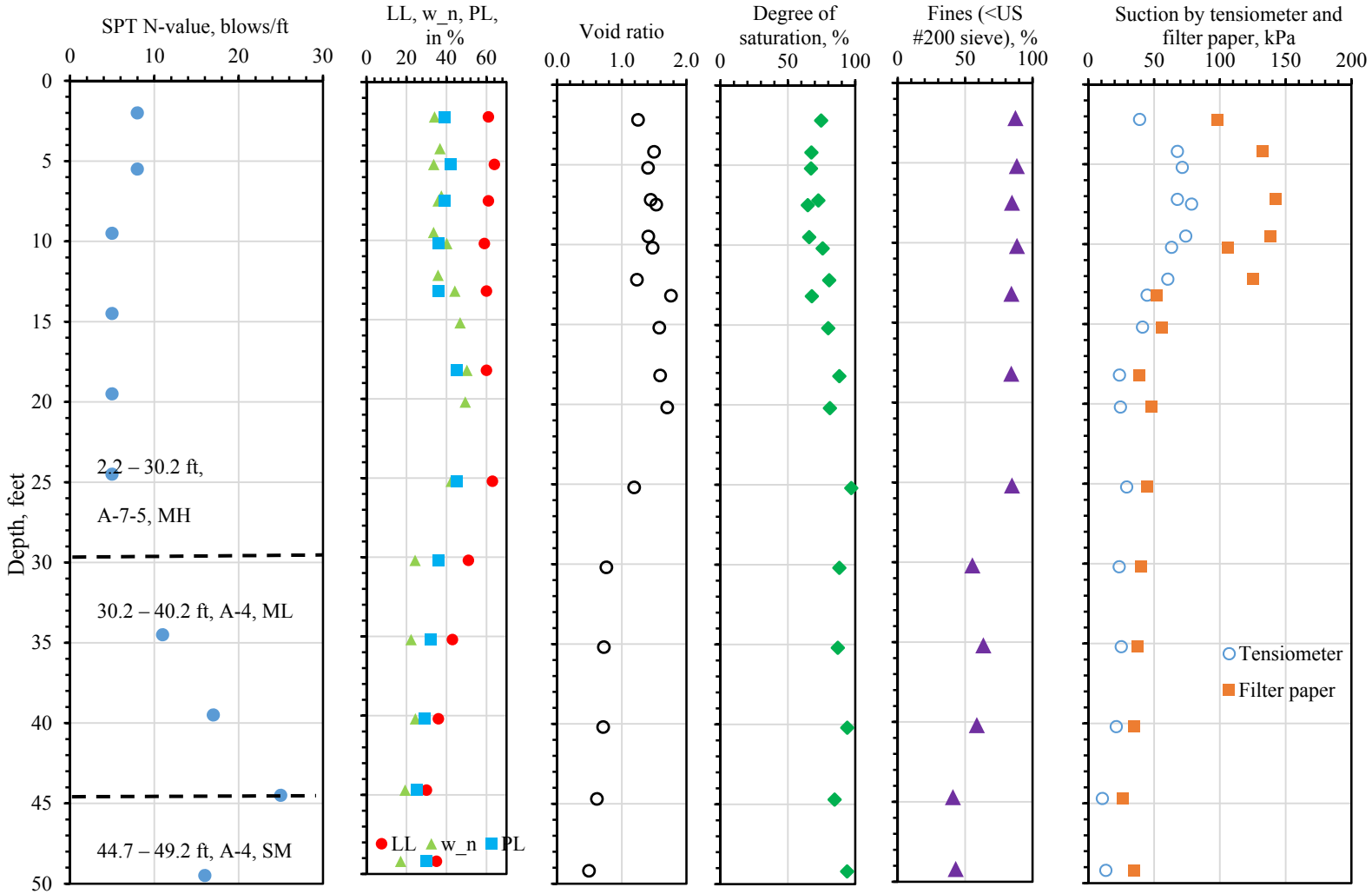

Profiles of SPT N-value, moisture content, void ratio, degree of saturation, fines, and suction for 404+50 3'LT

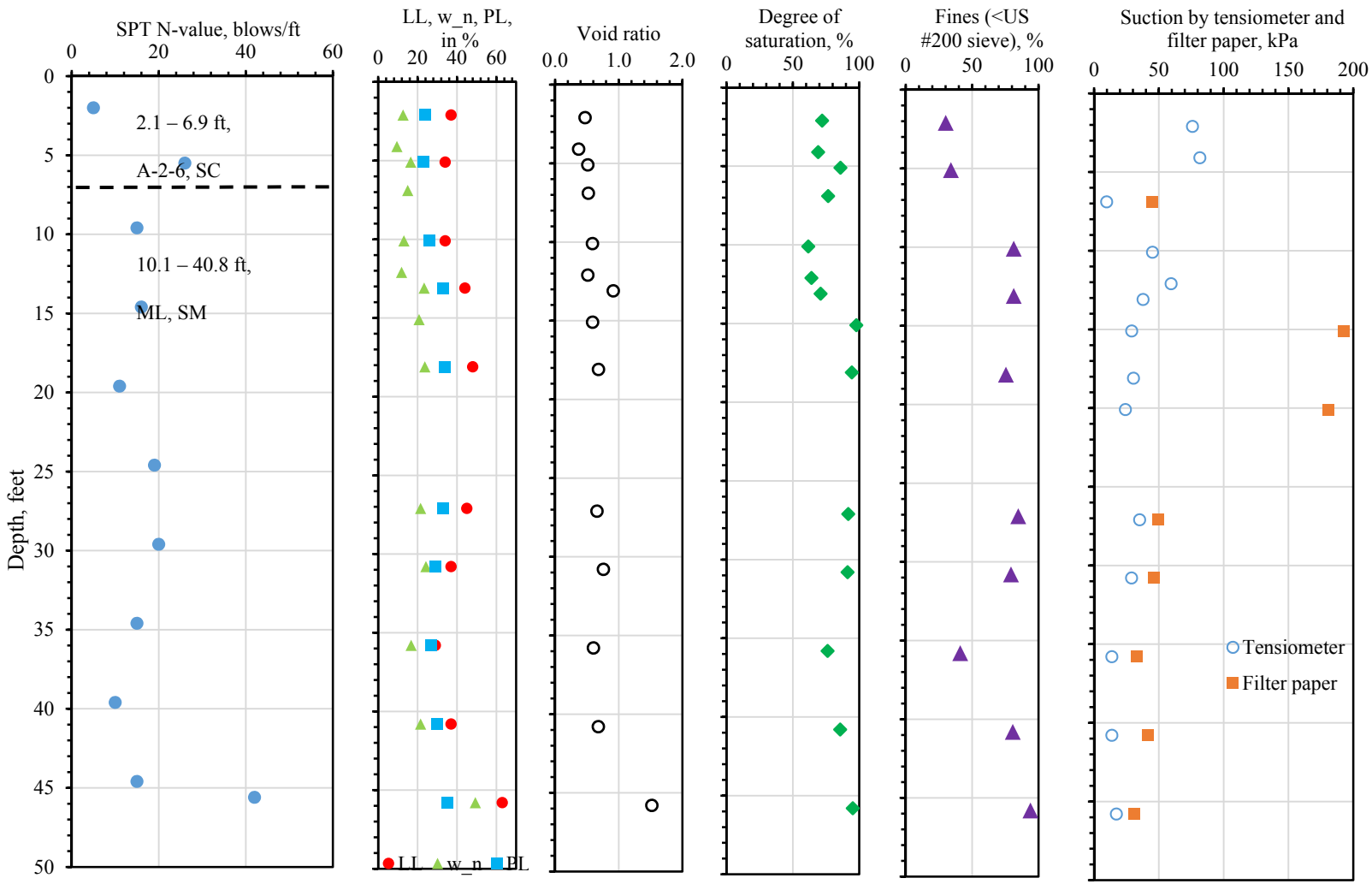

Profiles of SPT N-value, moisture content, void ratio, degree of saturation, fines, and suction for 403+45 3’LT

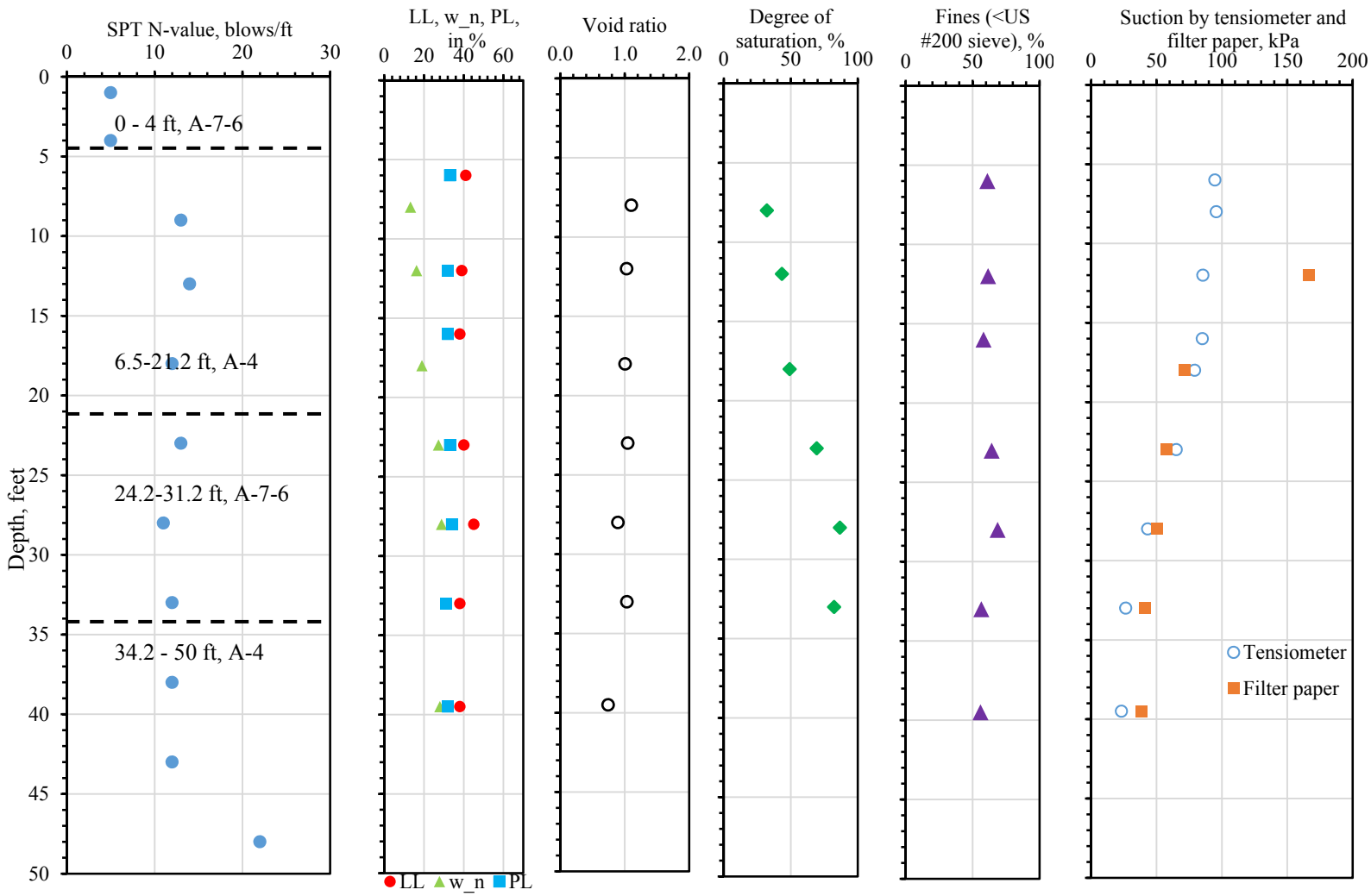

Profiles of SPT N-value, moisture content, void ratio, degree of saturation, fines, and suction for 404+50 86'RT

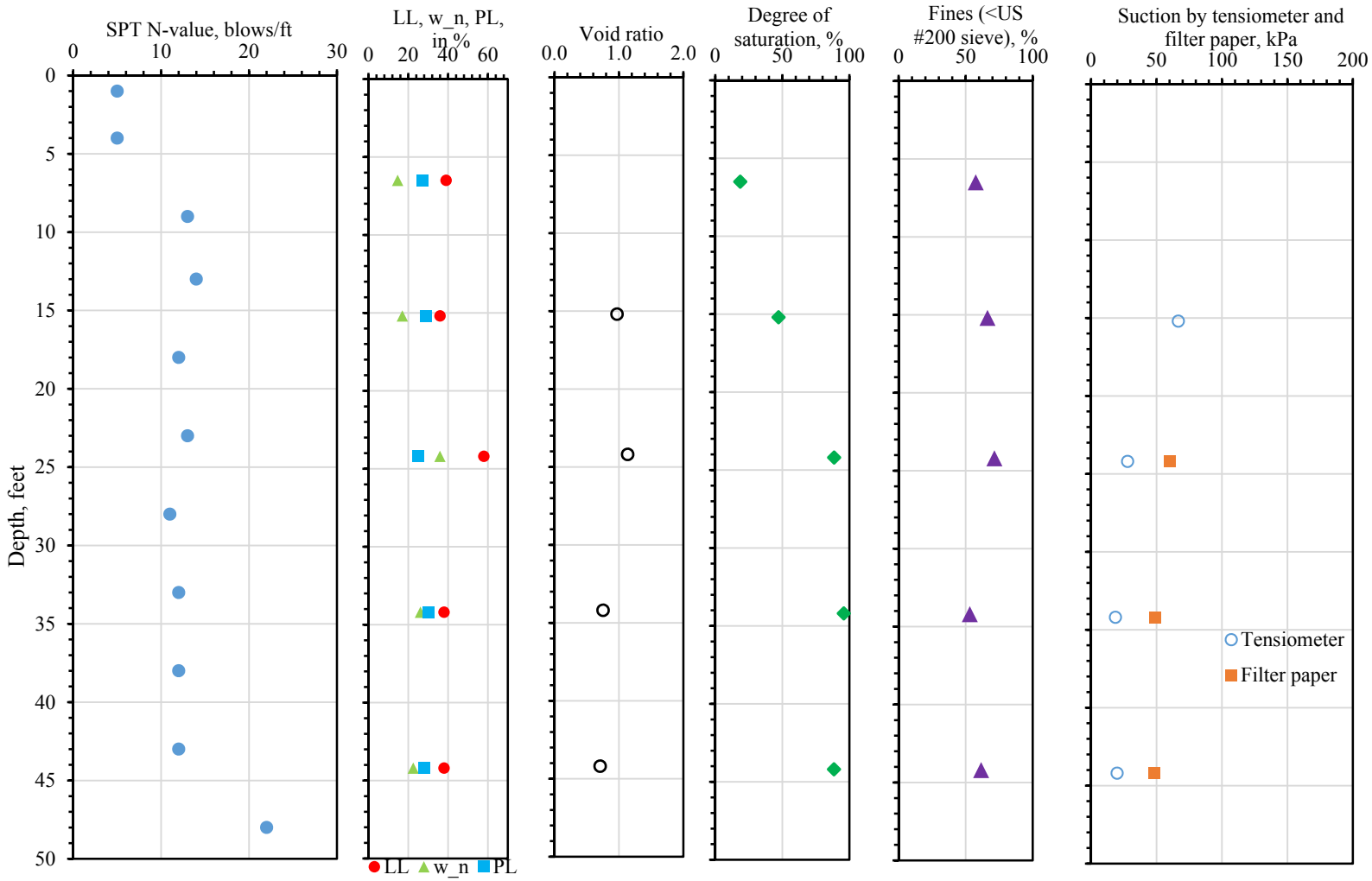

Profiles of SPT n-value, moisture content, void ratio, degree of saturation, fines, and suction for 404+50 94'RT

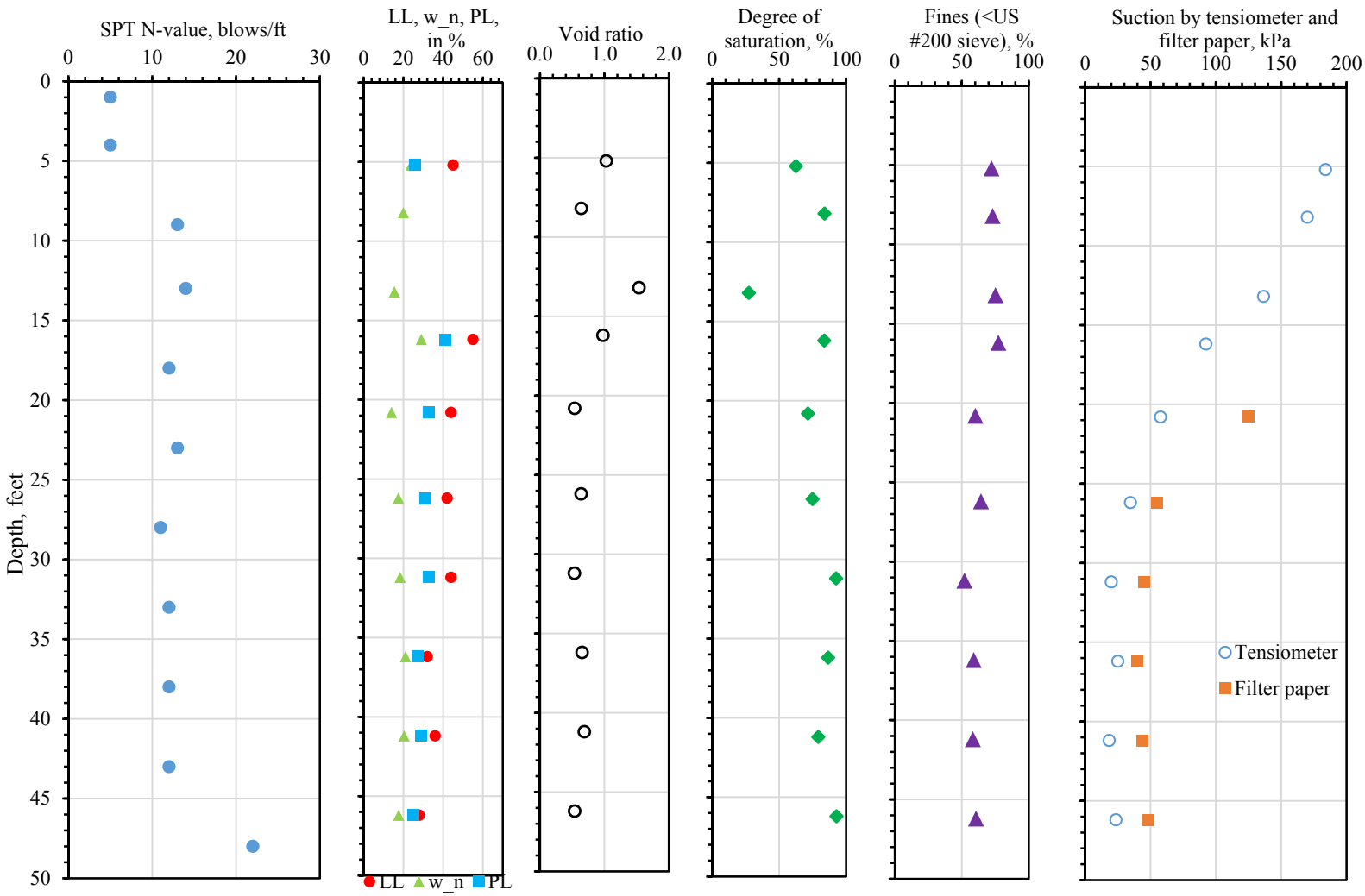

Profiles of SPT N-value, moisture content, void ratio, degree of saturation, fines, and suction for 404+50 102'RT

APPENDIX B: DATABASE OF SUCTION RELATED SOILPROPERTIES

ψ_t	Tensiometer suction
ψ_f	Filter paper suction
w_f	Filter paper sample water content

0.5:1 slope 405+70 3'LT																					
#	Depth	Soil Type		w	γ_d	γ_t	G_s	S	e	θ_w	θ_s	#200	5μm	2μm	LL	PL	PI	Tensiometer	ψ_t	Filter paper	ψ_f	w_f
	(ft)	(AASHTO)	(USCS)	(%)	(pcf)	(pcf)		(%)				(%)	(%)	(%)				time	(kPa)	time	(kPa)	(%)
ST36	2.0	A-7-5	MH	25.8	80	100	2.69	63	1.11	0.33	0.53	83.5	32.5	22.3	50	34	16	7/12/13	86.7			
	4.0			28.6	76	97		63	1.22	0.35	0.55							7/12/13	86.1	7/19/13	268.6	27.6
																		9/18/13	86.0	9/30/13	179.3	
ST37	5.0	A-7-5	MH	38.9	61	84	2.72	59	1.79	0.38	0.64	87.4	22.8	14.0	47	35	12	7/17/13	84.8			
	7.0			32.6	72	95		65	1.36	0.38	0.58							7/17/13	81.6	7/24/13	163.2	29.8
ST38	8.0	A-7-5	MH	29.5	61	79	2.72	45	1.79	0.29	0.64	94.6	31.7	21.5	61	40	21	7/17/13	73.9			
																		10/18/13	79.6	10/30/13	441.2	29.1
	10.0			35.0	67	91		62	1.52	0.38	0.60							7/17/13	77.1	7/24/13	128.1	33.0
ST39	16.0	A-7-5	MH	41.3	58	82	2.72	58	1.93	0.38	0.66	85.8	17.2	8.8	58	42	16	7/18/13	58.5			
																		10/16/13	58.7	10/30/13	53.9	40.9
	18.0			36.0	67	92		64	1.52	0.39	0.60							7/18/13	56.4	7/26/13	62.9	37.9
ST40	18.0	A-7-5	MH	42.2	66	94	2.74	73	1.59	0.45	0.61	85.8	17.2	8.8	58	42	16	7/18/13	48.8			
																		10/17/13	49.2	10/30/13	47.0	39.4
	20.0			17.5	71	83		34	1.42	0.20	0.59							7/18/13	45.7	7/26/13	57.4	20.3
ST41	25.0	A-7-5	MH	46.1	73	107	2.79	94	1.37	0.54	0.58	84.7	5.7	2.2	60	42	18	7/19/13	34.7	7/27/13	53.9	45.1
ST42	28.0	A-7-5	MH	42.6	78	111	2.76	97	1.22	0.53	0.55	89.2	10.9	5.0	50	37	13	7/26/13	14.2			
																		10/28/13	28.6	11/6/2013	45.3	40.6
	30.0			39.9	83	116		102	1.07	0.53	0.52							7/26/13	17.5	8/2/13	50.3	37.0
ST43	34.5	A-4	ML	20.1	110	133	2.81	96	0.59	0.36	0.37	76.7	8.0	2.0	31	27	4	7/30/13	13.9	8/6/13	48.3	20.4
ST44	38.9	A-6	ML	17.3	114	133	2.84	88	0.56	0.32	0.36	60.1	4.0	1.0	38	25	13	7/30/13	11.5	8/6/13	30.7	18.5
ST45	44.1	A-4	ML	20.5	115	139	2.88	105	0.56	0.38	0.36	68.2	14.7	10.4	34	27	7	8/6/13	18.3	8/14/13	38.3	19.6
ST46	49.5	A-4	ML	19.3	111	133	2.92	88	0.64	0.34	0.39	48.5	10.0	5.0	38	29	9	8/7/13	38.2	8/15/13	57.8	25.1

0.5:1 slope 405+70 9'RT PMT																						
#	Depth	Soil Type		w	γ_d	γ_t	G_s	S	e	θ_w	θ_s	%#200	5µm	2µm	LL	PL	PI	Tensiometer	ψ_t	Filter paper	ψ_f	w_f
	(ft)	(AASHTO)	(USCS)	(%)	(pcf)	(pcf)		(%)				(%)	(%)	(%)				time	(kPa)	time	(kPa)	(%)
ST88	6.4	A-7-5	MH	34.1	77	103	2.74	77	1.22	0.42	0.55	93.6	46.1	29.0	60	38	22	10/4/13	102.2	10/19/13	177.0	34.7
	8.4			33.9	56	75		46	2.03	0.31	0.67							10/4/13	102.2	10/21/13	182.0	32.4
ST89	11.4	A-7-5	MH	35.3	63	85	2.82	56	1.79	0.36	0.64	90.4	22.0	14.0	67	47	20	10/21/13	86.2	11/6/13	620.3	34.8
	13.4			46.3	53	78		57	2.30	0.40	0.70							9/20/13	86.7	9/30/13	104.5	45.5
ST90	16.4	A-7-5	MH	44.2	61	87	2.86	65	1.94	0.43	0.66	93.1	40.0	25.0	62	41	21	10/23/13	67.4	11/6/13	129.2	41.4
	18.4			51.3	66	100		86	1.71	0.54	0.63							8/21/13	63.4	9/8/13	61.0	45.7
ST91	21.4	A-7-5	MH	32.1	70	93	2.83	60	1.51	0.36	0.60	69.7	30.0	15.0	53	38	15	10/23/13	56.4	11/6/13	101.2	30.0
	23.4			35.2	81	109		83	1.19	0.45	0.54							8/23/13	54.0	9/8/13	61.4	32.8
ST92	28.4	A-7-5	MH	40.7	74	104	2.82	83	1.39	0.48	0.58	69.8	13.4	4.0	57	40	17	8/20/13	40.8	9/8/13	50.1	41.1
ST93	33.4	A-4	ML	24.0	98	121	2.83	84	0.81	0.38	0.45	66.4	11.5	4.3	40	31	9	9/13/13	27.2	9/30/13	43.2	25.4
																				9/30/13	40.6	25.5
ST94	39.4	A-7-5	MH	34.3	86	116	2.88	92	1.08	0.48	0.52	84.2	6.8	4.1	51	37	14	9/13/13	38.8	9/30/13	56.0	31.2
																					51.9	30.6

0.25:1 Slope 404+50 3'LT																						
#	Depth	Soil Type		w	γ_d	γ_t	G_s	S	e	θ_w	θ_s	%#200	5µm	2µm	LL	PL	PI	Tensiometer	ψ_t	Filter paper	ψ_f	w_f
3'LT	(ft)	(AASHTO)	(USCS)	(%)	(pcf)	(pcf)		(%)				(%)	(%)	(%)				time	(kPa)	time	(kPa)	(%)
ST47	2.2	A-7-5	MH	34.0	76	102	2.75	75	1.25	0.42	0.56	87.4	36.6	25.0	61	39	22	7/2/13	39.1	11/6/13	98.3	34.2
																		10/29/13	44.8			
	4.2			36.8	69	94		67	1.50	0.40	0.60							7/2/13	67.8	7/9/13	132.4	34.6
ST48	5.2	A-7-5	MH	33.6	73	97	2.81	67	1.41	0.39	0.58	88.4	36.2	24.0	64	42	22	7/2/13	71.5	11/6/13	218.5	34.3
																		10/30/13	72.8			
	7.2			37.4	72	98		73	1.45	0.43	0.59							7/2/13	67.8	7/9/13	142.4	33.5
ST49	7.5	A-7-5	MH	35.8	68	93	2.77	65	1.53	0.39	0.61	84.8	31.4	18.0	61	39	22	7/3/13	78.6	11/6/13	243.7	34.7
																		10/30/13	78.7			
	9.5			33.5	72	96		66	1.41	0.39	0.59							7/3/13	74.2	7/11/13	138.7	33.0
																		10/30/13	76.4			
ST50	10.2	A-7-5	MH	40.2	70	98	2.79	76	1.48	0.45	0.60	88.5	25.1	14.9	59	36	23	11/6/13	63.4	1/22/14	106.3	36.01
	12.2			35.7	78	106		81	1.24	0.45	0.55							7/12/13	60.5	7/19/13	125.5	35.3
ST51	13.2	A-7-5	MH	44.2	61	88	2.70	68	1.76	0.43	0.64	84.4	20.0	11.0	60	36	24	7/11/13	44.8	11/7/13	51.9	43.5
																		11/7/13	47.5			
	15.2			46.8	65	96		80	1.58	0.49	0.61							7/11/13	41.3	7/18/13	55.9	45.6
ST52	18.2	A-7-5	MH	50.2	67	101	2.80	88	1.60	0.54	0.61	84.3	13.0	2.0	60	45	15	7/3/13	23.8	7/11/13	38.5	48.7
	20.2			49.4	65	97		81	1.70	0.51	0.63							11/10/13	24.6	1/22/14	47.8	46.7
ST53	25.2	A-7-5	MH	42.3	78	111	2.73	97	1.19	0.53	0.54	84.8	17.5	7.0	63	45	18	8/8/13	29.3	8/18/13	44.7	38.7
ST54	30.2	A-7-5	MH	24.3	98	121	2.76	88	0.76	0.38	0.43	55.4	14.3	7.0	51	36	15	8/9/13	23.6	8/18/13	40.0	28.5
ST55	35.2	A-7-5	ML	22.3	102	125	2.83	87	0.72	0.37	0.42	63.6	9.7	4.0	43	32	11	8/7/13	25.1	8/15/13	37.6	25.5
ST56	40.2	A-4	ML	24.4	100	125	2.75	94	0.71	0.39	0.42	58.7	8.0	3.0	36	29	7	8/8/13	21.3	8/18/13	34.8	22.0
ST57	44.7	A-4	SM	19.3	104	124	2.70	85	0.62	0.32	0.38	41.0	11.0	5.0	30	25	5	7/3/13	10.8	8/14/13	25.9	19.0
ST58	49.2	A-4	SM	17.0	114	133	2.73	94	0.50	0.31	0.33	43.0	7.5	4.5	35	30	5	8/9/13	13.4	8/18/13	34.8	16.1

1:1 Slope 403+45 3'LT																					
#	Depth	Soil Type		w	γ_d	γ_t	G_s	S	e	θ_w	θ_s	%#200	5µm	2µm	LL	PL	PI	Tensiometer	ψ_t	Filter paper	ψ_f	w_f
	(ft)	(AASHTO)	(USCS)	(%)	(pcf)	(pcf)		(%)				(%)	(%)	(%)				time	(kPa)	time	(kPa)	(%)
ST59	2.1	A-2-6	SC	12.6	114	129	2.70	72	0.47	0.23	0.32	30.0	12.2	10.8	37	24	13	7/4/13	76.0	7/11/13	650.9	
	4.1			9.5	123	135		69	0.37	0.19	0.27							7/4/13	81.7			
ST60	5.1	A-2-6	SC	16.5	110	128	2.67	86	0.51	0.29	0.34	34.0	13.7	11.7	34	23	11					
	6.9			15.0	109	126		76	0.52	0.26	0.34							7/4/13	9.8	7/11/13	44.7	13.24
ST61	10.1	A-4	ML	13.0	109	123	2.78	62	0.59	0.23	0.37	81.3	23.3	16.1	34	26	8	7/5/13	45.2			
																		11/11/13	50.8			
	12.1			11.9	114	128		64	0.52	0.22	0.34							7/5/13	59.5			
																		11/11/13	60.5	7/12/13	148.4	19.16
ST62	13.1	A-7-5	ML	23.3	91	112	2.78	71	0.91	0.34	0.48	81.3	7.9	4.5	44	33	11	7/11/13	37.9			
																		11/20/13	50.0			
	15.1			20.7	109	132		98	0.59	0.36	0.37							7/11/13	29.1	7/18/13	192.9	19.17
ST63	18.1	A-7-5	ML	23.7	101	125	2.72	94	0.68	0.38	0.41	75.4	13.1	4.8	48	34	14	7/5/13	30.5			
	20.1																	7/5/13	24.3	7/12/13	181.0	20.55
ST64	27.1	A-7-5	ML	21.5	106	128	2.81	92	0.66	0.36	0.40	84.7	5.7	2.2	45	33	12	8/13/13	35.3	8/23/13	49.4	21.28
ST65	30.8	A-4	ML	24.2	101	126	2.86	91	0.76	0.39	0.43	79.2	12.0	7.1	37	29	8	8/13/13	29.0	8/23/13	45.9	19.88
ST66	35.8	A-4	SM	16.7	107	125	2.75	76	0.60	0.29	0.38	41.0	4.7	4.0	29	27	2	8/14/13	13.8	8/26/13	32.8	15.55
ST67	40.8	A-4	ML	21.5	101	122	2.71	86	0.68	0.35	0.41	80.5	5.9	3.0	37	30	7	8/14/13	13.8	8/26/13	41.5	20.70
ST68	45.8	A-7-5	MH	49.3	73	108	2.93	95	1.52	0.57	0.60	93.9	20.0	6.1	63	35	28	8/15/13	17.3	8/26/13	31.2	51.32
ST69	50.3	A-4	SM	14.4	119	137	2.75	91	0.44	0.28	0.30	43.4	4.9	3.2	31	27	4	8/15/13	12.5	8/26/13	30.2	11.65

Sheetpile wall 404+50 94'RT																					
#	Depth	Soil Type		w	γ_d	γ_t	G_s	S	e	θ_w	θ_s	%#200	5µm	2µm	LL	PL	PI	Tensiometer	ψ_t	Filter paper	ψ_f	w_f
	(ft)	(AASHTO)	(USCS)	(%)	(pcf)	(pcf)		(%)				(%)	(%)	(%)				time	(kPa)	time	(kPa)	(%)
ST26	6.5	A-6	CL	14.6	54	62	2.69	19	2.12	0.13	0.68	57.5	14.3	10.4	39	27	12					
ST28	15.2	A-4	ML	17.0	85	100	2.69	47	0.97	0.23	0.49	66.3	17.0	8.8	36	29	7	4/7/13	66.8			
ST30	24.2	A-7-5	CH	35.9	82	111	2.80	88	1.14	0.47	0.53	71.4	18.6	12.4	58	25	33	7/24/13	28.0	8/1/13	60.2	
ST32	34.2	A-4	ML	26.1	99	124	2.77	96	0.75	0.41	0.43	53.1	11.1	4.7	38	30	8	7/24/13	18.7	8/1/13	48.7	24.1
ST34	44.2	A-4	ML	22.5	102	125	2.79	88	0.71	0.37	0.42	61.5	10.9	1.5	38	28	10	7/24/13	20.0	8/1/13	48.0	22.9

Sheetpile wall 404+50 102'RT																						
#	Depth	Soil Type		w	γ_d	γ_t	G_s	S	e	θ_w	θ_s	%#200	5µm	2µm	LL	PL	PI	Tensiometer	ψ_t	Filter paper	ψ_f	w_f
	(ft)	(AASHTO)	(USCS)	(%)	(pcf)	(pcf)		(%)				(%)	(%)	(%)				time	(kPa)	time	(kPa)	(%)
ST70	5.2	A-7-5	CL	23.8	83	103	2.70	62	1.03	0.32	0.51	72.1	27.8	17.1	45	26	19	8/16/13	184.0	8/26/13	1124.9	21.1
ST71	8.2			20.0	102	122	2.68	84	0.64	0.33	0.39	72.9	21.0	12.0				10/8/13	170.0	10/19/13	776.3	18.0
ST72	13.2			15.5	67	77	2.71	27	1.54	0.17	0.61	75.1	16.3	11.8				10/3/13	136.6	10/19/13	464.5	14.9
																				10/19/13	431.0	15.9
ST73	16.2	A-7-5	ML	29.1	89	115	2.81	84	0.98	0.41	0.49	77.3	6.8	4.5	55	41	14	9/18/13	92.5	9/30/13	747.3	28.7
ST74	20.8	A-7-5	ML	14.0	111	127	2.74	71	0.54	0.25	0.35	60.0	11.5	5.7	44	33	11	9/9/13	57.8	9/19/13	124.8	15.9
																				9/19/13	128.2	15.6
																				3/12/14	176.9	19.5
ST75	26.2	A-7-5	ML	17.5	104	122	2.73	75	0.64	0.29	0.39	64.3	8.8	4.4	42	31	11	9/10/13	34.8	9/26/13	55.0	16.1
																				9/26/13	53.3	16.2
																				3/12/14	101.2	15.7
ST76	31.2	A-7-5	ML	18.3	110	130	2.69	92	0.53	0.32	0.35	51.9	8.0	1.5	44	33	11	8/21/13	20.1	9/8/13	44.9	19.0
ST77	36.2	A-4	ML	21.1	101	123	2.68	86	0.65	0.34	0.39	58.8	7.0	0.8	32	27	5	8/23/13	25.1	9/8/13	39.6	20.4
ST78	41.2	A-4	ML	20.3	99	119	2.68	79	0.69	0.32	0.41	58.2	5.4	1.8	36	29	7	8/22/13	18.6	9/8/13	44.2	19.0
ST79	46.2	A-4	ML	17.6	115	135	2.83	93	0.54	0.32	0.35	60.5	9.9	3.8	28	25	3	8/20/13	23.7	9/8/13	48.5	14.9
ST80	51.2	A-4	ML	21.0	107	130	2.68	101	0.56	0.36	0.36	59.0	6.5	1.9	34	29	5	8/26/13	28.7	9/9/13	44.5	20.3

Sheetpile wall 404+50 86'RT PMT																					
#	Depth	Soil Type		w	γ_d	γ_t	G_s	S	e	θ_w	θ_s	%#200	5µm	2µm	LL	PL	PI	Tensiometer	ψ_t	Filter paper	ψ_f	w_f
	(ft)	(AASHTO)	(USCS)	(%)	(pcf)	(pcf)		(%)				(%)	(%)	(%)				time	(kPa)	time	(kPa)	(%)
ST81	6	A-5	ML				2.68			0.17	0.52	61.0	21.0	13.3	41	33	8	7/19/13	94.7			
	8			13.2	80	90		32	1.10									7/19/13	95.7	7/27/13	379.5	15.4
ST82	12	A-4	ML	16.2	85	98	2.75	43	1.03	0.22	0.51	61.5	9.1	4.4	39	32	7	7/23/13	85.5	7/30/13	166.7	16.3
ST83	16	A-4	ML				2.61					58.1	3.1	2.3	38	32	6	7/23/13	85.1			
	18			18.9	81	97		49	1.00	0.25	0.50							7/23/13	79.1	7/30/13	71.7	18.5
ST84	23	A-4	ML	27.2	81	103	2.66	69	1.04	0.35	0.51	64.2	15.1	12.1	40	33	7	7/24/13	65.1	8/1/13	57.9	
ST85	28	A-4	ML	28.8	89	114	2.69	87	0.89	0.41	0.47	68.6	11.8	4.0	45	34	11	9/12/13	43.2	9/26/13	50.7	27.4
																				9/26/13	53.3	28.9
ST86	33	A-4	ML	31.1	84	110	2.73	82	1.03	0.42	0.51	56.5	12.0	6.0	38	31	7	9/12/13	26.5	9/26/13	41.1	28.0
																				9/26/13	41.3	29.4
ST87	39.5	A-4	ML	27.9	97	124	2.70	102	0.74	0.43	0.43	55.8	9.1	4.6	38	32	6	8/19/13	23.2	9/8/13	38.8	25.6

APPENDIX C: SOIL WATER CHARACTERISTIC CURVE

SWCC (A-5, ML)						
	ψ_p	θ_p			ψ_p	θ_p
ST28	0.1	0.435		ST61	0.1	0.422
	1	0.427			1	0.422
	30	0.38			20	0.403
	60	0.301			50	0.385
	130	0.212			100	0.338
	250	0.143			150	0.318
	480	0.107			200	0.299
ST32	0.1	0.509			300	0.28
	1	0.489			400	0.271
	20	0.435		ST64	0.1	0.442
	40	0.417			1	0.434
	80	0.345			20	0.37
	160	0.231			50	0.31
	330	0.171			100	0.247
	480	0.152			150	0.193
ST34A	0.1	0.518			200	0.153
	1	0.498			300	0.134
	20	0.402			400	0.121
	40	0.369		ST79	0.1	0.456
	80	0.289			1	0.455
	120	0.174			13.79	0.391
	240	0.148			27.579	0.36
	480	0.108			55.16	0.292
ST34B	0.1	0.461			68.95	0.253
	1	0.46			82.74	0.223
	13.8	0.378			96.53	0.204
	27.6	0.357			137.9	0.158
	41.4	0.333			206	0.132
	55.2	0.306			413.69	0.121
	68.95	0.287			482.63	0.1
	96.53	0.244				
	110.3	0.215				
	137.9	0.191				
	282.69	0.18				
	413.69	0.158				
	482.63	0.13				

SWCC A-7-5 MH						
	ψ_p	θ_p			ψ_p	θ_p
ST38A	0.1	0.61		ST36	0.1	0.541
	1	0.589			1	0.537
	15	0.554			13.79	0.454
	30	0.545			27.58	0.427
	70	0.437			62.1	0.39
	130	0.376			75.84	0.378
	240	0.346			103.4	0.359
	490	0.307			131	0.345
ST38B	0.1	0.611			213.74	0.316
	1	0.606			420.58	0.285
	17.2	0.558			482.6	0.28
	34.5	0.54		ST47	0.1	0.615
	68.95	0.454			1	0.6
	89.6	0.396			27.579	0.58
	124	0.352			67.569	0.525
	144.8	0.331			75.842	0.506
	179.3	0.312			137.895	0.441
	213.7	0.292			289.58	0.391
	234.4	0.279			420.58	0.375
	289.6	0.265			496.423	0.37
	358.53	0.251		ST70	0.1	0.533
	427.48	0.239			1	0.535
	482.63	0.231			10	0.483
ST50	0.1	0.594			20	0.465
	1	0.59			40	0.439
	13.79	0.544			80	0.4
	27.579	0.531			100	0.375
	62.1	0.496			150	0.347
	103.4	0.416			200	0.326
	144.79	0.357			300	0.311
	300	0.288			400	0.297
	480	0.253				
ST40	0.1	0.58				
	1	0.552				
	10	0.475				
	40	0.423				
	50	0.39				
	70	0.335				
	100	0.282				
	150	0.243				
	200	0.228				
	300	0.212				
	400	0.194				

APPENDIX D: DATA OF SUCTION AND MOISTURE SENSORS

FTC suction sensor																	
Location		405+70 0.5:1			404+50 0.25:1				403+45 1:1				Sheet pile wall				
Depth(ft)		3	6	10	3	6	10	20	3	6	10	20	3	5.7	10	13.75	20
Stage	Date\ #	37-02	36-18	37-03	37-09	37-10	37-11	37-06	36-21	36-23	36-20	36-19	37-05	36-22	37-01	37-07	37-04
	6/27/13	293.9	79.6	103.2	142.9	152.8	162.5	652.9	92.4	53.4	173.7	45.0	105.3	1638.1	173.6	387.3	102.8
	7/8/13	218.2	67.3	103.8	143.5	155.2	178.0	618.9	67.4	49.0	179.7	45.1	89.3	887.8	166.1		98.2
1st excavation starts	7/16/13	186.4	64.2	101.6	145.5	155.7	181.9	652.5	42.7	46.5	179.8	45.3	85.1	708.2	168.5	217.6	100.4
1st excavation ends	9/4/13	123.8	43.7	89.3	158.6	149.4	183.7	428.7	19.3	33.6	168.9	37.4	80.0	344.6	133.7		96.2
	9/23/13	125.0	30.7	74.6	149.1	134.4	166.2	421.4	11.8	28.0	154.3	35.7	77.1	279.1	146.0	205.8	98.4
2nd excavation starts	10/9/13	127.5	33.6	72.0	158.0	137.5	165.6	384.2	12.2	23.4	143.7	32.5	68.7	203.1	133.1	177.5	88.8
2nd excavation ends	10/25/13	136.9	37.9	71.4	160.4	133.2	152.6	328.8	11.0	18.7	127.9	31.1	64.3	200.8	124.8		83.0
	11/8/13	138.0	39.2	65.9	170.3		163.7	322.5	13.3	21.7	143.4	31.5	68.1	220.9	128.0		87.9
3rd excavation	11/22/13	163.5	49.6	70.1	175.4	150.0	169.8	325.4	15.7	19.6	133.5	29.5	69.9	221.8	120.9		86.1
ends on Dec	1/9/14	79.1	42.9	64.8	138.1	149.1	176.4	250.7	12.6	18.5	131.8	28.8	20.3	19.4	31.2		68.8
	1/23/14	75.9	30.1	53.8	127.8	134.2	161.6	227.4	11.9	15.7	118.5	27.2	5.3	6.5	5.1	64.0	57.0
Filtration starts	2/6/14	71.2	43.4	55.2	124.6	136.8	161.0	236.2	11.4	14.8	121.5	25.5					
	2/10/14	85.5	33.5	49.0	121.4	132.0	158.9	216.5	18.0	14.6	119.6	27.4					
	2/20/14	71.2	32.6	43.3	115.7	126.6	145.1	219.1	14.4	11.2	105.1	24.8	1.2	0.1	5.6		50.7
	3/4/14	76.3	29.3	34.7	109.5	114.9	140.8	189.5		10.1	95.4	18.9					
	3/10/14	69.4	35.5	37.6	111.1	125.8	150.8	197.8	11.8	10.9	100.6	20.3					

Calibrated data		Moisture content by sensors									
Site		0.5:1 Slope			0.25:1 Slope			1 : 1 Slope			
Location		405+70			404+50			403+45			
Depth		2	4	8	2	4	7	2	4	6	8
Stage	Date	Sensor 1	Sensor 5	Sensor 10	Sensor 4	Sensor 3	Sensor 2	Sensor 7	Sensor 6	Sensor 8	Sensor 9
	6/27/13	0.341	0.346	0.256	0.423	0.335	0.374	0.329	0.168	0.198	0.132
	7/8/13	0.348	0.349	0.259	0.431	0.338	0.378	0.330	0.170	0.200	0.135
1st excavation starts	7/16/13	0.352	0.352	0.260	0.435	0.340	0.380	0.330	0.171	0.202	0.137
1st excavation ends	9/4/13	0.360	0.361	0.265	0.437	0.343	0.388	0.335	0.183	0.207	0.141
	9/23/13	0.356	0.359	0.265	0.437	0.343	0.388	0.334	0.179	0.208	0.141
2nd excavation starts	10/9/13	0.356	0.357	0.267	0.435	0.342	0.390	0.330	0.177	0.208	0.141
2nd excavation ends	10/25/13	0.354	0.356	0.267	0.431	0.340	0.390	0.323	0.176	0.208	0.141
	11/8/13	0.356	0.356	0.267	0.427	0.342	0.390	0.318	0.176	0.207	0.141
3rd excavation ends	11/22/13	0.354	0.354	0.265	0.425	0.336	0.388	0.313	0.190	0.207	0.140
on Dec 20, 2013	1/9/14	0.362			0.425	0.340	0.400	0.368	0.174	0.205	0.140
	1/23/14	0.350		0.268	0.429	0.342	0.388	0.375	0.174	0.205	0.138
	2/6/14	0.370	0.367	0.268		0.342		0.367	0.179	0.204	0.141
	2/10/14	0.374	0.371	0.272	0.442	0.343	0.388	0.368	0.174	0.204	0.138
	2/19/14	0.374	0.375		0.460	0.347	0.403	0.372	0.183	0.337	0.138
	3/4/14	0.376	0.371	0.270	0.456	0.350	0.390	0.372	0.174	0.204	0.138
	3/10/14	0.376	0.374	0.272	0.446	0.343	0.396	0.375	0.183	0.204	0.140

Calibrated data		Moisture content by sensors					
Site		Sheet piles site					
Location				404+50			
Depth		2	3	4	5	6	12
Stage	Date	Sensor11	Sensor16	Sensor14	SensorN	Sensor15	Sensor13
	6/27/13		0.207		0.195		
	7/8/13	0.328	0.215	0.313	0.203	0.136	0.220
1st excavation starts	7/16/13	0.330	0.218	0.316	0.207	0.138	0.218
1st excavation ends	9/4/13	0.334	0.220	0.319	0.218	0.149	0.222
	9/23/13	0.336	0.220	0.321	0.219	0.146	0.226
2nd excavation starts	10/9/13	0.331	0.232	0.319	0.220	0.147	0.225
2nd excavation ends	10/25/13	0.330	0.226	0.316	0.221	0.147	0.228
	11/8/13	0.327	0.226	0.315	0.223	0.147	0.226
3rd excavation ends	11/22/13	0.326	0.225	0.311	0.226	0.149	0.226
on Dec 20, 2013	1/9/14	0.341	0.226	0.308	0.308	0.308	0.242
	1/23/14	0.345	0.242	0.303	0.322	0.321	0.253
	2/6/14						
	2/10/14						
	2/19/14	0.426	0.245	0.394	0.338	0.383	0.257
	3/4/14						
	3/10/14						

APPENDIX E: DATA OF WATER CONTENT AND SUCTION AT FINAL STAGE

0.5:1 SLOPE										
Suction profile		Depth (ft)	4'LT 04/20/14		4'LT 3/14/2014		Depth (ft)	AVG	MIN	MAX
	Final stage	0.1	53.1		52.83		0.1	53.1		
		2	37.3	48.9			2	43.1	5.8	5.8
		4	44	55.4	50.1		4	49.7	5.7	5.7
		6	49.6	54.1	60.5		6	51.9	2.3	2.3
		8	53.1		64.95		8	53.1		
		Depth (ft)	3'LT	9'RT PMT04/17/13	9'RT		Depth (ft)	AVG	MIN	MAX
	Initial stage	2	86.7				2	86.7		
		3.5		92.9			3.5	92.9		
		4	86.1				4	86.1		
		5	84.8				5	84.8		
		6.4			102.2		6.4	102.2		
		7	81.6				7	81.6		
		8	73.9							
		8.5		86.2	102.2		8.25	87.4	13.5	14.8
		10	77.1				10	77.1		
		11.4			86.2		11.4	86.2		
		13.4			86.7		13.4	86.7		
		16	58.5		67.4		16	63.0	4.5	4.5
		18	56.4				18.2	56.2	7.4	7.2
		18.1	48.8							
		18.4			63.4					
		19		52.7			19	52.7		
		20	45.7				20	45.7		

0.5:1 SLOPE										
Water content profile		Depth (ft)	3'LT	9'RT	3'RT (DOT)		Depth (ft)	AVG	MIN	MAX
	Initial stage	2	25.8				2	25.8		
		4	28.6				4	28.6		
		5	38.9				5	38.9		
		6.4		34.1			6.4	34.1		
		7	32.6				7	32.6		
		8	29.5				8	29.5		
		8.4		33.9			8.4	33.9		
		10	35		30.8		10	32.9		
		11.4		35.3			11.4	35.3		
		13.4		46.3			13.4	46.3		
		16	41.3				16	41.3		
		16.4		44.2			16.4	44.2		
		18	36				18	36.0		
		18.1	42.2				18.1	42.2		
		18.4		51.3			18.4	51.3		
		20	17.5				20	17.5		
		Depth (ft)	4'LT 04/20/2014				Depth (ft)	AVG	MIN	MAX
	Final stage	0.1	32.9				0.1	32.9		
		2	33.4	32			2	32.7	0.7	0.7
		4	29.1	31.5			4	30.3	1.2	1.2
		6	35.6	30.2			6	32.9	2.7	2.7
		8	28.3				8	28.3		

0.25:1 slope													
Suction profile		Depth (ft)	3'LT					AVG	Min	max			
	Initial stage	2.2	42.0					42.0					
		4.2	67.8					67.8					
		5.2	72.2					72.2					
		7.35	67.8	78.7				73.2	5.4	5.4			
		9.85	75.3	63.4				69.4	6.0	6.0			
		12.2	60.5					60.5					
		13.2	44.8					44.8					
		15.2	41.3					41.3					
		18.2	23.8					23.8					
		20	24.6					24.6					
								4.5'LT			7.5'LT		
		Depth (ft)	4.5'LT (lab)		7.5'LT (lab)			AVG	Min	Max	AVG	Min	Max
	Final stage	0.1	48.2		50.6			48.2			50.6		
		2	51.2	68.2	61.3	79.7		59.7	8.5	8.5	70.5	9.2	9.2
		4	65.3	80.8	70.5			73.1	7.8	7.8	70.5		
		6	73.4	81.8				77.6	4.2	4.2			
		8	73.6					73.6					

0.25:1 slope													
								3'LT					
		Depth (ft)	3'LT		3'RT (DOT)			AVG	Min	Max			
Water content profile	**Initial stage**	2.2	34					34.0					
		4.2	36.8					36.8					
		5.2	33.6					33.6					
		7.3	37.4	35.8	40.6			36.6	0.8	0.8			
		9.85	33.5		37.3			33.5					
		12.2	35.7					35.7					
		13.2	44.2					44.2					
		15.2	46.8		41.5			46.8					
		18.2	50.2					50.2					
		20	49.4		47.5			49.4					
								4.5'LT			7.5'LT		
		Depth (ft)	4.5'LT		7.5'LT			AVG	Min	max	AVG	Min	Max
	Final stage	0.1	25.253		29.439			25.3			29.4		
		2	38.324	35.583	36.252	35.492		37.0	1.4	1.4	35.9	0.4	0.4
		4	35.685	38.117	37.076			36.9	1.2	1.2	37.1		
		6	36.137	35.709				35.9	0.2	0.2			
		8	33.295					33.3					

1:1 slope													
		Depth (ft)	3'LT					AVG					
Suction profile	Initial state	2.1	76					76					
		4.1	81.7					81.7					
		10	48					48					
		12.1	60					60					
		13.1	37.9					37.9					
		15.1	29.1					29.1					
		18.1	30.5					30.5					
		20	24.3					24.3					
									1'RT			4'LT	
	Final state	Depth (ft)	1'RT		4'LT			AVG	Min	Max	AVG	Min	Max
		0.1	27.0	38.9	33.3	13.9		32.9	5.9	5.9	23.6		
		1	66.6					66.6					
		2	71.8	74.8	34.2	48.0		73.3	1.5	1.5	41.1	6.9	6.9
		4	74.0		52.6	71.5		74.0			62.1	9.5	9.5
		6	60.0		69.0	83.7		60.0			76.4	7.3	7.4
		8	74.5		67.8			74.5			67.8		

1:1 slope													
		Depth (ft)	3'LT	3'RT (DOT)				AVG	Min	Max			
Water content profile	**Initial state**	2.1	12.6					12.6					
		4.1	9.5					9.5					
		5.1	16.5					16.5					
		6.9	15	13.6				14.3	0.7	0.7			
		10	13	15				14	1	1			
		12.1	11.9					11.9					
		13.1	23.3					23.3					
		15.1	20.7					20.7					
		18.1	23.7					23.7					
		20		20.6				20.6					
		Depth (ft)	1'RT		4'LT			AVG	Min	Max	AVG	Min	Max
	Final state	0.1	14		21.9			14.0			21.9		
		2.1	10	10.6	13.3	14		10.3	0.3	0.3	13.7	0.4	0.4
		4.1	8.7		14.8	13.2		8.7			14.0	0.8	0.8
		6			12	13.9					13.0	0.9	1.0
		7.9			12.7						12.7		

Sheet pile wall						
		Depth (ft)	86'RT	86'RT PMT041013	94'RT	102'RT
Suction profile	Initial state	3		88.1		
		5.2				184
		6	94.7			
		8	95.7	87		
		8.2				170
		12	85.5			
		13		74.1		
		13.2				136.6
		15.2			66.8	
		16	85.1			
		16.2				92.5
		18	79.1	42.6		
		19				
		20.8				57.8
	Final state	Depth (ft)	15'RT to the wall 031214		7'RT to the wall 032814	
		0.1			9.3	
		1	8.1			
		2	43.1	40.9	18.6	
		4	21.7	35.7	7.2	
		6	17.5		21.6	
		8	58.8	65		
		10	107.6	94.7	29.8	

Sheet pile wall						
		Depth (ft)	86'RT	94'RT	94'RT (DOT)	102'RT
Water content profile	**Initial state**	5.2				23.8
		6.5		14.6		
		8	13.2			
		8.2				20
		12	16.2		19.2	
		13.2				15.5
		15.2		17		
		16.2				29.1
		18	18.9			
		20			21	14
			15'RT to the wall 031214		7'RT to the wall 032814	
	Final state	Depth (ft)				
		0.1	33.7		27.8	
		1	36.6			
		2	36	36.6	33.7	
		4	34	36.6	23.7	
		6	37.5	32.5	25.8	
		8	25.8	31.3		
		10	12.7		16.7	